UNDERSTANDING THE MECHANISM OF ACTION OF UV3, AN ANTI-CD54 MONOCLONAL ANTIBODY, IN THE THERAPY OF MULTIPLE MYELOMA

APPROVED BY THE SUPERVISORY COMMITTEE

Ellen S. Vitetta, Ph.D., Professor of Microbiology

Director, Cancer Immunobiology Center

Michael Bennett, M.D., Professor of Pathology

John Minna, M.D., Professor, Hamon Cancer Center

Jerry Niederkorn, Ph.D., Professor of Ophthalmology

Mark Siegelman, M.D., Ph.D., Associate Professor of Pathology

to my husband David

and to all my Families for your love and encouragement

UNDERSTANDING THE MECHANISM OF ACTION OF UV3, AN ANTI-CD54 MONOCLONAL ANTIBODY, IN THE THERAPY OF MULTIPLE MYELOMA

by

Elaine J. Coleman

DISSERTATION

Presented to the Faculty of the Graduate School of Biomedical Sciences

The University of Texas Southwestern Medical Center at Dallas

In Partial Fulfillment of the Requirements

For the Degree of

Doctor of Philosophy

The University of Texas Southwestern Medical Center at Dallas

Dallas, Texas

February, 2005

Acknowledgements

I especially thank my mentor, Dr. Ellen Vitetta, for her wisdom and counsel on this project. She is a talented scientist, and I am privileged to have trained under her. She is well-organized and a good teacher. She has given me the freedom to work independently, which has challenged me and taught me in so many ways.

I thank my committee members Dr. Michael Bennett, Dr. John Minna, Dr. Jerry Niederkorn, and Dr. Mark Siegelman for their guidance. I thank Dr. Jerry Niederkorn for his collaboration, counsel, and patience on the uveal melanoma project.

I thank Dr. Shiro Shimizu for the ILKM2 and ILKM3 cells and Dr. Michael Norgard for the 13G10 cells.

I thank my collaborators: Kim Brooks for her work with UV3 in the breast and prostate carcinoma model, for her contributions and assistance in the antibody production; Liz Mogelnicki for her work in evaluating VEGF levels in a panel of multiple myeloma cell lines and staining the cell lines with UV3; Jill Mooney and Namita Gandhi for their assistance and training in the ADCC and CDC assays; Dr. Larry Pop for his technical advice and assistance in the CDC and ADCC assays and for sharing his expertise as an oncologist; Dr. Joan Smallshaw for her assistance with the multiple myeloma model and for her technical support in molecular biology;

Dr. Camelia Spiridon for her work with UV3 in the breast and prostate carcinoma model; Dr. Shiuxan Wang for his work with UV3 in the uveal melanoma model.

I thank Ana Firan, Lien Le, Ming-Mei Liu for their technical support and for teaching me the art of antibody production. I thank Shane Scoggins for his technical advice and assistance in performing the microarrays, the Microarray Core for their work on the oligo arrays, and Dr. Noelle Williams for training me on quantitative PCR. I thank Dr. Jim Richardson, John Shelton, and the Molecular Histology lab for their technical support and advice. I thank Phyllis Baron for technical support.

I thank Linda Berry, Erica Garza, and Barbi McFatridge for their administrative support.

I thank my friends and families for their love, support, and encouragement. Thank you for the notes, the double chocolate brownies, and the mocha frappacinos. Finally, I thank David, my husband, who brings home flowers and has an endless supply of patience.

UNDERSTANDING THE MECHANISM OF ACTION OF UV3, AN ANTI-CD54 MONOCLONAL ANTIBODY, IN THE THERAPY OF MULTIPLE MYELOMA

Publication No. _____

Elaine J. Coleman

The University of Texas Southwestern Medical Center at Dallas, 2004

Supervising Professor: Ellen S. Vitetta, Ph.D.

Multiple myeloma is a hematopoietic malignancy involving the uncontrolled proliferation of a single clone of plasma cells or plasma cell progenitors in the bone marrow. Previously, a monoclonal antibody called UV3, which recognizes human CD54/ICAM-1, was developed for the therapy of multiple myeloma. UV3 is highly effective at treating advanced multiple myeloma in SCID mice with human multiple myeloma xenografts. UV3 does not inhibit homotypic tumor cell adhesion or their adhesion to the bone marrow. UV3 does not induce apoptosis of tumor cells or block cell growth. Previous work evaluating $F(ab)'_2$ fragments of UV3 demonstrated that they were effective in mediating anti-tumor activity, suggesting that other mechanisms also contributed to the anti-tumor activity of UV3.

One possibility to explain how UV3 exerts its anti-tumor activity could be that UV3 inhibits the secretion of pro-angiogenic cytokines and molecules, resulting in an

inhibition of angiogenesis. To this end, our goal was to evaluate the angiogenic signals from human multiple myeloma cells and determine whether UV3 would interfere with such signals. In addition, we further examined the role of the Fc portion of UV3 in mediating anti-tumor activity. We found that multiple myeloma cell lines secrete some pro-angiogenic cytokines and molecules, and although UV3 may induce a minor anti-angiogenic effect, the Fc portion of UV3 was critical for its anti-tumor activity. In addition, we found that UV3 prolonged the survival of SCID mice with Daudi lymphoma, which suggests UV3 may be effective in treating a variety of hematological malignancies.

Table of Contents

List of Figures

List of Tables

List of Abbreviations

ADCC	Antibody dependent cell cytotoxicity
bFGF	Basic fibroblast growth factor
CDC	Complement dependent cell cytotoxicity
CHO	Chinese hamster ovary (cells)
CHOP	Cyclophosphamide, doxorubicin, vincristine, prednisone
Cy	Cyanine
EDTA	Ethylene diamine tetraacetic acid
EGF	Epidermal growth factor
EGFR	Epidermal growth factor receptor
ELISA	Enzyme-linked immunosorbent assay
FACS	Fluorescently activated cell sorting
FcRn	Neonatal Fc receptor
FCS	Fetal calf serum
FU	Fluorouracil
GM-CSF	Granulocyte-macrophage colony stimulating factor
ICAM-1	Intercellular adhesion molecule-1
IL	Interleukin
IFN	Interferon
i.v.	Intravenously
LFA-1	Lymphocyte function-associated antigen
LV	Leucovorin

NFkB	Nuclear factor kappa B
NK	Natural killer (cells)
PBS	Phospho-buffered saline
PBSCs	Peripheral blood stem cells
SCID	Severe combined immunodeficiency
TE	Tris-EDTA
TGF	Transforming growth factor
TNF	Tumor necrosis factor
VAD	Vincristine, doxorubicin, dexamethasone
VEGF	Vascular endothelial growth factor

Introduction

A. Multiple Myeloma

The Disease

Multiple myeloma is a disease characterized by the uncontrolled proliferation of a single clone of plasma cells, or plasma cell progenitors in the bone marrow. There are approximately 45,000 Americans who currently have multiple myeloma, and the American Cancer Society estimates another 15,270 cases will be diagnosed in 2004 (1-3). The median age at diagnosis is 68 years. The incidence of multiple myeloma is slightly higher in men than women. African Americans and Native Pacific Islanders are affected more frequently than Caucasian Americans, and the frequency is lower in the Asian population (3,4). Without treatment, the median survival of patients diagnosed with multiple myeloma is only 17 months (5).

Clinical Presentation of Multiple Myeloma

Patients with multiple myeloma may present various symptoms such as general infection, anemia, renal disease, bone pain, or hypercalcemia. Blood tests of patients reveal a monoclonal Ig paraprotein, high levels of β2-microglobulin, low platelet counts, decreased hemoglobin concentrations, and high levels of C-reactive protein. Urine analysis reveals the presence of light

chain dimers, also known as Bence Jones Proteins. By following the levels of the monoclonal Ig in the serum and the Bence Jones Proteins in the urine over time, one can evaluate the progression of the disease (4,6-8).

Pathogenesis

Many genetic and biological factors contribute to the pathogenesis of multiple myeloma. In the development of a normal B cell, the V, D, and J segments of the immunoglobulin heavy chain genes rearrange to become a single V region gene. Once VDJ recombination occurs, somatic mutation and clonal selection occurs to improve antibody affinity, and isotype switching occurs (9). Occasionally, genetic alterations result in the activation of oncogenes or mutations in a tumor suppressor gene. Translocations at the Ig heavy-chain site 14q32 are found in approximately 75% of myelomas, and these translocations frequently result in the disregulation of cyclin genes *D1* and *D3*, fibroblast growth factor receptor 3, the nuclear protein multiple myeloma set domain (*MMSET*) that is involved in chromatin remodeling, and the transcription factors *c-MAF* and *MAFB*, which are proto-oncogenes (4,10-18). These types of genetic alterations are thought to occur early in the pathogenesis of multiple myeloma, and secondary translocations affecting oncogenes like *c-myc*, *ras*, and *p53* impact the progression of multiple myeloma (9,10,19-21). In addition, the monoallelic loss of chromosome 13q, which is thought to contain a tumor suppressor gene, is

common in multiple myeloma and is considered to be an important independent prognostic parameter (22).

Multiple myeloma cells home to the bone marrow microenvironment where the genetic alterations lead to complex interactions between the extracellular matrix and bone marrow stromal cells (23). The growth of multiple myeloma cells and disease progression are stimulated *via* multiple autocrine and paracrine loops (24). Interleukin (IL) -6 is a predominant growth factor for multiple myeloma (25,26). The majority of IL-6 production can be attributed to bone marrow stromal cells, although some multiple myeloma cell lines produce it. IL-6 stimulates the proliferation of multiple myeloma cells *via* a ras/MAPK pathway and induces the production of vascular endothelial growth factor (VEGF) by multiple myeloma cells. IL-6 interferes with antigen-presentation by dendritic cells, stimulates bone resorbtion, and enhances tumor cell survival (4,10,27).

Cytokines in Multiple Myeloma

Multiple myeloma cells can secrete VEGF, tumor necrosis factor alpha (TNF-α), and IL-1 β (28,29). VEGF influences the growth and migration of the multiple myeloma cells, the migration and tube formation of endothelial cells, and stimulates the bone marrow stromal cells to produce more IL-6 (30). TNF-α, which is also produced by stromal cells, activates NFκB, which regulates the transcription of cytokine genes and the expression of adhesion molecules. IL-1β is a potent osteoclast activator. IL-3, IL-8, IL-10, granulocyte-macrophage

colony-stimulating factor (GM-CSF), and interferon alpha (IFN-α) enhance the growth of multiple myeloma cells. The number of cytokines produced by both the multiple myeloma cells and the bone marrow stromal cells result in the proliferation of multiple myeloma cells, the extravasation of the multiple myeloma cells to secondary sites, and the stimulation of angiogenesis to generate blood vessels that provide nutrients and other factors for the growing tumor (4,10,22,27,31).

Treatment

Chemotherapy

Multiple myeloma is responsible for 20% of all hematological malignancy-related mortality (10). Without treatment, the median survival of patients with multiple myeloma is 17 months (5). For over 30 years, melphalan and prednisone have been the predominant choice of treatment (32). Melphalan is a nitrogen mustard, which is a type of alkylating agent. It damages DNA at all stages of the cell cycle (33,34). Prednisone is a corticosteroid, which acts as an immunosuppressant (35). Together, these agents extend the median survival to 3 years, with approximately 5% of patients achieving complete remissions (36).

In an effort to improve the clinical outcome, the efficacy of other conventional chemotherapeutic agents, such as vincristine, cyclophosphamide, and carmustine, have been evaluated. Vincristine is a plant alkaloid that inhibits

protein polymerization (34,37); cyclophosphamide is an alkylating agent that damages the DNA, predominantly, of proliferating cells (34,38); and carmustine is an alkylating agent that damages DNA at all stages of the cell cycle (34,39). Various combinations of vincristine, melphalan, cyclophosphamide, carmustine, and prednisone yield better response rates and slightly prolonged median survivals, but there is no improvement in the overall long-term survival (40,41).

Increasing the dosage of chemotherapy results in a 25-35% increase in the number of complete responders and a 12-13 month increase in the median overall survival (42). In addition, some of these combinations are not as toxic as melphalan. High dose melphalan generates a higher response rate among patients compared to conventional doses, but it leads to severe myelosuppression resulting, in some cases, in bone marrow failure (5,43).

Chemotherapy and Stem Cell Transplantation

Currently, the most successful therapy regimen for multiple myeloma involves the combination of chemotherapy and transplantation of autologous peripheral blood stem cells (PBSCs)(36,40-42). Patients receive a 4-day course of standard induction therapy consisting of vincristine, doxorubicin, and dexamethasone (VAD). Once PBSCs are collected, the patient receives a conditioning regimen that is commonly comprised of high dose melphalan with or without total body irradiation, followed by an autotransplantation of PBSCs (36,42). Phase II clinical trials using this protocol reported that up to 40% of

patients achieve complete responses with a median survival of 5 years (42,44,45). In an effort to reduce the rate of relapse and prolong survival, the use of two tandem autotransplants has demonstrated some success (5,41,46). Allotransplantation, however, yields the highest response rates with the lowest frequency of relapse, largely due to a graft-verses-myeloma effect. The disadvantage and limiting factor of allotransplantation is the high rate of transplantation-related mortality due to graft-verses-host disease (41,47-49).

Immunomodulatory Agents

In addition to chemotherapy and stem cell transplants, there are a few anti-angiogenic and immunomodulatory agents that hold promise for adjuvant and/or maintenance therapy. Thalidomide is one example (50). Thalidomide blocks basic fibroblast growth factor (bFGF) and VEGF- induced angiogenesis (51), promotes apoptosis of multiple myeloma cells, and interferes with the binding of multiple myeloma cells to the bone marrow stromal cells. Natural killer (NK) cell activity is also enhanced (52,53). The efficacy of thalidomide in treating multiple myeloma was first demonstrated in relapsed or refractory patients. One-third of patients responded in the dose-escalated phase II study resulting in prolonged event-free survival and overall survival (42,53,54). As a single agent, the ability to administer high doses is limited by the degree of treatment-induced peripheral neuropathy (42,54). However, thalidomide is not myelosuppressive, which, potentially, makes it very beneficial as an adjuvant therapy. Studies have

demonstrated therapeutic synergy between thalidomide and dexamethasone when given in combination, and current studies are evaluating this combination for induction or maintenance therapy (42,55). In addition, a variety of thalidomide analogs, such as Revimid, are being developed in effort to maintain efficacy and reduce the neurotoxic side effects (56,57).

Therapeutics Under Development

A variety of other anti-multiple myeloma agents are also in development. Bortezomib, also known as PS-341, is a proteosome inhibitor, which inhibits the activation of NFkB, induces apoptosis, and down-regulates adhesion molecules. Bortezomib, which was recently approved by the FDA for relapsed and refractory multiple myeloma, demonstrated a 28% overall response rate with mild to moderate toxicities including fatigue, nausea, diarrhea, constipation, thromobocytopenia, peripheral neuropathy, pyrexia, vomiting, and anemia (53,58). Other agents under development include 1) arsenic trioxide (59), which targets mitochondria, 2) an anti-CD20 antibody (52), which targets a B cell surface antigen detectable on some multiple myeloma cells and possibly multiple myeloma precursor cells, 3) an anti-CD40 antibody (60), which seeks to block the binding of CD40 ligand to CD40 resulting in the reduced secretion of pro-angiogenic and proliferative cytokines, 4) an anti-IL-6 antibody (61), which acts to interfere with the binding to its receptor, 5) an anti-HM1.24 antibody (62), which targets a plasma cell specific antigen, 6) VEGF inhibitors (53,63), which lower the

level of the proliferative and pro-angiogenic cytokines, and 7) anti-idiotypic vaccines (64), which seek to target the clonotypic idiotype of multiple myeloma.

B. Monoclonal Antibodies in Cancer

Technological Advantages

Specificity

Kohler and Milstein pioneered the technique and development of monoclonal antibodies nearly 30 years ago (65). Since that time, monoclonal antibodies have become an important field of study for the therapy of numerous diseases, including autoimmunity and cancer. Monoclonal antibodies are often referred to as “magic bullets” or “targeting missiles” because of their specificity for target cells (65,66). Monoclonal antibodies recognize unique cellular antigens on the surface of tumor cells, such as antigens that are overexpressed, antigens that are specific to one cell type, differentiation antigens, and viral antigens (67-69). Selective cytotoxicity provides a large therapeutic advantage resulting in fewer side effects.

Multiple Mechanisms of Action

In addition to specificity, monoclonal antibodies can activate multiple pathways of tumor destruction. They can recruit effector cells and molecules,

initiate signaling cascades, or block signals necessary for cell growth. In order to initiate effector functions, antibodies recruit complement components or effector cells, which are activated following their binding to the Fc portion of the antibody, resulting in cell lysis (67,69,70). Antibodies are able to alter signaling cascades directly, by inducing apoptosis or cell cycle arrest, or indirectly, by altering the tumor cell microenvironment. In addition, the binding of an antibody to its antigen can prevent other ligands and receptors from binding to the tumor cell. This interference can prevent a tumor cell from homing to a microenvironment favorable for growth, or it can block growth factors from further stimulating tumor cell proliferation and differentiation (70). Antibodies are therapeutically unique not only because they utilize several mechanisms to induce tumor cell destruction, but they often utilize more than one avenue of attack to produce an effect (71). This results in a potentially potent and versatile therapeutic modality.

Antibody Engineering

In addition to exerting their effect through multiple mechanisms, antibodies can be manipulated to improve their therapeutic efficacy. One of the first obstacles in early antibody therapy was their immunogenicity, since they were of mouse origin (72). Patients mounted an immune response, thus limiting therapeutic performance. In order to circumvent this problem, antibodies are now genetically engineered to have mouse variable regions with human constant domains (chimeric), mouse complementarity determining regions with the

remainder of the antibody being human (humanized), or antibodies can also be made completely human using Ig transgenic mice or phage display (70,73-75). By giving patients partial or fully human antibodies, there is little or no immune response, which gives the antibodies more time to exert their effect.

Other designs in antibody engineering strive to improve therapeutic efficacy by designing smaller antibody constructs, by altering the half-life of an antibody, or by conjugating antibodies to toxic payloads to enhance the cytotoxic effect (67,76). For example, smaller antibody constructs are able to penetrate deeper into a tumor mass (77). In addition, improving the avidity of an antibody or increasing binding of the antibody to the neonatal Fc receptor (FcRn) can prolong the length of time an antibody will remain at a tumor site or in the circulation (78). Conversely, decreasing the length of time in the circulation is advantageous when conjugating antibodies to radionucleotides, for example, because of their rapid clearance from the body, thus limiting whole body exposure to the radioactive isotope (67). The ability to genetically enhance the performance of monoclonal antibodies will greatly impact their future success.

FDA-Approved "Naked" Monoclonal Antibodies

Rituxan

Rituxan, also known as rituximab, recognizes CD20 on B cells and is a chimeric antibody approved for the treatment of non-Hodgkin's lymphoma

(68,76). Rituxan exerts its therapeutic effect by inducing antibody dependent cell cytotoxicity (ADCC), complement dependent cytotoxicity (CDC), and apoptosis of CD20+ cells. Clinical studies demonstrate that about half of all patients with low-grade non-Hodgkin's lymphoma respond to 4 doses of Rituxan therapy at a dose of 375 mg/m^2. In addition, patients with relapsed or refractory non-Hodgkin's lymphoma demonstrated a 31% overall response rate (67,79).

Rituxan demonstrates greater efficacy when given in combination with chemotherapy. The combination appears to have a synergistic effect and can reverse the sensitivity of chemo-resistant cells. In low grade and follicular non-Hodgkin's lymphoma, 95% of patients who received Rituxan plus cyclophosphamide, doxorubicin (an anthracycline) (80), vincristine, and prednisone (CHOP) responded, and there was no increase in toxicity compared to CHOP therapy alone. Rituxan is also currently being evaluated as maintenance therapy after high dose chemotherapy and autologous transplantation (67,81).

Herceptin

Herceptin, also known as trastuzumab, recognizes HER-2/neu (c-erbB-2), which is a member of the epidermal growth factor receptor (EGFR) family. It is a humanized antibody approved for the treatment of HER-2 positive metastatic breast cancer (67,76). Herceptin recruits effector cells, induces apoptosis, and decreases VEGF levels, leading to reduced angiogenesis (71). Studies have

demonstrated that 16% of patients with metastatic disease achieved an objective response and a median overall survival of 13 months, which was an improvement over the second line chemotherapy, and 30% of patients demonstrated stable disease. The combination of Herceptin and anthracycline chemotherapy increased response rates from 43% to 52% compared to the chemotherapy alone, and combination with a taxane regimen increased response rates from 16% to 42% and prolonged survival. Anthracyclines are cytostatic antibiotics that disrupt DNA structure, and taxanes inhibit cell mitosis by preventing tubulin dimer formation (34,67,68,82,83).

Campath

Campath, also known as alemtuzumab, is a humanized antibody approved for the treatment of chronic lymphocytic leukemia (76). Campath recognizes CD52 on B cells and T cells. In relapsed or refractory CLL, 42% of patients responded, and when tested as a first line therapy, all patients responded to Campath (67). Combinations of Campath with Fludarabine, which is an adenosine analog that inhibits adenosine deaminase (34,84), significantly increased the response rate in patients with refractory disease. The biggest concern with Campath therapy is the immunosuppression it causes, which can lead to reactivation of cytomegalovirus or Epstein-Barr virus. Campath is also being evaluated for the therapy of non-Hodgkin's lymphoma and for the depletion of B and T cells in donor grafts in allogeneic transplants (67,85).

Avastin

Avastin, also known as bevacizumab, recognizes VEGF and is a humanized antibody approved for the treatment of colorectal cancer. Avastin exerts its therapeutic effect by inhibiting neovascularization of the tumor. Although Avastin shows a modest effect as a single agent, it is primarily used in combination with irinotecan, 5-Fluorouracil (FU), and leucovorin (LV). Irinotecan targets replicating cells by preventing the repair of single strand nicks in the DNA (86); 5-FU inhibits DNA synthesis at all stages of replication; and LV (folate) raises the folic acid level (87,88). When these agents were given in combination, patients demonstrated a 20.3 month median survival verses 15.6 months in patients receiving chemotherapy alone, and the combination prolonged the progression-free survival and overall response. Toxicities from Avastin have not been substantial, but there was an increased incidence of bleeding, thromboembolism, and hypertension (89).

Erbitux

Erbitux, also known as cetuximab, is a chimeric antibody approved for the treatment of advanced colorectal cancer. It recognizes the extracellular domain of the EGFR and blocks epidermal growth factor (EGF) signaling. In addition, studies demonstrate that Erbitux blocks the production of VEGF, IL-8, and bFGF. As a single agent, 10.5% of patients with relapsed or refractory disease

responded and 36.8% demonstrated stable disease. When given in combination with irinotecan chemotherapy, the response rate doubled to 22.9% and the time to progression increased from 45 days to 126 days. The predominant side-effect of Erbitux is an acneiform rash, which correlated with a positive prognosis. Other toxicities were mild and included asthenia, fever, nausea, and allergic reactions (2,89).

C. Developing a New Therapy

The Generation of UV3

UV3 was developed in an effort to create a specific monoclonal antibody for the therapy of multiple myeloma. BALB/c mice were immunized once a month with alternating intraperitoneal injections of human multiple myeloma cell lines RPMI-8226 and U-266. Three days after the last injection, spleen cells from the immunized mice were fused with (SP2/0) mouse myeloma cells, and hybridomas that strongly reacted with the human multiple myeloma cell lines were further subcloned. Supernatants were screened by enzyme-linked immunosorbent assay (ELISA) and fluorescently activated cell sorting (FACS) to identify which clones produced an antibody that specifically recognized multiple myeloma cells. The antibody was purified by affinity chromatography on a protein G agarose column, and an ELISA was used to determine the isotype of the antibody, which was IgG_{2a}. The UV3 antibody was used to immunoprecipitate its antigen. The

antigen was an 83 kD protein that corresponded to the common intracellular adhesion molecule (ICAM-1), or CD54 (90,91).

In order to confirm the identity of the antigen, the ability of UV3 to bind to CD54 on various CD54 positive and negative cell lines was evaluated by flow cytometry. UV3 recognized and bound to an endothelial cell line known to be positive for CD54, and it recognized Chinese hamster ovary cells (CHO) transfected with CD54. UV3 did not, however, recognize and bind to non-transfected CHO cells, nor did it recognize a known CD54 negative human endothelial cell line. Studies also determined that UV3 recognizes **human** CD54, but not **mouse** CD54 (90).

The Therapeutic Success of UV3 in SCID Mice with Human Multiple Myeloma

The therapeutic success of UV3 was evident in both early and advanced disease. Severe combined immunodeficient (SCID) mice were irradiated and injected intravenously with human ARH-77 multiple myeloma cells and treatment was initiated either 1 day (early disease) or 15 days (advanced disease) following tumor cell injection. Mice with early disease received 0.8 μg/g of UV3 or an isotype-matched control antibody, and mice with advanced disease received 4 μg/g of UV3 or an isotype-matched control. By day 35 following tumor cell injection, mice receiving treatment with PBS or an isotype-matched control antibody developed hind-leg paralysis as a result of the growing tumor. However, tumor-bearing mice treated with UV3 in the early stages of disease

survived for 150 days at which point the experiment was terminated. Mice receiving UV3 in advanced stages of disease, survived for over 124 days following tumor cell injection at which point the experiments were terminated (92,93). This suggested not only that UV3 significantly prolonged the survival of mice with ARH-77 multiple myeloma, but UV3 accomplished its therapeutic effect at very low doses (67,92).

D. CD54 (ICAM-1)

Structure

CD54 is also known as ICAM-1, which is an abbreviation for immunoglobulin-like cell adhesion molecule. CD54 belongs to the immunoglobulin supergene family, and it is a transmembrane glycoprotein with 5 immunoglobulin-like domains and a charged cytoplasmic tail. The molecular weight of CD54 varies due to differentially glycosylated forms, and its surface distribution is thought to be regulated by the cytoskeleton (94-96).

Expression

CD54 is expressed on endothelial cells, epithelial cells, fibroblasts, leukocytes, and tumor cells. The expression of CD54 is regulated by a number of various cytokines, steroid hormones, and physical factors. Prominent inducers of CD54 expression include TNF-α, interferon gamma (IFN-γ), and IL-1, and

glucocorticoids are important inhibitors of expression. IL-6, an important cytokine in the progression of multiple myeloma, assists in the regulation of CD54 transcription, along with NFkB. CD54 expression is regulated differently by each cell type, and the regulation of CD54 can depend on the differences in post-transcriptional machinery, the activity of glycosylation enzymes, the availability of transcription factors and receptors for extracellular signaling, and signal transduction pathways. With the majority of its expression regulated by *in vivo* factors, the role of CD54 expression in normal and disease states is difficult to elucidate *in vitro* (94,97,98).

Function

CD54 binds to the integrins lymphocyte function-associated antigen (LFA-1) and Macrophage-1 (Mac-1), CD43, rhinoviruses and coxsackie viruses, and to soluble fibrinogen. The affinity of CD54 for its target can be altered due to conformational changes resulting from the phosphorylation of the cytoplasmic domain, a negative molecular charge possibly resulting from an increase in sialic acid residues, or differentially glycosylated forms of CD54. All of these variations result in cell-specific ways that CD54 aids in cell-cell adhesion, cell signaling, cell migration, and the co-stimulatory activation of NK cells and cytotoxic T cells (94, 98-102).

In addition to the membrane(m) bound version of CD54, a soluble(s) version of CD54 also exists (103). Much is still unknown about the role and

regulation of sCD54 and the functional relationship between sCD54 and mCD54. The levels of sCD54 do not necessarily correlate with mCD54, and various isoforms of sCD54 have been detected. sCD54 can compete with mCD54 for ligand binding, and sCD54 has been specifically implicated as playing a role in a number of diseases (104-108).

Pathophysiology

The role of CD54 as a regulator of inflammatory and immune responses in the pathology of a variety of diseases is under investigation. Expression is upregulated in a number of autoimmune and inflammatory diseases (109), such as multiple sclerosis, atherosclerosis, and asthma. The importance of CD54 in inflammation is demonstrated, in part, by the use of glucocorticoids in asthmatic inhalers, which lower CD54 expression levels. As a receptor for rhinoviruses, CD54 is involved in the response to a majority of the common colds, and CD54 aids in organ transplant rejection (110). In malignancy, CD54 expression can be elevated or reduced, depending on the tumor type. In general, a reduced expression of CD54 correlates with an aggressive, more malignant disease, which is probably due to reduced recognition of the tumor by the immune system (111-113). Conversely, high levels of CD54 expression have been found on some tumor cells, such as multiple myeloma (114) and melanoma (115), but the presence of increased sCD54 may compete for ligand binding and interfere with immune recognition (106,112,116-118).

E. Determining the Mechanism of Action of UV3

In vivo studies demonstrated the therapeutic success of UV3 in both early and advanced stages of multiple myeloma (92). However, given the multiple functional activities of CD54 and the variability in its expression and regulation, the mechanism of action of UV3 was unknown. Studies performed to understand UV3's mode of action revealed that UV3 did not interfere with either homotypic tumor cell adhesion or the adhesion of tumor cells to stromal cells; it did not inhibit proliferation or induce apoptosis; and, because $F(ab)'_2$ fragments of UV3 showed some efficacy in treating multiple myeloma, it was concluded that though the Fc played a role in UV3's anti-tumor activity, it was not solely responsible for UV3's anti-tumor effect (92). With these possibilities excluded, the search began for other possible anti-tumor effects of UV3. Based on the role of UV3 in adhesion and inflammation (94), the ability of sCD54 to induce angiogenesis *in vitro* and *in vivo* (104), and the influence of angiogenic cytokines on CD54 expression (119), it was hypothesized that UV3 interfered with angiogenesis in the murine model of multiple myeloma.

F. Angiogenesis

Angigogenesis is a remodeling process that involves the sprouting of new blood vessels from pre-existing ones. It is essential for normal development, tissue regeneration, and remodeling, and in adults, it primarily occurs in the

female reproductive system, in wound healing, and in disease. The disregulation of angiogenesis is a component of a number of pathological conditions. The absence of angiogenesis contributes to conditions such as limb ischemia and ulcers, but the presence of increased angiogenesis contributes to disease progression in psoriasis, rheumatoid arthritis, and cancer (120-122).

The angiogenesis cascade involves a number of steps, each of which is regulated by a variety of factors. First, there is an increase in the local production of growth factors prompted by the tumor cells and their microenvironment. This stimulates an increase in proteases, such as matrix metalloproteinases, which degrade the basement membrane. Endothelial cells can then migrate toward the angiogenic stimulus, which is further influenced by cell adhesion molecules, and endothelial cell proliferation is induced. These steps are followed by the tube formation by the endothelial cells and remodeling of the vasculature to a more mature state (123-125).

Angiogenesis in Cancer Progression

Angiogenesis is critical to the growth and development of a tumor (126,127). In order for a tumor to expand and metastasize, it needs a vascular network that will expand with the tumor to provide oxygen and other nutrients. There are a number of promoters and inhibitors that regulate angiogenesis in a healthy host, and the combination of upregulating promoters and downregulating inhibitors leads to an ‘angiogenic switch’ (123). Promoters of angiogenesis

include growth factors and cytokines, such as the VEGF family or IL-8, serine proteases and metalloproteinases, integrins, and extracellular matrix proteins, such as fibrin (128-130). Natural inhibitors of angiogenesis include proteolytically cleaved products of extracellular matrix proteins, such as angiostatin and endostatin, cytokine antagonists, such as angiopoietin-2, and cytokines, such as IL-12 and IFN-α (124,129,131).

Previously, it was thought that the initiation of tumor angiogenesis was responsible for turning a dormant tumor into a progressive one (132). However, there are highly vascularized benign tumors, such as adrenal adenomas, and recent studies reveal the importance of genetic and environmental factors in initiating tumor progression. Genes that influence cell growth, senescence, differentiation, and neoplastic transformation play a role in both the angiogenic switch and in tumor progression. In addition, stress factors such as hypoxia, low pH, and iron deficiencies also play a role (126,133,134).

Anti-Angiogenesis Therapy

Angiogenesis inhibitors are an important asset in the therapy of malignant disease. They are less-toxic; they are able to affect chemotherapy-resistant tumor cells; tumor cells are less likely to develop resistance to the therapy; and, they can be used in combination with chemotherapy or other anti-angiogenic agents in an effort to target the tumor *via* multiple pathways (133). Anti-angiogenesis strategies target growth factors, growth factor receptors, receptor

tyrosine kinase activity, endothelial cell proliferation, and endothelial cell adhesion molecules (131,135-138). The clinical development of many angiogenesis inhibitors is under development. Giving angiogenesis inhibitors in combination with other types of therapy is advantageous. Both Avastin, an inhibitor of VEGF, and Erbitux, an inhibitor of EGFR signaling, improved survival when given in combination with chemotherapy to patients with colorectal cancer (89). In addition, the use of thalidomide in combination with dexamethasone, which is a corticosteroid with immunosuppressive and anti-inflammatory properties, is beneficial as maintenance therapy for multiple myeloma (42,55).

G. Objectives

The objectives of this study were as follows: 1) to determine whether ARH-77 cells expressed angiogenic genes and whether the trait is characteristic of ARH-77 cells only or of other multiple myeloma cell lines, 2) to determine whether ARH-77 cells secreted angiogenic proteins, 3) to determine whether the angiogenic proteins would affect endothelial cell growth and proliferation, 4) to determine whether UV3 would block this cascade of angiogenic events by interfering with angiogenic gene expression, protein secretion, or by binding soluble angiogenic proteins, 5) to determine whether there is evidence *in vivo* of a reduced vascular supply in UV3-treated SCID/ARH-77 mice, and 6) to re-evaluate the role of the Fc portion of UV3 in mediating anti-tumor activity.

Materials and Methods

A. Cell culture

Human Multiple Myeloma Cell Lines

ARH-77, U-266, RPMI-8226, IM-9, HS-Sultan, and SKO-007

The human multiple myeloma cell lines ARH-77 (American Type Culture Collection CRL-1621, Manassas, VA)(139), U-266 (American Type Culture Collection TIB-196)(140), RPMI-8226 (American Type Culture Collection CCL-155)(141), IM-9 (American Type Culture Collection CCL-159)(142), HS-Sultan (American Type Culture Collection CRL-1484)(143), and SKO-007 (American Type Culture Collection CRL-8033-1)(144) were cultured at 5 x 10^5 cells/ml in RPMI-1640 medium (Sigma-Aldrich, St. Louis, MO) containing 10% heat-inactivated fetal calf serum (FCS) (HyClone, Logan, Utah), 2 mM L-glutamine (GIBCO/Invitrogen, Carlsbad, CA), 100 U/ml penicillin (GIBCO), and 0.1 mg/ml streptomycin (GIBCO) (complete medium). All cells were cultured at 37°C, 5% CO_2/95% air.

ILKM-2 and ILKM-3 Cell Lines

The ILKM-2 and ILKM-3 human multiple myeloma cell lines (gifts from Dr. Shiro Shimizu, Ishikawa, Japan)(145) were cultured at 5 x 10^5 cells/ml in RPMI-

1640 medium containing 10% FCS, 2 mM L-glutamine, 100 U/ml penicillin, 0.1 mg/ml streptomycin, and 2 ng/ml IL-6 (Sigma-Aldrich) (complete medium). The cells were cultured at 37°C, 5% CO_2/95% air.

MC/CAR Cell Line

The human multiple myeloma cell line MC/CAR (American Type Culture Collection CRL-8083)(146), was cultured at 5 x 10^5 cells/ml in IMDM medium (GIBCO) containing 20% FCS, 2 mM L-glutamine, 100 U/ml penicillin, and 0.1 mg/ml streptomycin (complete medium). The cells were cultured at 37°C, 5% CO_2/95% air.

NCI-H929 Cell Line

NCI-H929 (American Type Culture Collection CRL-9068)(147), human multiple myeloma cells were cultured at 5 x 10^5 cells/ml in RPMI-1640 medium containing 15% FCS, 4 mM L-glutamine, 100 U/ml penicillin, 0.1 mg/ml streptomycin, 10 mM Hepes buffer (GIBCO), and 1 mM sodium pyruvate (GIBCO) (complete medium). Cells were cultured at 37°C, 5% CO_2/95% air.

Daudi Human Burkitt's Lymphoma Cell Line

The Daudi human Burkitt's lymphoma cells (American Type Culture Collection CCL-213)(148) were cultured at 5 x 10^5 cells/ml in RPMI-1640 medium (Sigma-Aldrich) containing 10% heat-inactivated fetal calf serum

(HyClone), 2 mM L-glutamine (GIBCO/Invitrogen), 100 U/ml penicillin (GIBCO), and 0.1 mg/ml streptomycin (GIBCO) (complete medium). Cells were cultured at 37°C, 5% CO_2/95% air.

UV3 and 13G10 Hybridoma Cell Lines

Hybridoma cells secreting the murine anti-CD54 (intracellular adhesion molecule, ICAM-1) antibody (90) and hybridoma cells secreting the IgG_{2a} isotype control 13G10 against the syphilis causing bacterium *Treponema Pallidum* (a gift from Dr. Michael Norgard at UTSW Medical Center, Dallas, TX) (149) were grown at 5 x 10^5 cells/ml in DMEM medium (Sigma-Aldrich) containing 10% FCS and 2 mM L-glutamine (complete medium). Cells were initially cultured in 150 mm^3 tissue culture flasks (BD Falcon, Bedford, MA) at 37°C, 5% CO_2/95% air. Cells were then transferred to 2 L roller bottles (Fisher) and passaged 1:10. The bottle caps were unscrewed a quarter of a turn, and the bottles were placed at 37°C, 5% CO_2/95% air for 24 hours. Bottle caps were screwed tightly, and roller bottles were incubated for 7 days at 37°C.

Human Umbilical Vein Endothelial Cells (HUVECs)

HUVECs (Cascade Biologics, Portland, OR) were purchased cryopreserved at the end of primary culture and were grown in Medium 200 (Cascade Biologics, Portland, OR) containing low serum growth supplement (Cascade Biologics, Portland, OR) (complete medium). HUVECs were harvested using a Trypsin-

ethylene diamine tetraacetic acid (EDTA) solution (Cascade Biologics, Portland, OR), and the activity of the trypsin was inhibited with a Trypsin Neutralizer solution (Cascade Biologics, Portland, OR). HUVECs were harvested, cultured, and frozen according to company instruction. Cells were cultured for no more than 16 population doublings, and the cells were seeded at 2500 cells/cm2 following each passage. Cells were maintained in a humidified, 37°C, 5% CO_2/95% air incubator (Forma Scientific).

B. In Vitro Antibody Treatment

When any cell type received antibody treatment, the selected cells were first centrifuged (RC3C Sorvall Centrifuge, DuPont, Wilmington, DE) in a 50 ml conical tube (BD Falcon) at 4°C, 300 x g for 10 min. The cells were resuspended in their corresponding complete medium without FCS at 5 x 10^5 cells/ml and centrifuged at 300 x g for 10 min at 4°C to wash the cells. Finally, the cells were resuspended at 5 x 10^5 cells/ml in their respective, complete medium. Five milliliters of cells, or 25 x 10^5, were seeded in a 25cm^2 tissue culture flask (BD Falcon), with one flask for each treatment condition. One flask was set aside as an untreated control sample. Cells cultured with UV3 or the isotype control antibody received 100ug of affinity purified antibody per 5 x 10^5 cells. The antibody was suspended at a high concentration (≥3 mg/ml) in a PBS solution so that the cell medium would not be diluted when the antibody was added to the cell culture. The cells were incubated at 37°C, 5% CO_2/95% air for 24 or 48 hours.

C. Antibody Production

UV3

Approximately 250L of hybridoma cells secreting UV3 were grown for this project. The cells were centrifuged in a Sorvall RC3B Centrifuge (DuPont) at 1850 x g for 30 minutes at 4°C to remove cells and debris. The cell supernatant was poured into clean, two liter roller bottles (BD Falcon), and a PBS-azide solution (0.005% final concentration) was added to the supernatant to prevent contamination. The supernatant was passed over 25 milliliters of protein-G sepharose (Amersham Biosciences) in a 2.5 cm x 10 cm column (BioRad, Hercules, CA) at a rate of 3 ml/minute at 4°C. With a hybridoma culture yield of 15-20 mg/L, a column could purify up to 160 mg of the UV3 antibody (6-8L). The flow through from the hybridoma supernatant was collected at 4°C and stored for a second passage over a cleaned column at a later time. Following the processing of 6-8L of hybridoma supernatant, the column was washed with 300 ml of PBS. The protein was eluted with 0.1M Glycine-HCl, pH 2.8, until all the antibody had been eluted. This was determined by following the peaks on the fraction recorder. When a flat line appeared after a tall peak and the $O.D._{280}$ of the eluate was less than 0.075, the elution of the protein was stopped. Three milliliter fractions of the eluted protein were collected in 12x75mm glass tubes (Fisher), containing 0.5 ml of 1.0M Tris-HCl, pH 8.0, and the fractions were analyzed by a Beckman DU-62 spectrophotometer. Fractions containing UV3

were pooled and dialyzed against PBS. UV3 was concentrated, 10 ml at a time, using a 50 ml Amicon Ultra Centrifugal Filter Device (Millipore, Bedford, Massachusetts), which excludes anything lower than 30,000 molecular weight. UV3 was dialyzed against PBS and filtered through a 150 ml, 0.22μm Stericup filter (Milipore).

cUV3

UV3 was chimerized (cUV3) by Dr. Joan Smallshaw (150). Using previously determined sequence data (Peter Hudson at WEHI, Melbourne, Austrailia, personal communication), primers were designed to PCR amplify the heavy and light variable domains of UV3, and these were cloned into a pUC18 utility vector. The sequence was checked for accuracy, and new primers were designed to modify the ends for insertion into the human γ_1 heavy and κ light chain expression vectors, pAH4604 and pAG4622 (provided by Dr. Sherrie Morrison, UCLA, CA)(151). The two constructs were co-transfected into SP2/0 cells, a non-secreting murine myeloma line (ATCC). Positive lines were selected by an ELISA assay when antibody from co-transfection supernatant was recognized by both an anti-heavy chain antibody, coating the bottom of the plate, and an anti-light chain antibody conjugated to alkaline phosphatase. When the nitrophenyl phosphate substrate solution was added, a yellow color developed to reveal which co-transfection supernatants contained the cUV3 antibody. cUV3 was grown and purified for our use in the RAID program by the Biological

Resources Branch of the Division of Cancer Treatment and Diagnosis at the National Cancer Institute.

Isotype Control

The 13G10 antibody was grown, collected, and purified in the same way as the UV3 antibody, as described.

D. F(ab)'$_2$ production and purification

F(ab)'$_2$ Production

One hundred to one hundred fifty milligrams of UV3 was dialyzed for 5 hours at 4°C against an acetate buffer, pH 3.7-3.8 (1760 ml of 0.2 M acetic acid and 240 ml of 0.2 M sodium acetate). The dialyzed UV3 was transferred to clean, 50 ml conical tubes (BD Falcon), and for each 100 mg of UV3 to be digested, 25 mg of pepsin (Sigma) was added to the tube. The UV3-pepsin solution was incubated for 17 hours on a Labquake™ Shaker (Barnstead/Thermolyne) at 37°C, after which electrophoresis was used to examine the F(ab)'$_2$ fragments before purification.

PhastGel System

A 20 µl sample of the digest was taken for electrophoresis on a PhastGel™ (Amersham Biosciences, Piscataway, NJ) under reducing and non-reducing conditions to examine the relative levels of the F(ab)'$_2$ fragments. Samples (10 µl) were mixed 1:1 with either reducing (1.25 ml 1.0 M Tris-HCl, pH 6.8, 4 ml 10% sodium dodecyl sulfate, 1.0 ml 2-mercaptoethanol, 2.0 ml glycerol, 1.25 ml distilled water, 0.5 ml of 0.1% Bromophenol Blue) or non-reducing buffer (reducing buffer without 2-mercaptoethanol) and heated in a 100°C heat block for 3 minutes. Three microliters of each sample was pipetted onto a strip of parafilm that covered a sample well mold. Capillary action drew 1 µl of each

sample into the teeth of the loading comb, which was then transferred to the comb slot in the gel holder. Samples were analyzed on 4-15% SDS Page gels using the PhastSystem (Amersham Biosciences). Samples were electrophoresed for 30 minutes until the voltage reached 65V. The gels were removed from the separation and control unit, which operates the electrophoresis, and transferred to the development unit for the staining and destaining process. PhastGels (Amersham Biosciences) were stained with PhastGel™ Blue R (Amersham Biosciences) and destained according to set programming for Coomassie Blue stains (5 minutes, 8 minutes, and 10 minute washes) with a 10% acetic acid, 30% methanol, and distilled water solution.

F(ab)'$_2$ Purification

The 50 ml conical tube of digested UV3 (containing IgG, F(ab)'$_2$, and Fab' fragments) was removed from the shaker and centrifuged at 2500 x g for 10 minutes at 4°C to pellet the pepsin. The supernatant was poured into to a clean 50 ml conical tube (BD Falcon), and 1.0 M Tris-HCl was added to bring the pH to 7-7.5. The digest was then dialyzed against PBS.

The UV3 digest, at 100 mg or less, was passed over a 1 ml (100 mg packed volume) HiTrap™ Protein A column (Amersham Biosciences) at a rate of 1 ml per minute to eliminate any remaining IgG. The column capacity was 20 mg of IgG. The flow through from the column and the wash, which contained the F(ab)'$_2$ fragments, were saved. The column was eluted with 10 ml of 0.1 M

glycine-HCl, and the eluate was collected and analyzed by spectrophotometry (Beckman) to determine whether there was any loss. The eluate was discarded when it contained less than 1 mg, or 1% of the digest, of IgG.

F(ab)'$_2$ Purification by HPLC

F(ab)'$_2$ fragments from the protein A column were concentrated using a 50 ml Amicon Ultra Centrifugal Filter Device (Milipore), which excludes anything with a molecular weight of less than 30,000, to 15-20 mg/ml (maximum 10 ml volume) in PBS. The concentrated 10 ml sample in PBS was loaded onto an HPLC column (LKB Bromma) run with PBS at a flow rate of 5 ml per minute. One ml fractions were collected into clean, borosilicate glass tubes (Fisher). A fraction recorder monitored the amount of protein eluting from the column. The fractions were analyzed by spectrophotometry (Beckman DU-640) to identify which of the collected tubes corresponded to which peaks. Using the PhastGel™ System (see above), electrophoresis of fractions within each peak revealed whether a peak corresponded to IgG, F(ab)'$_2$, or Fab' fragments. Two peaks appeared on the fraction recorder correlating with F(ab)'$_2$ fragments (major peak) and Fab' fragments (secondary peak). Fraction tubes containing the F(ab)'$_2$ fragments were pooled, and the F(ab)'$_2$ sample was concentrated using an Amicon Ultra Centrifugal Filter Device (Milipore) to 5-10 mg/ml and filtered for use with a Millex®-GS 0.22µm syringe filter unit.

A sample of the final, "ultra-pure F(ab)'$_2$" was analyzed on a PhastGel™ (Amersham Biosciences, see above for details) for viewing. The gel was scanned using a LKB UltraScan XL (Pharmacia/Pfizer, New York, NY) which took the scanned image and translated it into a graph of peaks corresponding to the number and size of the bands in the gel. The area under each peak was calculated using GelScan-XL (Pharmacia), and the values obtained corresponded to the relative amount of UV3 IgG, F(ab)'$_2$, and Fab'. A F(ab)'$_2$ preparation was considered to be ultra-pure when the IgG was less than 1% of the total preparation and the amount of Fab' fragments were less than 10%.

E. RNA Isolation

TRIzol Total RNA Isolation

Cells were collected, counted, and centrifuged at 300 x g for 10 minutes at 4°C. One milliliter of TRIzol (Invitrogen, Carlsbad, CA) was added for 5-10 x 10^6 cells in a 1.5 ml RNase-free eppendorf tube. Cells were lysed by repetitive pipetting through 5 repetitions and incubated for 5 minutes at room temperature. For each ml of TRIzol added, 0.2 ml of chloroform (Sigma) was added. The sample was mixed by shaking by hand for 15 seconds and incubated for 2-3 minutes at room temperature. The sample was centrifuged (Eppendorf Centrifuge 5417C) at 12,000 x g for 15 minutes at 4°C. The top, aqueous phase was removed with a 200 µl pipetman and transferred to a new 1.5 ml RNase-free eppendorf tube. The RNA was precipitated by adding 0.5 ml of isopropanol (Sigma) for each ml of TRIzol used, and the sample was incubated for 10 minutes at room temperature. The sample was centrifuged at 12,000 x g for 10 minutes at 4°C. The supernatant was discarded, and the pellet was resuspended in 1 ml of 75% ethanol for each ml of TRIzol used. The sample was centrifuged at 7500 x g for 5 minutes at 4°C. The supernatant was discarded, and the sample was air-dried. The RNA was dissolved in 100 µl of DEPC-water and quantitated on a spectrophotometer (Beckman Coulter, Inc., Fullerton, CA).

Samples were treated with DNase using Ambion's DNA-free kit (Ambion, Inc., Austin, TX) and accompanying protocol. 10x DNA-free buffer was added to the RNA sample at 1/10 of the RNA volume. For each ≤100 µl sample of RNA, 1 µl of DNA-free enzyme was added. The sample was vortexed and incubated for 25-30 minutes at 37°C. The DNase Inactivation Reagent was vortexed and added at 1/10 of the total volume, and the sample was incubated for 2 minutes at room temperature and mixed by vortexing it after each minute. The sample is centrifuged for 1 minute at 10,000 x g to pellet the DNase Inactivation Reagent. The sample, minus the pellet, was transferred to a 1.5 ml RNase-free tube with a pipetman, and the RNA was stored at -80°C.

F. Gene arrays

SuperArray, Inc. Membrane Arrays

Angiogenesis-1 and Angiogenesis-2 GEArray™ kits were purchased from SuperArray, Inc. Each kit contains two identical nylon membranes spotted with angiogenesis-specific cDNA fragments. Total RNA was isolated using the TRIzol reagent with the protocol described above. The microarray assay was performed according to kit instructions: pre-hybridization of the membrane, cDNA synthesis, and hybridization of the cDNA probe to the membrane.

Pre-hybridization

15 ml of hybridization solution (kit component), in a 15 ml conical tube, was warmed to 68°C in a water bath (Precision). 155 µl of salmon sperm DNA (Sigma) was added to a 0.5 ml eppendorf tube and heated to 100°C using a DeltaCycler II™ (Ericomp) thermal cycler. After 5 minutes, the salmon DNA was placed on ice, and 151.5 µl of the denatured DNA was added to the 15 ml of hybridization solution. The nylon membrane microarray was moistened with distilled, deionized water and placed in a 35 x 150 mm glass hybridization tube (Fisher Scientific, Hampton, NH). For pre-hybridization of the membrane, 10 ml of the hybridization solution was added to the tube, and the tube was placed in an Isotemp Hybridization oven (Fisher Scientific) set at 68°C, 5-10 rpm for 1-2 hours.

cDNA synthesis

One to five micrograms of the sample RNA was added to a 0.5 ml RNase-free eppendorf tube and mixed with 2 µl of the kit primer mix (buffer A) and RNase-free water to a volume of 20 µl. In a second 0.5 ml RNase-free eppendorf tube, the following reagents were added and mixed: 8 µl of kit labeling buffer (buffer B), 1 µl RNase inhibitor, 2 µl Moloney Murine Leukemia Virus (MMLV) Reverse Transcriptase (Promega, Madison, WI), and 4 µl of kit RNase-free water. The tube containing the RNA was placed in a thermal cycler (Ericomp) at 70°C for 2 minutes, followed by 2 minutes at 42°C. The second tube containing the labeling mix received 5 µl of ^{32}P during the RNA incubation at 70°C. It was then added to the thermal cycler for the 42°C incubation to warm the solution to the same temperature as the RNA. After 2 minutes at 42°C, the labeling mix (20 µl) was added to the RNA and further incubated at 42°C for 25 minutes. Five microliters of stop solution (buffer C) and 5 µl of denaturing solution (buffer D) were added after the 25 minute incubation, and the sample was incubated at 68°C for 20 minutes. Finally, 50 µl of neutralization solution (buffer E) was added, and the sample was incubated for 10 minutes at 68°C.

Hybridization

The radiolabeled cDNA probe (100 µl) was added to the remaining 5 ml of hybridization solution. The pre-hybridization solution was discarded, and the

cDNA probe was added to the membrane. The membrane array was incubated overnight in the hybridization oven at 68°C, 5-10 rpm.

Wash

Wash solutions were prepared according to kit instructions, as follows: 1) 10 ml of 20x saline-sodium citrate (SSC) (175.3 g NaCl, 88.2 g Na_3Citrate.2H_2O, water to 1 L), 5 ml of 20% sodium dodecyl sulfate (SDS) and 85 ml of distilled, deionized water; 2) 0.5 ml of 20x SSC, 2.5 ml of 20% SDS, and 97 ml of distilled, deionized water. The hybridization solution containing the cDNA probe was discarded. Half of the first wash solution was added to the membrane array, and the array was incubated at 68°C and rotated at 10 rpm for 20 minutes for the first wash. This wash was discarded, and the step was repeated 3 times, first with the remaining wash solution 1, followed by 2 washes with wash solution 2.

Data Acquisition

The membrane array was removed from the hybridization oven and covered in Glad® Cling Wrap (Oakland, CA). It was placed in a cassette for exposure to a Phosphor Screen (Molecular Dynamics/Amersham Biosciences, Piscataway, NJ) overnight. The screen was scanned using a Storm Phosphoimager (Molecular Dynamics/Amersham Biosciences), and the image was analyzed by ImageQuant (Molecular Dynamics/Amersham Biosciences). The expression of a gene correlated directly with the intensity of radioactivity,

which was reflected in the computer image by the darkness of the spot. The degree of expression of a particular gene was determined relative to the intensity of expression of the positive control genes (β-Actin and GAPDH) printed on the array.

Microarray Core Spotted, Microchip Arrays

RNA was isolated using the TRIzol isolation method described above. cDNA was synthesized and purified by the Microarray Core. The control ARH-77 cell cDNA was labeled with Cy-3, and the UV3-treated ARH-77 cell cDNA labeled with Cy-5. The labeled probes were hybridized to a human 22K oligo microarray chip, and the data were analyzed using GenePix Pro 3.0 (Axon/Molecular Devices Corp., Sunnyvale, CA).

cDNA synthesis

Five micrograms of RNA was diluted to 10 µl with nuclease-free water in a 0.5 ml RNase-free eppendorf tube. One microliter of T7-d24 primer was added, and the sample was incubated for 10 minutes at 70°C. First Strand master mix was made as follows: 4 µl of 5x First Strand Buffer, 1 µl of 10 mM mix of deoxynucleoside triphosphates (dNTP), 2 µl of 100 mM dithiothreitol (DTT), 1 µl of Superscript II reverse transcriptase, and 1 µl of Rnase Inhibitor. Nine microliters of this first strand master mix was added to the RNA, and the sample was incubated for 2 hours at 42°C. The samples were then placed at 4°C.

Second Strand Master Mix was made as follows: 20 µl of 5X second strand buffer, 3 µl of 10 mM dNTP mix, 51 µl of nuclease free water, 4 µl of DNA polymerase I, 1 µl of *E. Coli* DNA ligase, and 1 µl of Rnase H. Eighty microliters of this second strand master mix was added, and the sample was incubated for 2 hours at 16°C. One microliter of T4 DNA Polymerase was added, and the sample was incubated for 10 minutes at 16°C. Finally, 10 µl of 0.5M EDTA was added to inhibit all DNA working enzymes.

cDNA Purification

The cDNA was transferred from a 0.2 ml RNase-free eppendorf tube to a 1.5 ml DNase-free eppendorf tube. Fifty microliters of nuclease-free water was added, followed by 600 µl of cDNA binding buffer. The tube was vortexed for 3 seconds, at which point the mixture appeared yellow. Three hundred eighty microliters of the mixture was added to a cDNA Cleanup Spin Column (Qiagen), and the column was centrifuged at 8000 x g until the entire sample flowed through the column. The flow through was re-loaded onto the column and centrifuged again at 8,000 x g for 30 seconds. The flow through at this point was discarded. This process was repeated until all of the cDNA solution has passed over the column.

The column was transferred to a new 2.0 ml collection tube. The column was loaded with 750 µl of cDNA wash buffer, centrifuged at 8,000 x g for 30 seconds, and the flow through discarded. The cap was opened and the column

was centrifuged further at maximum speed (11,000-15,000 x g) for 5 minutes. The column was transferred to a new 1.5 ml collection tube, and 14 µl of nuclease-free water was added to the column. The elution buffer was allowed to remain on the column for 3 minutes at room temperature before being centrifuged at maximum speed for 1 minute. The column was discarded.

Antisense RNA (aRNA)

Eight microliters of cDNA was added to a 0.5 ml nuclease-free eppendorf tube. This was followed by 2 µl of each of the following reagents (Ambion MessageAmp aRNA kit): T7 adenosine triphosphate (ATP), T7 cytidine triphosphate (CTP), T7 guanosine triphosphate (GTP), T7 uridine triphosphate (UTP), T7 10x Reaction Buffer, and T7 Enzyme Mix. The contents of the tube were vortexed, and the tube was centrifuged. The sample was incubated at 37°C for 10 hours and then transferred to a 1.5 ml nuclease-free eppendorf tube and stored at 4°C.

The GeneChip Sample Clean-up Module (Affymetrix, Santa Clara, CA) was used to purify the aRNA. Sixty microliters of nuclease-free water was added to the sample. The sample was vortexed, centrifuged briefly, and 350 µl of aRNA binding buffer (included in the kit) was added. The tube was vortexed, centrifuged briefly, and 250 µl of 100% ethanol was added. The sample was mixed by pipetting, and the mixture was loaded onto the aRNA clean-up spin column (included in the kit). The column was centrifuged (Eppendorf) at

maximum speed at room temperature until the mixture had all flowed through the column. The flow-through was loaded onto the column two more times to ensure that all of the aRNA had been isolated. Five hundred microliters of aRNA wash buffer (included in the kit) was loaded onto the column, and the column was centrifuged at 8,000 x g for 30 seconds. The flow through was discarded, and the column was transferred to a new 2.0 ml collection tube (included in the kit). Five hundred microliters of 80% ethanol was added to the column, and the column was centrifuged at 8,000 x g for 30 seconds. The flow through was discarded, the cap on the column was opened, and the column was centrifuged at maximum speed for 5 minutes at room temperature to dry the column. The column was transferred to a new 1.5 ml collection tube (included in the kit), and 20 µl of nuclease free water, pre-heated to 60°C, was loaded onto the column. The column was incubated at room temperature for 3 minutes and centrifuged at maximum speed for 1 minute. This step was repeated with another 20 µl of pre-heated nuclease-free water. The column was discarded, and the flow through, containing the purified aRNA was quantified using a spectrophotometer.

Cy3/Cy5 labeling

The control ARH-77 cell aRNA and the UV3-treated ARH-77 aRNA were labeled with cyanine (Cy) -3 and Cy-5, respectively, using the Micromax ASAP™ RNA labeling kit (Perkin-Elmer, Boston, MA). For Cy-3 labeling, a 0.5 ml nuclease-free eppendorf tube received 2 µg of control aRNA, 5 µl of ASAP™

labeling buffer (included in the kit), 1 µl of ASAP™ Cy-3 reagent, and nuclease-free water up to 10 µl. For Cy-5 labeling, a second 0.5 ml nuclease-free eppendorf tube received 2 µg of aRNA from UV3-treated cells, 5 µl of ASAP™ labeling buffer, 1 µl of ASAP™ Cy-5 reagent, and nuclease-free water up to 10 µl. Each tube was mixed gently by vortexing and centrifuged briefly. The samples were incubated at 85°C for 15 minutes in a thermal cycler (Mini-cycler, MJ Research Inc., Reno, NV). The tubes were incubated on ice for 2.5 minutes, and 2.5 µl of the stop solution (included in the kit) was added.

The labeled probes were combined into a 1.5 ml nuclease-free eppendorf tube, and 450 µl of RNase-free 1x Tris-EDTA (TE) buffer (10 mM Tris, 1 mM EDTA, Sigma) was added. The mixture was vortexed and loaded onto the Amicon Microcone 30 column (Millipore). The column was centrifuged at 11,600 x g at room temperature for 8 minutes, and the flow-through was discarded. The column was loaded with 400 µl of RNase-free 1x TE buffer and centrifuging the column for 8 minutes. The column was inverted and transferred to a new 1.5 ml collection tube (included in the kit) and centrifuged at maximum speed for 2 minutes. The sample was dried in a vacuum to a volume less than 5 µl. The labeled probes were mixed with 50 µl of ASAP™ hybridization buffer (included in the kit) that had been pre-heated to 70°C for 5 minutes, and the mixture was hybridized to the microarray chip.

Data Analysis

Data were reviewed and evaluated using GenePix Pro 3.0. Data were normalized using the MarC-V software (152,153). Genes were selected that had been up-regulated or down-regulated by 2 fold or more as a result of treatment with UV3.

Affymetrix GeneChip Array

RNA Isolation

RNA was isolated using the RNeasy Lipid Tissue Mini kit (Qiagen, Valencia, CA). ARH-77 human multiple myeloma cells were treated with UV3 or 13G10 (isotype control) as described above. Five million cells from each of the antibody-treated cultures were collected in 50 ml conical tubes (BD Falcon) and centrifuged (Sorvall) at 300 x g for 10 minutes at 4°C. The cell supernatant was aspirated by vacuum suction with a glass pipet to remove the cell media. One milliliter of QIAzol lysis reagent was added to the tube, and the cells were lysed by plunging the cell suspension through a 20 gauge needle, 5 times. The homogenized sample was transferred to a 1.5 ml RNase-free eppendorf tube, and the sample was incubated for 5 minutes at room temperature. Two hundred microliters of chloroform (Sigma) were added to the tube, and the sample was vigorously mixed by shaking by hand for 15 seconds. The sample was incubated for 2-3 minutes at room temperature and centrifuged (Eppendorf Centrifuge) at

12,000 x g for 15 minutes at 4°C. The top, aqueous phase was removed using a 200 µl pipetman and transferred to a new 1.5 ml RNase-free tube. An equal volume of 70% ethanol (approximately 500 µl, Pharmco, Brookfield, CT) was added, and the RNA-ethanol solution was mixed well by pipetting. Seven hundred microliters of the solution was transferred to an RNeasy mini spin column (included in the kit) nested in a 2 ml collection tube (included in kit) and centrifuged (Eppendorf Centrifuge) at 8000 x g for 15 seconds at room temperature. The flow through was discarded, and the remaining RNA-ethanol solution was added to the column for a second centrifugation until all of the RNA had passed over the column.

The RNA was treated with RNase-Free DNase (Qiagen) while on the column, according to the RNA isolation kit instructions. Three hundred and fifty microliters of Buffer RW1™ (a wash buffer included in the kit) was added to the column to wash, and the column was centrifuged (Eppendorf Centrifuge) at 8000 x g for 15 seconds at room temperature. The flow through was discarded. Ten microliters of DNase 1 was added to a 500 µl RNase-free eppendorf tube and mixed with 70 µl of Buffer RDD™ (included in the kit) by pipetting. The mixture was added to the column and incubated for 15 minutes at room temperature. Following the incubation, the column was washed with 350 µl of Buffer RW1™ and centrifuged in an Eppendorf Centrifuge at 8000 x g for 15 seconds at room temperature. The flow through was discarded, and the column was transferred to a new, RNase-free eppendorf tube.

The column was washed with 500 µl of Buffer RPE™ (a wash buffer included in the kit) and centrifuged (Eppendorf Centrifuge) at 8000 x g for 15 seconds at room temperature. The flow through was discarded, and a second wash with 500 µl Buffer RPE™ was added. The column and tube were centrifuged in an Eppendorf Centrifuge at 8000 x g for 2 minutes at room temperature. The flow through was discarded, and the column and tube were centrifuged in an Eppendorf Centrifuge at room temperature for an additional 1 minute at 8000 x g. The RNeasy column was transferred to a new 1.5 ml RNase-free eppendorf tube. Twenty microliters of RNase-free water was added to the column, and the column was centrifuged in an Eppendorf Centrifuge at room temperature for 1 minute at 8000 x g. This step was repeated with an additional 20 µl of water and 1 minute centrifugation. The column was discarded, leaving ARH-77 RNA in an RNase-free eppendorf tube, in RNase-free water.

A 10 µl sample of the RNA was diluted 1:50 in RNase-free water and read in a spectrophotometer (Beckman) at an O.D.260 and an O.D.280. The A260/A280 ratio was used to determine the quality of the RNA. Pure RNA has an A260/A280 ratio of 1.8-2.1, and all ARH-77 RNA had a quality ratio $\geq$2. The quantity of the RNA was determined by the following equation: O.D.260 x 40 x dilution factor = the concentration in µg/ml.

cDNA Synthesis and aRNA Probe

The RNA was submitted to the Simmons Cancer Center Genomics Core (University of Texas Southwestern Medical Center) for preparation of biotin-labeled aRNA (Message Amp kit, Ambion). For first strand cDNA synthesis, 1-5 µg of total RNA was mixed with 1 µl of the T7-oligo (dT) (included in the kit) and RNase-free water up to 12 µl in a 0.5 ml RNase-free eppendorf tube. The sample was heated to 70°C for 10 minutes, spun briefly, and placed at 42°C. The sample was maintained at this temperature while adding the following reagents: 2 µl of 10x first strand buffer (included in the kit), 1 µl of RNase inhibitor (included in the kit), 4 µl of a dNTP mixture (included in the kit), and 1 µl of reverse transcriptase (included in the kit). The sample was mixed gently and incubated at 42°C for 2 hours.

The sample was centrifuged briefly and placed on ice, while the following reagents were added for second strand cDNA synthesis: 61 µl of RNase-free water, 10 µl of 10x second strand buffer (included in the kit), 4 µl of dNTP mixture, 2 µl of DNA polymerase (included in the kit), 1 µl of DNA Polymerase I (Invitrogen), 1 µl of E.coli DNA ligase (Invitrogen) and 1 µl of RNase H (included in the kit). The sample was mixed gently, centrifuged, and incubated at 16°C for 2 hours. The sample received 1 µl of T4 DNA Polymerase (Invitrogen) and was incubated for 10 minutes at 16°C. Finally, 10 µl of 0.5 M EDTA was added to inhibit all enzymes.

In order to purify the cDNA, the cDNA was transferred to a 1.5 ml RNase-free eppendorf tube containing 50 µl of nuclease-free water and 600 µl of cDNA binding buffer (included in the kit). The sample was vortexed, centrifuged, and 760 µl of the sample was loaded onto a column (included in the kit). The column was centrifuged at maximum speed until the entire sample has passed through. The column was transferred to a new 2.0 ml collection tube (included in the kit) and loaded with 750 µl of cDNA wash buffer (included in the kit). The column was centrifuged at 8,000 x g for 30 seconds at room temperature, and the flow-through was discarded. The caps of the columns were opened, and the columns were centrifuged at maximum speed for 5 minutes at room temperature. The column was transferred to a new 1.5 ml collection tube (included in the kit) and 11.5 µl of nuclease-free water was added onto the center of the column membrane. The column was centrifuged at maximum speed for 1 minute at room temperature, and the column was discarded.

Ten and a half microliters of the column flow-through, which contained the purified cDNA, was transferred to a new 0.5 nuclease-free eppendorf tube, and the following reagents were added to begin synthesis of biotin-labeled aRNA: 4 µl of T7 ATP (included in the kit), 3 µl of T7 CTP (included in the kit), 4 µl of T7 GTP (included in the kit), 3 µl of T7 UTP (included in the kit), 4 µl of T7 10x reaction buffer (included in the kit), 4 ul of T7 enzyme mix (included in the kit), 3.75 ul of biotin CTP (New England Biolabs, Beverly, MA), and 3.75 ul of biotin UTP (New England Biolabs). The sample was mixed gently, centrifuged briefly, and

incubated at 37°C for 10 hours. Two microliters of DNase I (included in the kit) was added to the tube, and the tube was spun briefly and incubated at 37°C for 30 minutes.

Using the GeneChip Clean-up Module (Affymetrix) to purify the aRNA, the sample was transferred to a 1.5 ml nuclease-free eppendorf tube containing 60 µl of nuclease-free water. The tube was vortexed, centrifuged, and 350 µl of aRNA binding buffer (included in the kit) was added. The tube was vortexed, centrifuged, and 250 µl of 100% ethanol was added. The solution was mixed gently by pipetting, and the 700 µl of mixture was loaded onto the column (included in the kit). The column was centrifuged at maximum speed until all of the mixture had flowed through the column. Five hundred microliters of aRNA wash buffer was loaded onto the column, and the column was centrifuged at 8,000 x g for 30 seconds at room temperature. The flow-through was discarded, and the column was transferred to a new 2.0 ml collection tube (included in the kit). Five hundred microliters of 80% ethanol was loaded onto the column, and the column was centrifuged at 8,000 x g for 30 seconds. The flow-through was discarded. The cap of the column was opened, and the column was centrifuged at maximum speed for 5 minutes to dry the column. The column was transferred to a new 1.5 ml collection tube (included in the kit), and 20 µl of RNase-free water, pre-heated to 60°C, was added to the center of the column membrane. The column was centrifuged at maximum speed for 1 minute. This wash step

was repeated a second time, and the flow-through was saved for quantification of the purified biotin-labeled aRNA.

Affymetrix hybridization

The aRNA probes were submitted to the Microarray Core (University of Texas Southwestern Medical Center) for processing and hybridization to Affymetrix human U-133 2+ microarrays (Affymetrix). Following fragmentation and hybridization of the biotinylated aRNA to the Affymetrix chip, the array was stained with streptavidin phycoerythrin and washed in the Affymetrix GeneChip fluidics station. The array was scanned using the GeneChip® Scanner 3000 (Affymetrix), and data were acquired with the GeneChip® Operating Software (Affymetrix), which normalized data prior to analysis.

Data Analysis

The resulting data were analyzed using GeneSpring (Silicon Genetics, Redwood City, CA). Data were normalized initially using the GeneChip® Operating Software (G-COS, Affymetrix), and further normalization of the data was performed in GeneSpring. Genes were selected for further evaluation based on a variety of criteria. The expression of the gene must be "present" (p value <0.05, as determined by comparison of results from multiple probes for a given gene) or "marginal" (p value 0.05-0.065) in at least one of the samples (control or treated). In addition, the gene expression must have changed 5 fold or more in

UV3-treated samples. Once these genes were selected, the data were searched for similarities in physiogical function using both GeneSpring and the Stanford Source program (154).

G. Polymerase Chain Reaction (PCR)

Semi-Quantitative PCR

cDNA synthesis

Cells were treated with antibody as described above, and RNA was isolated from cells according to the TRIzol protocol described above. The following reagents were added in a 0.5 ml RNase-free tube: 6 µl of Reverse Transcription 5x Buffer (Promega), 3 µl of a deoxynucleotide tri-phosphate mixture (dNTPs) containing 10 mM each of dATP, dCTP, dGTP, and dTTP (Sigma), 0.5 µl of Recombinant RNasin® Ribonuclease Inhibitor (Promega), 1.5 µl of Avian Myeloblastosis Virus (AMV) Reverse Transcriptase (Promega), 3 µl of $Oligo(dT)_{15}$ Primer (Promega), 1 µg of RNA, and nuclease-free water to a final volume of 30 µl. The sample was incubated in a thermal cycler (Perkin Elmer Cetus 480, Norwalk, CT) at 42°C for 40 minutes, followed by 5 minutes at 99°C and 5 minutes at 4°C.

PCR

The expression of IFN-γ, VEGF, transforming growth factor-β (TGF-β), and Glyceraldehyde-3-phosphate dehydrogenase (GAPDH, a housekeeping gene in ARH-77 cells) was evaluated. Primer pairs were used to amplify their respective genes from 5 different dilutions of ARH-77 cDNA (IFN-γ, VEGF, and TGF-β) or

10 different dilutions of cDNA (GAPDH), for a total of 25 PCR reactions. A master mix for 30 PCR reactions was made by combining the following reagents in a 1.5 ml DNase-free eppendorf tube; 150 µl of Thermophilic DNA Polymerase 10x Buffer (Promega), 120 µl of 25 mM $MgCl_2$ (Promega), 60 µl of 10 mM dNTP (Sigma), 15 µl of 5 units/µl Taq DNA Polymerase (Promega), and 555 µl DNase-free water.

For IFN-γ, VEGF, and TGF-β, 180 µl of this master mix was pipetted into each of three 0.5 ml DNase-free eppendorf tubes, and 30 µl of each primer in the respective primer pair was added. All primer pairs were purchased from Integrated DNA Technologies, Inc. (IDT, Coralville, IA). The IFN-γ primers were A) 5' – GCA GGT CAT TCA GAT GTA G – 3' and B) 5' – GAC AGT TCA GCC ATC ACT TGG – 3'. The VEGF primers were A) 5' – GGA CAT CTT CCA GGA GTA – 3' and B) 5' – TGC AAC GCG AGT CTG TGT – 3'. The TGF-β primers were A) 5' – TCC GCA AGG ACC TCG GCT GGA – 3' and B) 5' – ATC ATG TTG GAC AGC TGC TCC – 3'. To the remaining 360 µl of master mix, 60 µl of each GAPDH primer was added to the 1.5 ml eppendorf tube. The GAPDH primers were A) 5' – CAC CAT GGA GAA GGC – 3' and B) 5' – TGC CAG TGA GCT TCC – 3'.

Each of the 3 master mixes containing IFN-γ, VEGF, or TGF-β primers were divided into 5, 40 µl aliquots in 0.5 ml DNase-free eppendorf tubes. The master mix containing primers for GAPDH was divided into 10, 40 µl aliquots in 0.5 ml DNase-free eppendorf tubes.

Serial dilutions of ARH-77 cDNA were prepared in DNase-free water at a 1:1 ratio to obtain concentrations of cDNA at 1/2, 1/4, 1/8, and 1/16. A 1:10 dilution was prepared from the 1/16 concentration, followed further by 9, 1:1 dilutions. For IFN-γ, VEGF, and TGF-β, each of the 5 aliquots of master mix plus primers received a 10 µl dilution of ARH-77 cDNA ranging from undiluted (0.33 µg) to a dilution of 1/16. For the 10 GAPDH PCR reactions, each of the 10 aliquots of master mix plus primers received a 10 µl dilution of ARH-77 cDNA ranging from 1/160 to 1/81,820.

PCR reactions were placed in a thermal cycler (Perkin Elmer) and incubated as follows: 5 minutes at 94°C; 34 cycles of 30 seconds at 94°C, 30 seconds at 55°C, 60 seconds at 72°C; 10 minutes at 72°C; hold at 4°C (for up to 10 hours).

Gel Electrophoresis

A 1.5% agarose (Fisher Scientific) solution was prepared in DNase-free water and heated in a microwave (General Electric, Louisville, KY) on high for 3 minutes to dissolve the agarose into solution. The ends of the casting tray (Bio-Rad, Hercules, CA) were sealed with labeling tape (TimeMed Labeling Systems, Inc., Burr Ridge, IL), and when the agarose solution cooled to the point of being able to hold the glassware in hand, the solution was slowly poured into the casting tray until it had filled half the depth of the tray. A gel comb was added to one end of the gel, approximately 0.5 inches from the top. The gel incubated at

room temperature until it solidified, and the gel comb and tape were removed. The gel and casting tray were placed in a Wide Mini Sub® gel electrophoresis chamber (Bio-Rad), and tris-acetate EDTA buffer (TAE buffer: 0.04M Tris-acetate and 0.001M EDTA) was poured into the chamber until it covered the gel surface. Two microliters of 6x gel-loading buffer (0.25% bromophenol blue (Sigma), 0.25% xylene cyanol FF (Sigma), 40% sucrose (Sigma) in water) were mixed with 10 µl of each PCR reaction, and 10 µl from each PCR reaction plus loading buffer was pipetted into respective gel wells. The gel was electrophoresed for 1 hour at 100 V in a Power Pac 300 electrophoresis machine (Bio-Rad).

The gel was stained in an ethidium bromide (Sigma) solution (100 ml of DNase-free water plus 50 µl of ethidium bromide) for 5 minutes, followed by destaining in dH_2O for 10 minutes. Bands were viewed using a Foto/Eclipse (Fotodyne, Inc. Hartland, WI), and data were analyzed using the Alpha Imager™ (Alpha Innotech, San Leandro, CA). The computer measured the brightness of each band relative to background and gave a corresponding numerical value that represented the intensity of expression of a particular gene at the corresponding cDNA dilution. From these values, a standard curve for GAPDH was generated, and the standard curve was used to determine the relative expression values of the other genes in ARH-77 cDNA.

SYBR™ Green Quantitative RT-PCR

cDNA Synthesis

For each reverse transcription, the following reagents were mixed in a 0.5 ml RNase-free eppendorf tube and incubated for 10 minutes in a thermal cycler (Ericomp) at 70°C; 2 µg of RNA (ARH-77 RNA isolated using TRIzol or Stratagene Reference RNA), 0.5 µl of Random Oligos (Gibco), 0.5 µl of Oligo dT (Gibco), and RNase-free water up to 11 µl. There were two tubes set up for each RNA sample. One tube receives all reagents, while the other tube receives all reagents except the Superscript reverse transcriptase.

The tubes containing the RNA and oligos were placed on ice. Four microliters of 5X First Strand Buffer (Gibco), 1 µl of 10 mM dNTPs (Gibco), 1 µl 0.1 M DTT (Gibco), and 1 µl of Superasin (Ambion) was added to each tube and mixed by vortex. One of the tubes for each RNA mixture received 1 µl of Superscript II reverse transcriptase (Gibco), and the second tube, lacking reverse transcriptase, was designated as a "-RT" control. Each sample was incubated for 10 minutes at room temperature, followed by 50 minutes in a thermal cycler (Ericomp) at 42°C and 10 minutes at 70°C. Each sample was placed on ice for 2 minutes, and 1 µl of RNAse H (Gibco) was added. Finally, each sample was incubated for 20 minutes at 37°C and diluted to 100 µl with DNase-free water (20 ng/ul final cDNA concentration).

PCR

Primers (IDT) were designed using Primer Express 1.5 (Applied Biosystems, Foster City, CA) and Net Primer (155). The primers were dissolved in sterile, distilled water at 100 pmol/µl. A 10 pmol/µl working solution of each primer was made by diluting the stock 1:10 in sterile, dH_2O. Before using new primer pairs on test cDNA, various concentrations (100 nM, 250 nM, 500 nM, and 1000 nM) of each primer set was tested on the reference cDNA, which had been reversely transcribed from Stratagene Reference RNA (LaJolla, CA) to determine the optimal primer concentration that would not yield primer-dimers.

Samples of the ARH-77 cDNA were diluted in DNase-free water to 20 pg/µl for GAPDH, the housekeeping gene, and 200 pg/µl for angiopoietin. Reference cDNA was diluted in DNase-free water in two different ranges as follows: five 1:10 serial dilutions beginning at 200 pg/µl were made to obtain a GAPDH standard curve, and 5 serial dilutions of 1000 pg/µl, 200 pg/µl, 100 pg/µl, 50 pg/µl, and 10 pg/µl was prepared to obtain a standard curve for angiopoietin. Five microliters of each reference cDNA dilution was pipetted in duplicate into respective wells of a MicroAmp® Optical 96 well reaction plate (Applied Biosystems), followed by the addition of 5 µl of each "-RT" reference cDNA dilution in duplicate. Five microliters of ARH-77 cDNA or ARH-77 "-RT" cDNA, at 20 pg/µl or 200 pg/µl, were pipetted into their respective wells.

A master mix of PCR reagents was made for each gene by adding the following to a 0.5 ml DNase-free eppendorf tube: 10 µl/reaction of SYBR™

Green (Qiagen), 0.5 µl/reaction of each 10 µM primer (IDT), and 4 µl/reaction of DNase-free water. Fifteen microliters of the GAPDH master mix was pipetted into each well containing the 200 pg/µl – 0.02 pg/µl reference cDNA standard and into respective wells containing 20 pg/µl of ARH-77 cDNA. Fifteen microliters of the angiopoietin master mix was pipetted into each well containing the 1000 pg/µl – 10 pg/µl reference cDNA standard and into respective wells containing 200 pg/µl ARH-77 cDNA. This process was performed carefully to avoid introducing air bubbles, and it was repeated for all respective "-RT" controls. The 96-well plate was sealed with Optical Caps (8 caps/strip from Applied Biosystems) using the Cap Installing Tool (Applied Biosystems) and centrifuged (Beckman Coulter Allegra 6R) at 300 x g for 1-2 minutes at room temperature.

Data were acquired using the ABI PRISM 7700 (Applied Biosystems, Foster City, CA). Thermal cycling conditions were set at 95°C for 15 minutes followed by 40 cycles of 15 seconds at 95°C and 60 seconds at 60°C. The volume of the reaction was changed to 20 µl and the Dye Layer was set for SYBR™ green. Results were analyzed using Sequence Detection Systems 1.9 (Applied Biosystems). A threshold is set within the liner range of amplification of all genes, and the cycle number at which a given gene amplification reached the threshold was used to determine relative difference between the expression of each gene. For example, the cycle threshold number from each concentration of the reference cDNA was used to generate a standard curve, and from this curve,

the relative amount of GAPDH and angiopoietin expressed by ARH-77 cells was determined.

Finally, a melt curve analysis was performed to ensure that the results obtained represented a single, uniform product. To this end, the thermal cycler was set at 95°C for 15 seconds, 60°C for 20 seconds, and 95°C for 15 seconds, with a ramp time of 19 minutes and 59 seconds. The melt curve for each product was viewed using the Sequence Detection Systems Dissociation Curves software (Applied Biosystems), which shows a change in signal at each temperature. A single uniform product appeared as a single peak.

H. Fluorescent Activated Cell Sorting (FACS)

Twenty million cultured cells were collected into a 50 ml conical tube (BD Falcon) and centrifuged (Sorvall centrifuge) at 300 x g for 10 minutes at 4°C. The cells were washed with complete medium lacking FCS and centrifuged (Sorvall centrifuge) at 300 x g for 10 minutes at 4°C. The cells were resuspended at 10^7 cells/ml in PBS containing 1% FCS, and 100 µl of the cell suspension was placed in each tube (12 x 75 round-bottom, BD Falcon). One microgram of mouse (PharMingen/BD Biosciences) or human control antibody (purified from human serum, Sigma) was added to respective tubes and incubated in the dark for 5 minutes at 4°C to block binding to Fc receptors.

Antibodies (0.5 µg, 1 µg, or 2 µg) were added to the respective tubes, and the cells were vortexed briefly. The cells were incubated on ice in the dark for 15 minutes at 4°C, vortexed briefly, and incubated for another 15 minutes under the same conditions. One milliliter of PBS containing 1% FCS was added to each tube. The cells were vortexed briefly and centrifuged (Sorvall) at 300 x g for 5 minutes at 4°C. After aspirating the supernatant, 400 µl of 1% paraformaldehyde (Sigma) was added to the cells, and the tubes were vortexed briefly.

Data were acquired within 24 hours using a FACScan (BD Biosciences). Results were analyzed using CellQuest (BD Biosciences).

I. Thymidine Incorporation

Cells were centrifuged for 10 minutes at 300 x g at 4°C. The cells were washed with complete medium lacking FCS and centrifuged (Sorvall) for 10 minutes at 300 x g at 4°C. The cells were resuspended in complete medium at 5 x 10^5 cells/ml. One hundred microliters of the cell suspension was added to each well of a 96-well tissue culture plate (BD Falcon).

Antibodies, which were previously dialyzed into serum-free medium, were diluted in complete medium to 2 mg/ml, and four, 1:10 serial dilutions were prepared ranging from 0.2 - 200 µg/ml. One hundred microliters of each dilution were added to the respective wells. The 1:1 dilution of treatment to cells gave a final concentration of 1 mg/ml (maximum) antibody for 5 x 10^4 cells. Doxorubicin (GensiaSicor Pharmaceuticals, Irvine, CA) was added at a final concentration of 0.5 µg/ml as a positive control.

The cells were incubated at 37°C with 5% CO_2/95% air for 24 or 48 hours. Eight hours before the end of the incubation, 1 mCi/ml thymidine (Amersham Biosciences, Piscataway, NJ) was diluted 1:10 in complete medium, and 10 µl of the thymidine dilution was added per well. At the end of the incubation time, cells were harvested onto a FilterMAT (Skatron, Sterling, VA) using a Skatron cell harvester (Skatron, Sterling, VA). FilterMATs were counted using a β-counter (Wallac 1410, Pharmacia/Pfizer, New York, NY).

J. Enzyme-Linked Immunosorbent Assay (ELISA)

VEGF ELISA

Accucyte® competitive human VEGF ELISA kits were purchased from Cytimmune Sciences, Inc (College Park, MD). Cells were collected and treated with antibody as described above. The cells were centrifuged (Sorvall) at 300 x g for 10 minutes at 4°C, and the supernatant was isolated for immediate analysis of VEGF production. The assay was carried out according to kit instructions.

The VEGF standard (included in the kit) was diluted to 200 ng/ml in 1 ml of serum-free medium, and 5 serial dilutions at 1:4 were prepared from this initial concentration. One hundred microliters of each dilution was added to the respective wells of a 96 well plate pre-coated with goat anti-rabbit secondary antibodies (included in the kit). One hundred microliters of cell supernatant was added in duplicate to the wells. Each well received 25 µl of rabbit anti-human VEGF antibody (included in the kit), and the plate was covered with an acetate plate sealer (included in the kit) and incubated at room temperature for 3 hours. Twenty five microliters of human VEGF conjugate (included in the kit) was added to each well, and the plate was incubated at room temperature for 30 minutes.

Wash buffer was diluted to 1 L with deionized water. A multi-channel pipet was used to dispense 250 µl of the diluted wash buffer into each well. The plate was inverted over the sink, flicked to eliminate fluid, and blotted on clean paper towels. This washing procedure was repeated until the plate had been washed a

total of five times. During the fifth wash, the plate was incubated in wash buffer for 10 minutes at room temperature before the buffer was discarded.

Each well received 50 µl of streptavidin-alkaline phosphatase (included in the kit), and the plate was sealed with a plastic cover (kit) and incubated at room temperature for 30 minutes. During this time the color reagents A & B, provided in the kit, were brought to room temperature.

The plate was washed 5 times as before, and the color reagents A & B were mixed at a 1:1 dilution. Each well received 200 µl of the prepared color reagent, and the plate was re-sealed and incubated at room temperature for 25 minutes.

The color of the sample was measured at 492 nm using a Molecular Devices ThermoMax microplate reader. Once the plate had incubated for 15 minutes, measurements were taken every two minutes until the end time-point. The amount of VEGF present in unknown samples was calculated from the standard curve where known concentrations of VEGF were used.

sCD54/ICAM-1 ELISA

Human CD54 ELISA kits were purchased from Chemicon International, Inc. (Temecula, CA). ARH-77 cells were collected and treated with antibody as described above. Since UV3 may competitively bind to sCD54, UV3 was added to all wells immediately before harvesting. The cells were centrifuged (Sorvall) at 300 x g for 10 minutes at 4°C, and the supernatant was isolated for immediate

analysis of sCD54 production. The assay was carried out according to kit instructions.

Wash buffer (included in the kit) was diluted 1:20 in distilled water. Each well received 2 washes with 300 µl of the diluted wash buffer. The wells were aspirated with a glass pipet following each wash. After the second wash, the plate was blotted on a clean paper towel to remove any residual wash buffer.

One hundred microliters of the sample diluent (included in the kit) was added to the wells designated for the standard, except for the duplicate wells designated for 100 ng/ml of sCD54. Two hundred microliters of sCD54 standard (100 ng/ml) was added to the wells. Dilutions of the standard were made 1:1 in the wells, beginning with the transfer of 100 µl of the 100 ng/ml standard into 100 µl of sample diluent to obtain 50 ng/ml. This process was repeated until a standard range of 6.25 - 100 ng/ml of sCD54 was obtained.

One hundred microliters of the sample diluent was added to the blank wells, and 90 µl of sample diluent was added to the wells designated for cell supernatant. Ten microliters of each cell supernatant sample was added to respective wells and was mixed by pipetting. A 10% horse radish peroxidase (HRP) conjugate solution (kit) was made by mixing 10 µl of HRP conjugate with 990 µl of assay buffer (kit). Fifty microliters of diluted HRP-conjugate was added to all wells, and the wells were covered with a plate cover and incubated at room temperature for 1 hour.

The wells were washed 3 times with diluted wash buffer using the procedures outlined at the beginning of the protocol. A substrate solution was prepared by mixing substrate solution I (kit) and substrate solution II (kit) at a 1:1 ratio. One hundred microliters of this substrate mixture was added to each well, and the plate was incubated for 15 minutes in the dark at room temperature. The enzymatic reaction was stopped by pipetting 100 µl of the stop solution (1 M phosphoric acid) into each well.

The absorbance of each sample was measured at 450 nm using a Molecular Devices ThermoMax microplate reader.

K. ADCC

Isolation of Splenocytes

BALB/c mice, 10-14 weeks of age, were sacrificed (one mouse for every 40-60 million splenocytes needed). A 1 inch transverse cut was made across the abdominal wall, and the spleen was removed using stainless steel surgical scissors (Fisher). The spleen(s) were placed in a 50 ml conical tube (BD Falcon) containing 50 ml of Hank's Balanced Salt Solution (HBSS) (Gibco) containing 1% FCS.

In a laminar flow hood (Nuaire, Plymouth, MN), 40-45 ml of the HBSS medium in the 50 ml conical tube was poured out into a waste container. The remaining 5-10 ml of HBSS medium plus spleens was poured into a sterile petri dish (BD Falcon) containing 15 ml of fresh HBSS medium. The spleens were sliced into smaller pieces using 2 microscope slides with frosted ends, which were then homogenized between the two frosted ends of the slides. The splenocyte suspension was pipetted into a clean 50 ml conical tube (BD Falcon). The petri dish was washed 3 times with 10 ml of fresh HBSS to collect any remaining splenocytes, and the washes were added to the splenocyte mixture. In order to allow debris to settle, the splenocytes were incubated for 3 minutes at room temperature, and the supernatant was transferred to a clean 50 ml conical tube (BD Falcon).

The cell suspension was filtered through a nylon mesh (BD Falcon) into a 50 ml conical tube (BD Falcon). The cells were centrifuged (Sorvall) at 200 x g for 10 minutes at 4°C, and the supernatant was poured off. M-lyse buffer from the Mouse Erythrocyte Lysing Kit (R & D Systems, Minneapolis, MN) was diluted 1:10 in distilled water, and the splenocytes were resuspended in the diluted buffer (2 ml per spleen). The cells were incubated at room temperature for 10 minutes, and the remainder of the 50 ml tube was filled with PBS containing 1% FCS. The cells were centrifuged (Sorvall) at 200 x g for 10 minutes at 4°C. The splenocytes were resuspended at 3 x 10^6 cells/ml in DMEM medium containing 10% FCS, 1% L-glutamine, 1% non-essential amino acids (Gibco), 1% sodium pyruvate, and 1% penicillin-streptomycin. Twenty thousand units of Interleukin-2 (Chiron) was added for each milliliter of cells to activate natural killer cells. A 14 M stock solution of β-mercaptoethanol (Sigma) was diluted 1:2500 in DMEM medium, and 5 µl of the dilution was added per milliliter of cells. Indomethacin (Sigma) was added to the cell suspension at 0.5 µg/ml. Two milliliters of cell suspension were pipetted into each well of a 24 well tissue culture plate (Falcon), according to the number of cells needed, and the plate was incubated for 5 days at 37˚C, 10% CO_2/90% air.

Target Cells

Target cells were removed from culture, pipetted into a 50 ml conical tube (BD Falcon), and centrifuged (Sorvall) at 300 x g for 5 minutes at 4°C. The cells

were resuspended in complete medium at 3 times the initial volume and centrifuged (Sorvall) at 300 x g for 5 minutes at 4°C. The cells were resuspended at 10^7 cells/ml in serum-free medium. Five hundred microliters of the cell suspension was transferred to a 15 ml conical tube (BD Falcon) containing 150 µCi (150 µl) of chromium-51 (185 MBq, Amersham). The cells were vortexed and incubated for 1 hour in the dark at 37°C. During the incubation, the tube was inverted at 20 minutes and 40 minutes to enhance the labeling.

The 15 ml tube was filled with serum-free media, the cells were centrifuged at 300 x g for 5 minutes at room temperature, and the wash was repeated. The supernatant was discarded in liquid radioactive waste containers, and the cells were resuspended in 500 µl of serum-free medium. One hundred microliters of cell suspension was dispensed into individual glass tubes (Fisher). Five micrograms of UV3 or control antibodies were added to respective tubes, and one tube of cells was left untreated. The tubes were incubated at 4°C for 15 minutes, vortexed, and incubated at 4°C for 15 minutes. The cells were centrifuged at 300 x g for 5 minutes at 4°C. The cells were resuspended in an equal volume of serum-free medium, centrifuged at 300 x g for 5 minutes at 4°C, and the wash was repeated. The cells were resuspended in complete medium at 5 x 10^4 cells/ml, and 100 µl of the target cells (treated or untreated) were added to respective wells of a 96 well plate (Costar).

Effector Cells

Splenocytes were removed from culture and centrifuged at 300 x g for 5 minutes at 4°C. The cells were resuspended in complete target cell medium at 3 times the volume and centrifuged at 300 x g for 5 minutes at 4°C. The cells were resuspended at 5 x 10^6 cells/ml in complete target cell medium, and serial dilutions of 1:1 (2.5 x 10^6 cells/ml) and 1:5 (5 x 10^5 cells/ml) were prepared. One hundred microliters of these three concentrations were added to wells designated 100:1 (effector:target), 50:1, and 10:1, respectively.

^{51}Chromium Release Assay

The cells were incubated at 37°C, 5% CO_2/95% air for 4 hours. Cell medium containing 2% Triton X-100 (Sigma) was added to control wells to determine the maximum chromium released. The plates were centrifuged at 300 x g for 4 minutes at room temperature, and the contents of each well were transferred to 12 x 75 mm glass tubes (Fisher) for analysis in a γ-counter (Wallac Wizard, PerkinElmer). The percentage of specific lysis was calculated using the following equation:

$$\text{Specific percent lysis} = 100 \times \frac{\text{test } ^{51}\text{Cr released} - \text{control } ^{51}\text{Cr released}}{\text{maximum } ^{51}\text{Cr released} - \text{control } ^{51}\text{Cr released}}$$

L. CDC

Target Cells

Target cells were labeled with ^{51}Chromium as described under ADCC.

^{51}Chromium Release Assay

Rabbit serum (Chemicon) was diluted in serum-free RPMI at 1:2.5, 1:12.5, and 1:25. One hundred microliters of each complement dilution was added to respective wells in a 96 well tissue culture plate (Falcon). One hundred microliters of serum-free RPMI containing 2% Triton X-100 (Sigma) was used as a positive control to measure maximum chromium release. One hundred microliters of target cells were added to respective wells, and the tissue culture plate was incubated for 4 hours at 37°C, 5% CO_2/95% air.

The plates were centrifuged at 300 x g for 4 minutes at room temperature, and the contents of each well were transferred to 12 x 75 mm glass tubes (Fisher) for analysis in a γ-counter (Wallac Wizard, PerkinElmer). The percentage of specific lysis was calculated using the following equation:

$$\text{Specific percent lysis} = 100 \times \frac{\text{test } ^{51}\text{Cr released} - \text{control } ^{51}\text{Cr released}}{\text{maximum } ^{51}\text{Cr released} - \text{control } ^{51}\text{Cr released}}$$

M. Migration Assays

Preparation of HUVECs

HUVECs (Cascade Biologics), cultured in 75 mm^3 tissue culture flasks, were selected for use when they reached 80% confluency. The medium was pipetted out of the HUVEC flask and discarded. Fifteen milliliters of fresh, HUVEC complete medium containing 2 µl/ml of Vybrant™ Di-I labeling solution (Molecular Probes, Eugene, OR) was added to the HUVEC culture. The cells were then incubated for 2 hours in a humidified 37°C incubator (Forma Scientific) with 5% CO_2/95% air.

ARH-77 cells

ARH-77 cells were cultured in medium containing 1% FCS. Cells were centrifuged in a 50 ml conical tube (BD Falcon) at 300 x g for 10 minutes at 4°C and resuspended in serum-free medium to wash the cells. Cells were centrifuged at 300 x g for 10 minutes at 4°C and resuspended in 1% complete medium at 10^7 cells/ml. The cells were diluted in 1% complete medium to the respective, test concentrations.

Assay

BD Biocoat Angiogenesis systems for endothelial cell migration (BD Biosciences, Bedford, MA) were used for this assay. Fluorescently-labeled

HUVECs were washed and harvested, as described above. The HUVECs were resuspended in serum-free RPMI-1640 medium at 2 x 10^5 cells/ml. 250 µl of the HUVEC suspension (5 x 10^4 cells) was seeded onto the fibronectin FluroBlok membrane within the top chamber of the respective wells. For each chamber with HUVECs, a control chamber was included that had only serum free RPMI-1640 (no cells) in the top chamber. To the bottom chamber, 750µl of control (serum free medium, 1% medium, etc.) or test stimulant (ARH-77 cells) was added. The plate was incubated for 20-24 hours in a humidified 37°C incubator (Forma Scientific) with 5% CO_2/95% air. The plate was scanned each hour from the 20-24 hour incubation with a Tecan Spectrafluor Plus (Maennedorf, Switzerland). The data acquisition was set to measure the amount of fluorescence in the bottom chamber, which reflected the migration of fluorescent HUVECs in response to the stimulus in the bottom chamber.

N. SCID Xenografts

Multiple Myeloma Cells

Female NOD/SCID mice (Jackson Labs, Bar Harbor, ME), 6-7 weeks of age, were irradiated with 150 rads of γ-irradiation using a Mark I Irradiator (J. L. Shepherd and Associates, San Fernando, CA). Twenty four hours later, mice were injected intravenously (i.v.) into the tail vein with 100 µl of 10^7 ARH-77 cells suspended in sterile PBS. Antibody therapy began 14 days after tumor cell injection. For four consecutive days, 4 ug/g of UV3 or the isotype control antibody was injected i.v. Mice receiving $F(ab)'_2$ fragments were injected with 8 ug/g/day i.v. on days 14-17. Control mice received 100 µl of sterile PBS. Mice were followed by weight and by observation for signs of the following: visible tumor, paralysis, 20% weight loss, and sickness. When mice exhibited two of these signs, animals were sacrificed.

Daudi Lymphoma Cells

Fox Chase Inbred SCID mice (Taconic, Germantown, NY) were injected i.v. with 100 µl of 10^7 Daudi cells. Beginning one day following tumor cell injection, mice received daily i.v. treatment for four consecutive days. Mice receiving UV3, cUV3, or isotype control antibody were injected with 0.8 µg/g of antibody each day. Mice receiving $F(ab)'_2$ fragments were injected with a 10 fold higher dose, or 8 µg/g. Mice receiving $F(ab)'_2$ fragments plus IgG (UV3) were

injected with a regular dose of $F(ab)'_2$ (8 μg/g), plus 10, 20, or 30% of the UV3 IgG dose (0.08 μg/g, 0.16 μg/g, or 0.24 μg/g). Animals were sacrificed when they developed hind-leg paralysis.

Results

A. Evidence for Angiogenesis in Multiple Myeloma

ARH-77 Cells Expressed Angiogenic Genes.

ARH-77 cells were examined for their expression of angiogenic genes using small, pathway-specific membrane microarrays from SuperArray, Inc. These microarrays are printed with cDNA fragments of 20 common pro-angiogenic and anti-angiogenic genes. ARH-77 cells expressed the pro-angiogenic genes angiopoietin-1, angiogenin, endothelin receptor type B, fibroblast growth factor receptor (FGFR) 3, tie-2, VEGF, and VEGF-D. ARH-77 cells expressed anti-angiogenic genes interferon-α 2 and collagen type 18 (**Figure 1**). The relative levels of expression of these genes were determined as a percent of the positive controls, β-actin and GAPDH. Although these genes became the focus of study, other membrane arrays from SuperArray that contained more extensive sets of angiogenic genes were also examined, revealing that ARH-77 cells expressed more angiogenic genes than presented here (data not shown).

Several Multiple Myeloma Cell Lines Expressed CD54

A panel of multiple myeloma cell lines was examined by flow cytometric analysis in order to determine whether each line expressed CD54. Human multiple myeloma cell lines HS-Sultan, NCI-H929, IM-9, ARH-77, RPMI-8226 and U-266 expressed CD54. SKO-007 human myeloma cells also expressed CD54, although the percentage of positive cells was slightly lower than that of the other multiple myeloma cell lines (**Figure 2**). This difference in cell surface expression did not correlate with the degree of expression of angiogenic genes (**Figure 3**), nor did it correlate with whether a cell line had been transformed with Epstein Barr Virus (EBV).

Cells From A Panel of Multiple Myeloma Cell Lines Displayed Similar Angiogenic Profiles.

The expression of angiogenic genes among a panel of multiple myeloma cell lines was examined using pathway-specific membrane microarrays from SuperArray, Inc. The human multiple myeloma cell lines RPMI-8226, NCI-H929, SKO-007, IM-9, U-266, and HS-Sultan expressed the pro-angiogenic genes angiopoietin-1, angiogenin, FGFR-3, Tie-2, VEGF, and VEGF-D, and they expressed the anti-angiogenic gene IFN-α 2 (**Figure 3**). There was no correlation between the expression of angiogenic genes and whether a cell line had been EBV transformed. This panel of human multiple myeloma cell lines

expressed the same angiogenic genes as ARH-77 cells (**Figure 1**). In addition, the expression levels of each gene were similar among the multiple myeloma cell lines, though the expression of angiopoietin-1 and IFN-α 2 by NCI-H929 cells was significantly higher than the expression observed in ARH-77 cells.

ARH-77 Cells Expressed Angiogenic Genes As Determined by Semi-Quantitative PCR.

In order to quantitate the expression of angiogenic genes, ARH-77 cells were examined for expression of pro-angiogenic genes and anti-angiogenic genes using semi-quantitative PCR. ARH-77 cells expressed the pro-angiogenic genes VEGF and TGF-β and the anti-angiogenic gene IFN-γ (**Figure 4**). Each of these angiogenic genes was amplified from the same range of cDNA concentrations, yet, as compared to IFN-γ, VEGF and TGF-β were expressed at higher levels. This suggests that in ARH-77 multiple myeloma cells, pro-angiogenic genes might have a more intense level of expression than the anti-angiogenic genes.

ARH-77 Cells Secreted VEGF.

ARH-77 cells were cultured at 5 x 10^5 cells/ml for 24 or 48 hours, and the cell supernatants were evaluated in an ELISA assay immediately after collection to determine whether VEGF was secreted. The average VEGF levels in ARH-77

cell supernatant were 2.9 ng/ml and 3.5 ng/ml, respectively (**Figure 5**). There was no significant difference between the two time-points in the amount of VEGF secreted (*P*=0.39). Background levels of VEGF in ARH-77 complete medium have been subtracted to give the values presented. These data indicate that although VEGF is secreted by ARH-77 cells, the VEGF levels did not accumulate in the cell medium over time, suggesting that ARH-77 cells may metabolize the VEGF that they secrete.

Other Multiple Myeloma Cell Lines Secreted VEGF.

Other human multiple myeloma cell lines were also examined to determine whether the secretion of VEGF was common to all. HS-Sultan, ILKM2, ILKM3, IM-9, MC-CAR, RPMI-8226, SKO-007, and U-266 cells were cultured for 24 hours in a 24-well plate at a starting concentration of 10^5 cells/ml, and immediately after collection the cell culture supernatants were evaluated by ELISA for levels of VEGF. After subtracting any background levels of VEGF found in the cell media, the average VEGF levels (ng/ml) in the supernatant of each cell line was determined (**Figure 6 and Table 1**). Human multiple myeloma lines MC-CAR and U-266 appeared to be the highest secretors of VEGF. However, when the standard deviations (**Figure 6 and Table 1**) were considered, all of the multiple myeloma lines, including ARH-77, secreted comparable levels of VEGF (**Figure 5**).

ARH-77 cells Secreted sCD54.

sCD54 induces angiogenesis both *in vitro* and *in vivo* (104). In addition, sCD54 stimulates tumor growth *in vivo* (156). Supernatants of ARH-77 cells were examined using an ELISA assay to determine whether they secreted sCD54. ARH-77 cells were plated at an initial concentration of 2.5 x 10^5 cells/ml, 5 x 10^5 cells/ml, or 10 x 10^5 cells/ml and cultured for 72 hours. The average levels of sCD54 in ARH-77 cell supernatant were 4.6 ng/ml, 6.9 ng/ml, and 7.9 ng/ml, respectively (**Figure 7**). This suggests that ARH-77 cells not only secrete sCD54, but that the level of sCD54 secreted increased with the number of ARH-77 cells cultured.

ARH-77 Cells Stimulated the Migration of Endothelial Cells

Since ARH-77 cells expressed angiogenic genes and secreted angiogenic proteins, ARH-77 cells were co-cultured with HUVECs to determine whether they could stimulate the migration of endothelial cells. HUVECs were grown in the top chamber of a transwell on a fibronectin-coated membrane while various concentrations of ARH-77 cells were placed in the bottom chamber. As illustrated in **Figure 8**, 5 x 10^5 ARH-77 cells/ml stimulated 2.6 fold more endothelial cell migration than ARH-77 cell medium alone, and 5 x10^6 ARH-77 cells/ml stimulated 6.6 fold more endothelial cell migration than ARH-77 cell

medium alone. This trend suggested that ARH-77 cells stimulate the migration of endothelial cells, and that the degree of migration was directly proportional to the number of ARH-77 cells plated in the bottom chamber. However, the increase in endothelial cell migration due to ARH-77 cells was not statistically significant compared to controls (P=0.24, 5 x 10^5 cells/ml; P=0.09, 5 x 10^6 cells/ml). In addition, there was no significant difference between the migration induced by 5 x 10^6 ARH-77 cells/ml as compared to 5 x 10^5 cell/ml (P=0.22).

Figure 1. As Determined by Microarray Analysis, ARH-77 Cells Expressed Angiogenic Genes.

ARH-77 cells expressed a number of angiogenic genes according to the SuperArray microarrays. RNA was isolated from ARH-77 cells and reverse transcribed to cDNA in the presence of ^{32}P. The radiolabeled cDNA was hybridized to a nylon membrane printed in duplicate with cDNA fragments of angiogenic genes. The radioactivity revealed the relative expression levels of various angiogenic genes as compared to positive controls. The following angiogenic genes were expressed by ARH-77 cells: angiopoietin-1 (A1 & A2), angiogenin (A5 & A6), collagen type 18 (B1 & B2), endothelin receptor type B (B5 & B6), FGFR-3 (D1 & D2), IFN-α 2 (E3 & E4), tie-2 (F5 & F6), VEGF (G1 & G2), VEGF-D (H1 & H2). The pUC-18 bacterial plasmid (A7 & B7) served as a negative control, and β–actin (C7 & D7) and GAPDH (E7, F7, G7, H5-7) served as positive controls. Figure 1 is representative of greater than 7 experiments.

Figure 1.

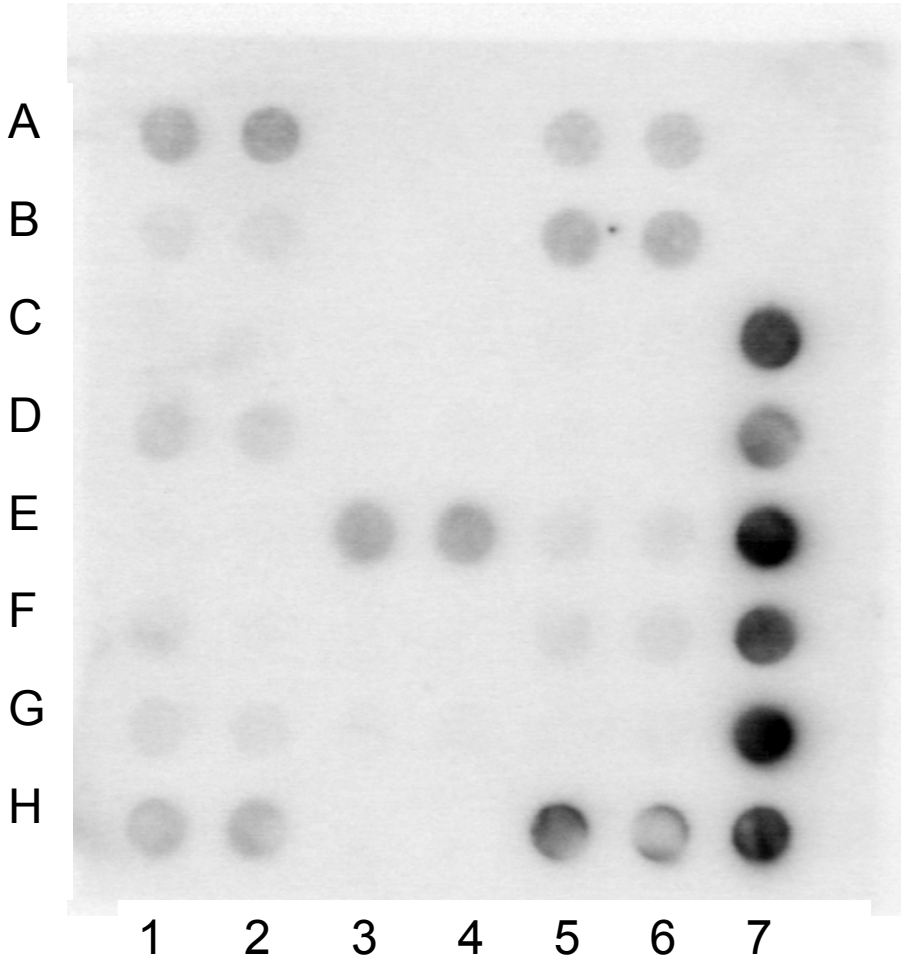

Figure 2. Several Multiple Myeloma Cell Lines Expressed CD54.

A panel of 7 multiple myeloma cell lines were stained with UV3 and analyzed by flow cytometry. The bars in the graph represent the average percentage of positive cells minus staining with an isotype-matched control. All of the multiple myeloma cell lines expressed CD54 on their cell surface. The LnCap prostate carcinoma cell line was a negative control. The number of experiments performed for each cell line is indicated below the graph.

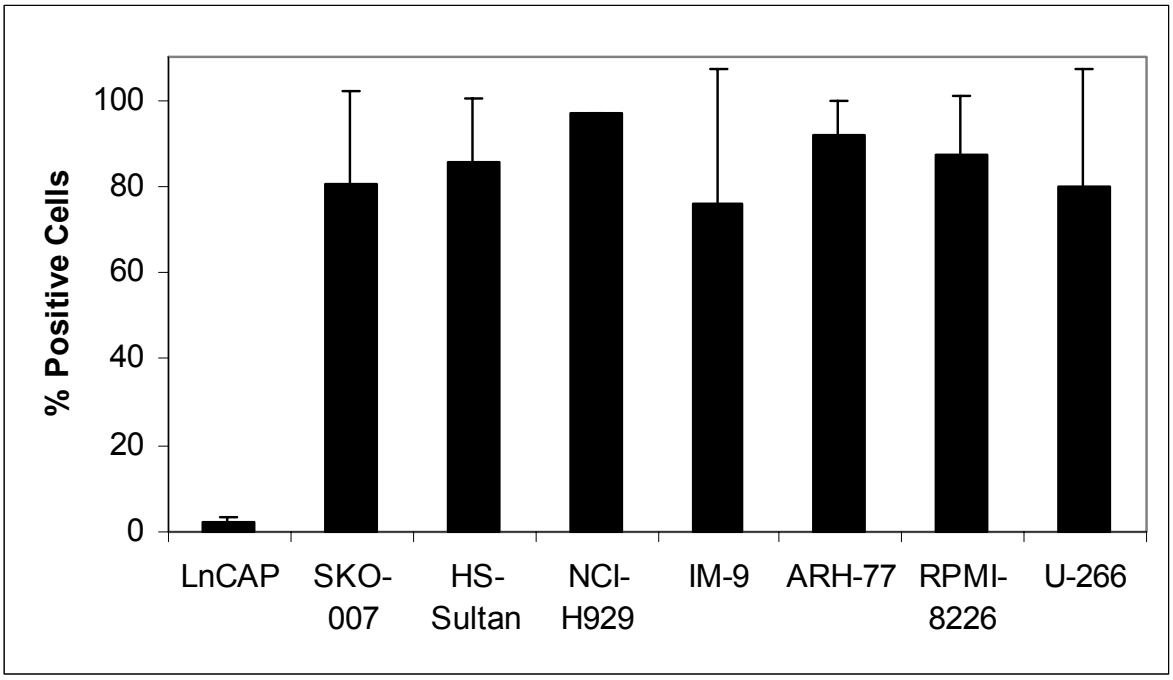

No. of Exps:	2	2	3	1	3	4	4	4

Figure 3. As Determined by Microarray Analysis, Several Multiple Myeloma Cell Lines Expressed Angiogenic Genes.

RNA was isolated from a panel of cultured multiple myeloma cell lines, and subjected to microarray analysis (SuperArray). As shown below, many of the multiple myeloma lines expressed the same angiogenic genes at similar levels. NCI-H929, however, demonstrated a significant increase in the expression of Angiopoietin-1 (P=0.0005) and IFN-α2 (*P*=0.0007). The expression of VEGF-D by NCI-H929 was increased compared to ARH-77 cells, but the increase was not significant (*P*=0.44). The graph represents the average of 3 experiments.

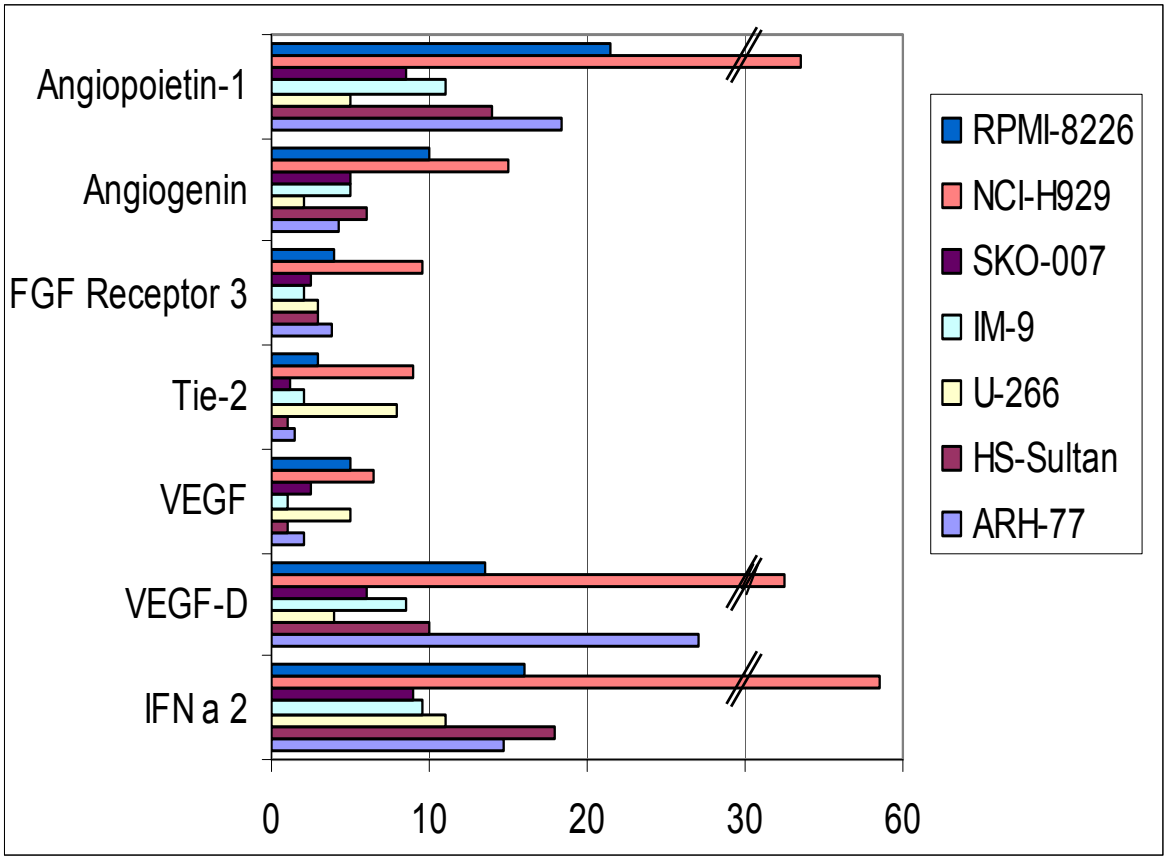

Figure 4. As Determined by Semi-Quantitative PCR, ARH-77 Cells Expressed Angiogenic Genes.

RNA was isolated from ARH-77 cells and cDNA was reverse transcribed. IFN-γ, VEGF, and TGF-β were PCR-amplified from various concentrations of ARH-77 cDNA. Lane 1 – undiluted cDNA (0.33 µg); lane 2 – cDNA 1/2; lane 3 – cDNA 1/4; lane 4 – cDNA 1/8; lane 5 – cDNA 1/16. GAPDH was PCR-amplified from various concentrations of ARH-77 cDNA. Lane 1 – 1/160 cDNA; lane 2 – 1/320 cDNA; lane 3 – 1/640 cDNA; lane 4 – 1/1280 cDNA; lane 5 – 1/2560 cDNA; lane 6 – 1/5120 cDNA; lane 7 – 1/10,240 cDNA; lane 8 – 1/20,480 cDNA; lane 9 – 1/40,960 cDNA; lane 10 – 1/81,820 cDNA. PCR products were analyzed by densitometry. The values obtained for the "housekeeping gene", GAPDH, were used to generate a standard curve, and the levels of IFN-γ, VEGF, and TGF-β expressed were determined from the standard curve. The data revealed the expression of both pro-angiogenic genes (VEGF and TGF-β) and anti-angiogenic genes (IFN-γ) in ARH-77 cells. The figure is representative of greater than 3 experiments.

Figure 4.

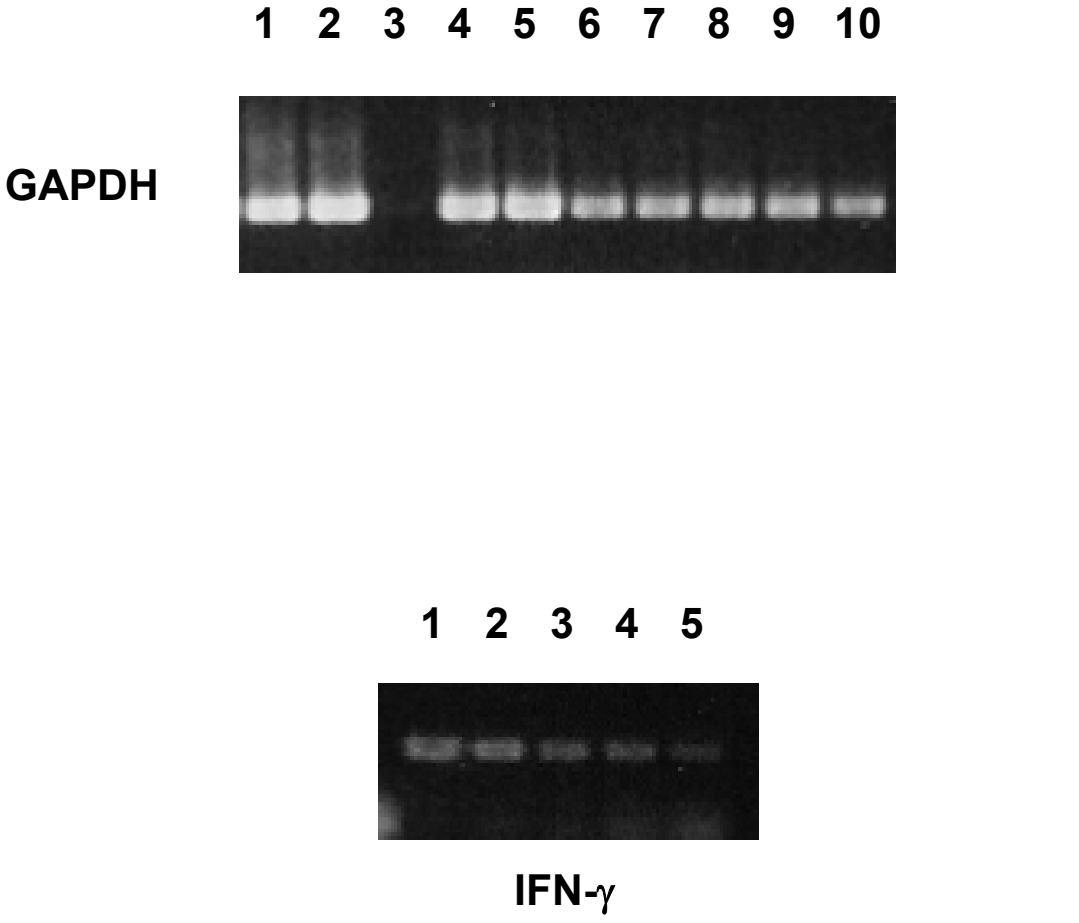

Figure 5. ARH-77 Cells Secreted VEGF.

ARH-77 cells were cultured for 24 or 48 hours. The cells were centrifuged, and the supernatants were collected. The VEGF secreted by the ARH-77 cells was measured using an ELISA assay. The amount of VEGF in the supernatant of the ARH-77 cells was compared to a standard, and cell medium alone served as a negative control. The amount of VEGF secreted after 48 hours of cell culture was not significantly different from the amount of VEGF secreted at 24 hours (*P*=0.39). This graph represents an average of 6 experiments.

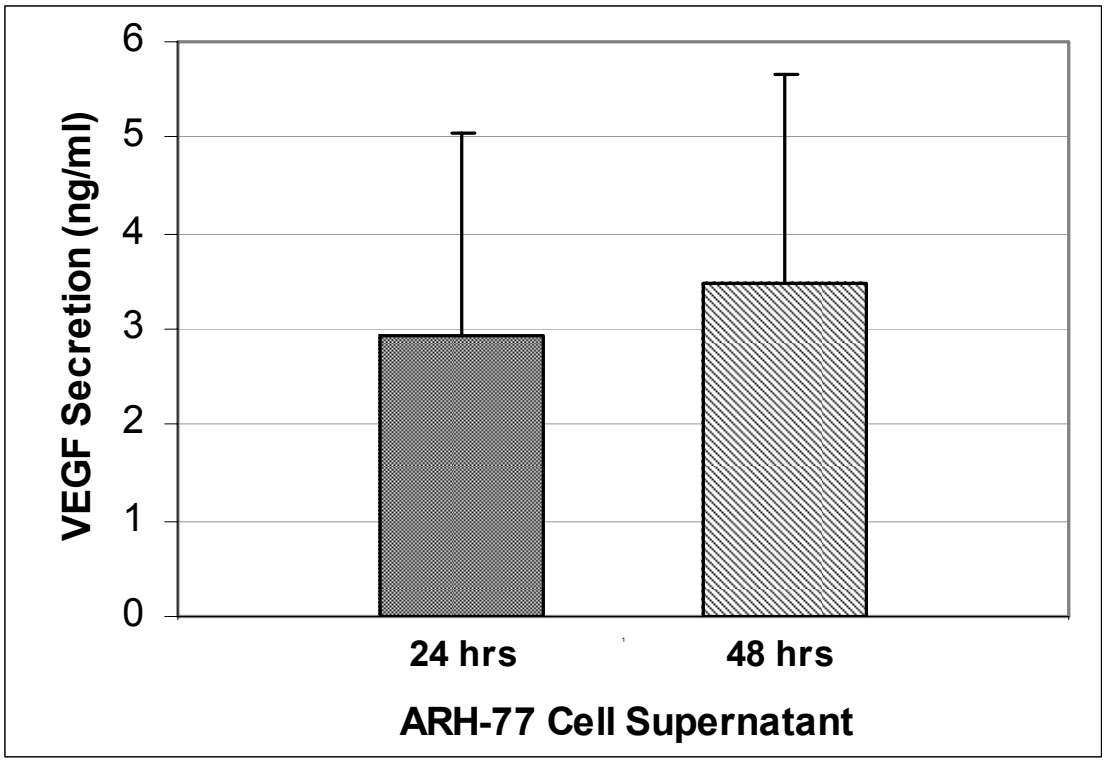

Figure 6. Other Multiple Myeloma Cell Lines Secreted VEGF.

Cell supernatants were collected from a panel of multiple myeloma cell lines that had been in culture for 24 hours. The amount of VEGF in the cell supernatants was measured using an ELISA, and the results are shown below and in Table 1. The amount of VEGF in the cell supernatants were compared to a standard, and cell medium alone served as a negative control. Other multiple myeloma lines secreted amounts of VEGF that were similar to those secreted by ARH-77 cells. The number of experiments performed for each cell line is indicated below the graph.

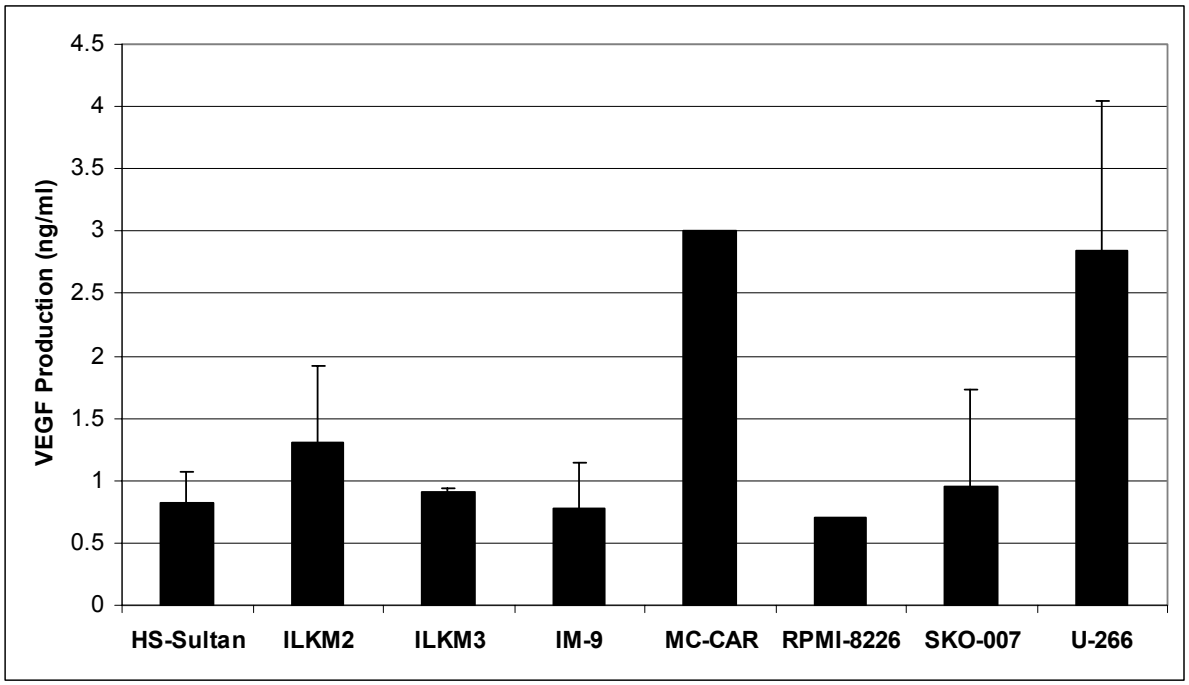

No. of Exps:	3	3	2	3	1	1	2	2

Table 1. Other Multiple Myeloma Cell Lines Secreted VEGF

	HS-Sultan	ILKM2	ILKM3	IM-9	MC-CAR	RPMI-8226	SKO-007	U-266
Average Secretion (ng/ml)	0.82	1.3	0.92	0.77	3	0.71	0.96	2.85
Standard Deviation	0.25	0.62	0.02	0.38	n/a	n/a	0.77	1.20

n/a – The VEGF levels were measured once.

Figure 7. ARH-77 Cells Secreted sCD54.

ARH-77 cells were cultured for 72 hours in complete medium at various cell concentrations. Cell supernatants were collected, and the amount of sCD54 was measured using an ELISA. As indicated in the figure, ARH-77 cells secreted sCD54. This graph is representative of 3 experiments performed.

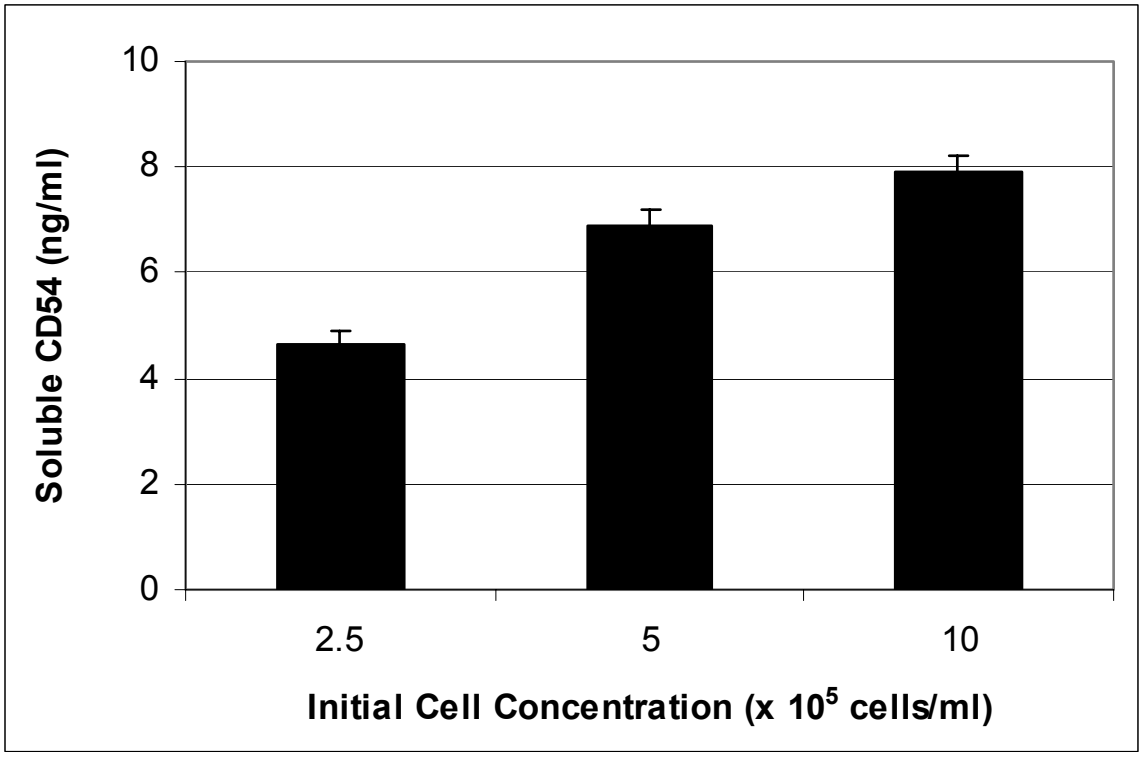

Figure 8. ARH-77 Cells Appeared to Stimulate the Migration of HUVECs.

Fluorescently-labeled HUVECs were seeded onto a fibronectin layer in the top chamber of a transwell. Various concentrations of ARH-77 cells or cell medium were added to the bottom chamber, and the transwells were incubated for 24 hours at 37°C. The amount of fluorescence measured in the bottom chamber reflected the number of HUVECs migrating in response to the stimulus. HUVEC migration was expressed as the fold migration relative to medium alone from ARH-77 cells. This graph is based on the average of 3 experiments, and suggests that ARH-77 cells stimulate the migration of HUVECs. Stimulation appeared to be proportional to the number of ARH-77 cells added. There was, however, no significant difference between the migration of HUVECs induced by 5×10^5 ARH-77 cells/ml (P=0.24) or by 5×10^6 cells/ml (P=0.09) and that induced by ARH-77 cell medium. There was no significant difference between the migration induced by 5×10^6 ARH-77 cells/ml as compared to 5×10^5 cells/ml (P=0.22).

Figure 8.

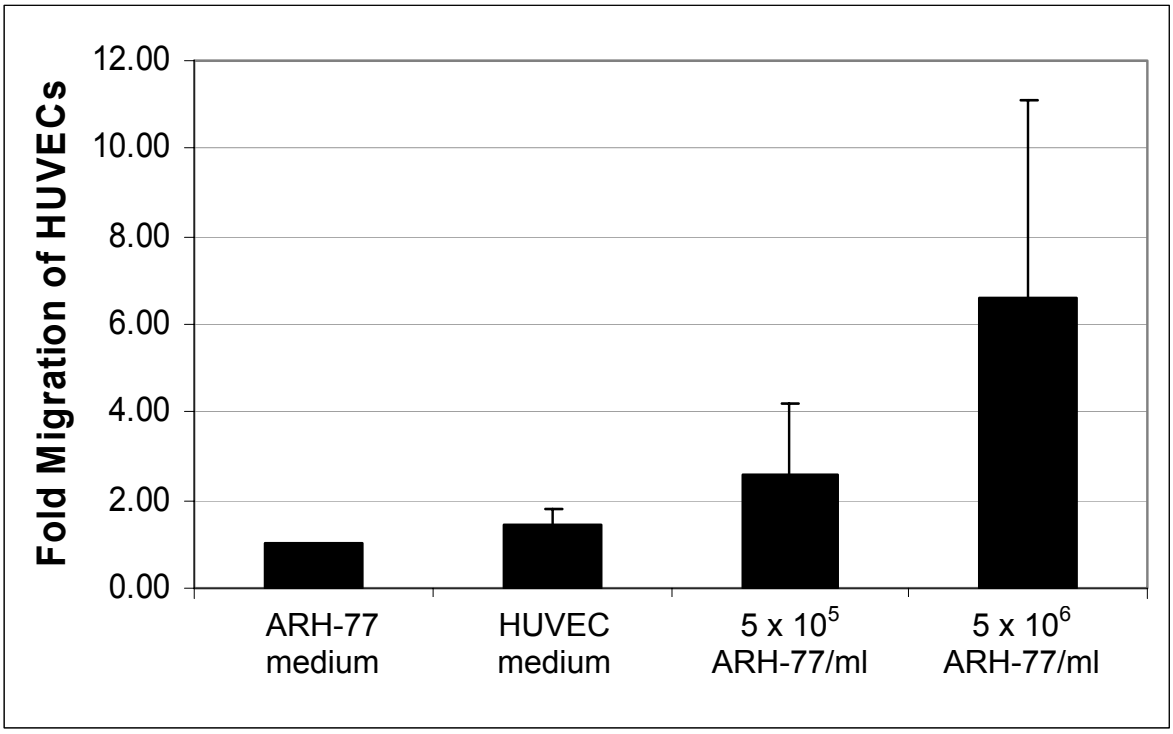
Fold Migration of HUVECs
12.00
10.00
8.00
6.00
4.00
2.00
0.00
ARH-77 medium
HUVEC medium
5 x 10^5 ARH-77/ml
5 x 10^6 ARH-77/ml

B. UV3 Had a Modest Effect in Inhibiting Angiogenesis in ARH-77 Cells

UV3 Decreased the Expression of Angiogenic Genes in ARH-77 Cells.

The expression of angiogenic genes from untreated, isotype-matched control treated, or UV3-treated ARH-77 cells was examined using a pathway-specific membrane microarray from SuperArray, Inc. The resulting data were compared to determine whether UV3 altered the expression of angiogenic genes in ARH-77 cells. UV3 induced a decrease in the expression of the pro-angiogenic genes Angiopoietin-1, Angiogenin, Endothelin Receptor B, FGFR-3, Tie-2, VEGF, and VEGF-D, and UV3 induced a decrease in the expression of the anti-angiogenic genes Collagen type 18, IFN-α2 (**Figure 9**). Although UV3 appeared to decrease the expression of both pro-angiogenic and anti-angiogenic genes, UV3 induced a statistically significant decrease in the expression of only the pro-angiogenic genes Angiopoietin-1 (P=0.00003), FGFR-3 (P=0.04), and VEGF-D (P=0.05). UV3 did not induce a significant increase in any gene, suggesting that UV3 may induce a down-regulation of pro-angiogenic genes, rather than an up-regulation of anti-angiogenic genes.

The Expression of Several Cytokines Not Involved in Angiogenesis Remained Unchanged in UV3-Treated ARH-77 Cells.

RNA from control-treated and UV3-treated ARH-77 cells was examined using a cytokine pathway-specific microarray from SuperArray, Inc. to determine whether UV3 could induce a down-regulation of cytokine genes. As shown in **Figure 10**, UV3 treatment of ARH-77 cells induced an increase in the expression of IL-2 and a decrease in the expression of IL-1α, IL-3, IL-10, IL-11, IL-16, and TNF-α. Although many cytokine genes appeared to be affected, only two of the seven genes were significantly altered as a result of treatment with UV3, IL-10 (P=0.05) and TNF-α (P=0.05), suggesting that UV3 induces the down-regulation of some cytokines.

UV3 Decreased the Expression of Pro-Angiogenic Genes and Increased the Expression of Anti-Angiogenic Genes.

In order to obtain more precise quantitation of the changes in expression of angiogenic genes in UV3-treated ARH-77 cells, semi-quantitative PCR was performed on control-treated and UV3-treated ARH-77 cell cDNA. The levels of expression of IFN-γ, VEGF, and TGF-β were determined relative to a standard curve of expression of the positive control, GAPDH. UV3 induced a 4-fold increase in the expression of IFN-γ. UV3 induced an 8-fold decrease in the expression of VEGF and a 6-fold decrease in the expression of TGF-β (**Figure**

11). These data suggest that UV3 may induce an up-regulation in the expression of pro-angiogenic genes and a down-regulation in the expression of anti-angiogenic genes.

UV3 Inhibited the Secretion of Pro-Angiogenic sCD54.

Due to previous findings illustrating the pro-angiogenic activity of sCD54 (104), the levels of sCD54 in cell supernatants from isotype-matched control-treated and UV3-treated ARH-77 cells were examined using an ELISA. All samples received UV3 immediately prior to the assay. As shown in **Figure 12**, supernatants from ARH-77 cells collected from 5 x 10^5 cells treated with an isotype-matched control antibody contained 6.8 ng/ml sCD54. Supernatant from the same number of cells treated with UV3 contained 3.3 ng/ml of sCD54 (P=0.0000001). Cell supernatant collected from 10 x 10^5 cells treated with an isotype control antibody contained 8.3 ng/ml of sCD54, and supernatant from the same number of cells treated with UV3 contained 4.3 ng/ml of sCD54 (P=0.00007). Thus, UV3 decreased the secretion of sCD54 by 50%.

UV3 Had a Modest Effect on ARH-77 Cell-Stimulated Migration of HUVECs.

In order to determine whether the effect of UV3 may have a downstream biological effect *in vitro*, control-treated and UV3-treated ARH-77 cells were examined for their ability to induce the migration of HUVECs. In an average of 3

experiments, ARH-77 cells stimulated a 5-fold increase in the migration of HUVECs as compared to the serum-free medium. Relative to serum free medium, ARH-77 cells cultured with UV3 stimulated a 2-fold increase in the migration of HUVECs, which was the same amount of migration observed in the low-serum medium condition (**Figure 13**). Culturing ARH-77 cells with an isotype-matched control antibody had no effect on the ability of ARH-77 cells to induce the migration of HUVECs (data not shown). This suggested that UV3 interferes with the migration of HUVECs *in vitro*. However, in comparing the results of 3 experiments, there was no significant difference between the amount of migration induced by ARH-77 cells vs. UV3 treated ARH-77 cells (P=0.44).

Figure 9. UV3 Decreased the Expression of Angiogenic Genes in ARH-77 Cells

RNA was isolated from ARH-77 cells cultured with UV3, an isotype control Ig, or cells received UV3 prior to harvesting (sham). The RNA was reverse transcribed into cDNA in the presence of ^{32}P, and the radiolabeled cDNA was hybridized to a nylon membrane printed in duplicate with cDNA fragments of angiogenic genes. The radioactivity revealed the relative expression levels of various angiogenic genes as compared to positive controls. The expression of angiogenic genes from ARH-77 cells treated with UV3 decreased compared to sham and isotype treated controls. The expression of VEGF-D, FGFR-3, and Angiopoietin-1 decreased significantly as a result of UV3 treatment (Angiopoietin-1, P=0.00003; FGFR-3, *P*=0.04; VEGF-D, *P*=0.05). This graph represents the average of greater than 7 experiments.

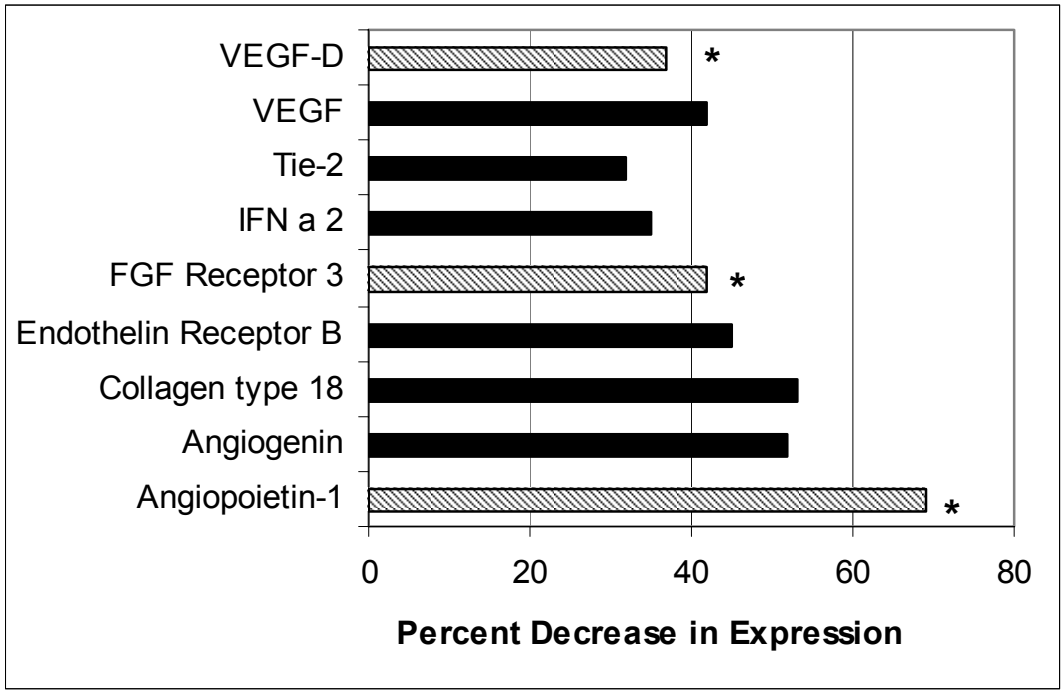

Figure 10. The Expression of Several Cytokines Not Involved in Angiogenesis Remained Unchanged in UV3-Treated ARH-77 Cells.

RNA was isolated from ARH-77 cells treated with UV3 or an isotype control antibody. The RNA was reverse transcribed into cDNA in the presence of ^{32}P, and the radiolabeled cDNA was hybridized to a nylon membrane printed in duplicate with cDNA fragments of various cytokine genes. The radioactivity revealed the relative expression levels of cytokine genes as compared to positive controls. In general, cytokines did not change significantly as a result of treatment with UV3. Exceptions included Interleukin-10 and TNF-α, which did change significantly. Bar 1 - IL-1α (*P*=0.15); Bar 2 - IL-2 (*P*=0.62); Bar 3 - IL-3 (*P*=0.36); Bar 4 - IL-10 (*P*=0.05); Bar 5 - IL-11 (*P*=0.64); Bar 6 - IL-16 (*P*=0.37); Bar 7 – TNF-α (*P*=0.05). This is the average of three experiments performed.

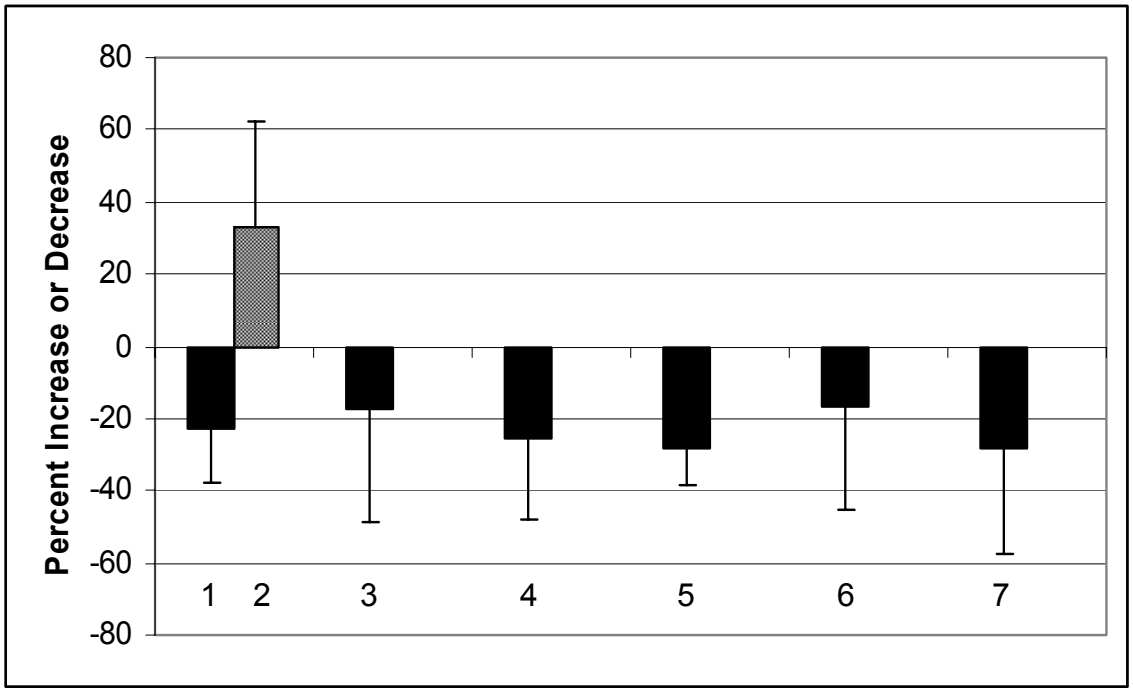

Figure 11. UV3 Decreased the Expression of Pro-Angiogenic Genes and Increased the Expression of Anti-Angiogenic Genes.

RNA was isolated from ARH-77 cells cultured in the presence or absence of UV3 and was reverse transcribed into cDNA. IFN-γ, VEGF, TGF-β, and GAPDH were PCR-amplified from various concentrations of each cDNA, and PCR products were analyzed by densitometry. The values obtained for the "housekeeping gene", GAPDH, were used to generate a standard curve.

In UV3-treated ARH-77 cells, the expression of GAPDH remained unchanged, but the expression of IFN-γ, an anti-angiogenic gene, increased 4 fold. In addition, the expression of VEGF and TGF-β, both pro-angiogenic genes, decreased 8 and 6-fold, respectively. The graph below represents the average of 2 experiments.

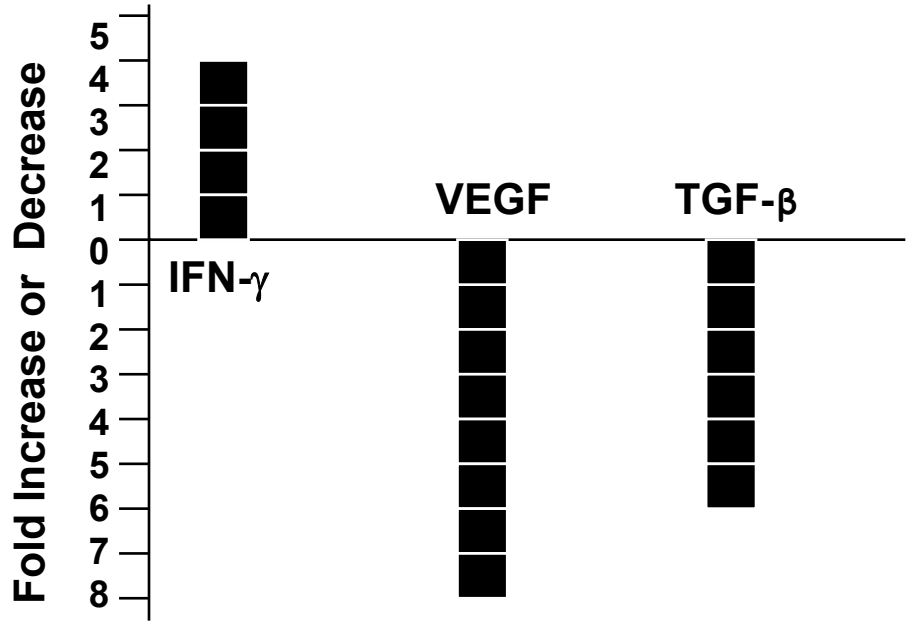

Figure 12. UV3 Inhibited the Secretion of sCD54.

ARH-77 cells, plated at various cell concentrations, were cultured for 72 hours in complete medium alone or in complete medium containing UV3 or an isotype-matched control antibody. UV3 was added to all cultures immediately before the assay to make sure it did not competitively interfere with the measurement. Cell supernatants were collected, and the amount of sCD54 was measured using an ELISA. UV3 significantly decreased the amount of sCD54 secreted by ARH-77 cells (P=0.0000001, 5 x 10^5 cells/ml; P=0.00007, 10 x 10^5 cells/ml). This graph depicts the average of 2 experiments.

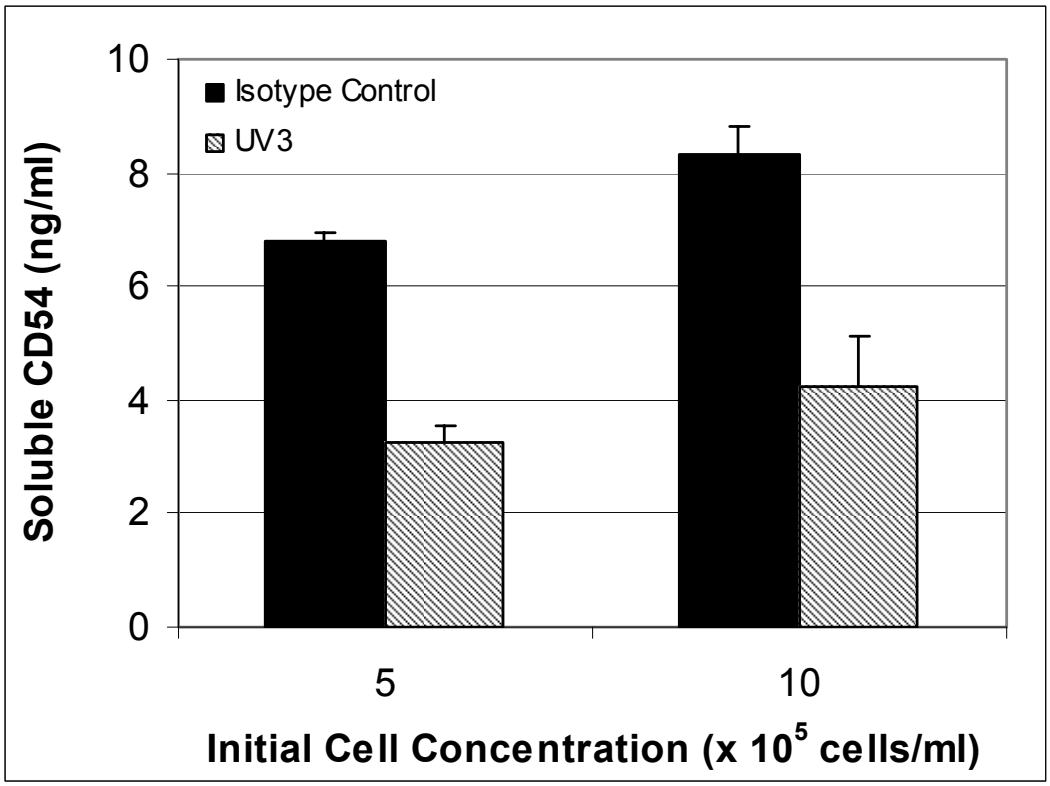

Figure 13. UV3 Had a Modest Effect on ARH-77 Cell-Stimulated Endothelial Cell Migration.

Fluorescently labeled HUVECs were harvested and plated at 2 x 10^5 cells/ml onto a fibronectin membrane in the top chamber of a transwell. In the bottom chamber of the transwell, various conditions of cell medium were added with or without ARH-77 cells, which had been cultured under low serum conditions. The transwell plate was incubated in the dark at 37˚ for 22-23 hours, and the amount of fluorescence present in the bottom chamber was measured, which reflected the number of migrated HUVECs. The degree of HUVEC migration under various conditions is demonstrated in the graph below relative to serum free medium. ARH-77 cells cultured with or without an isotype-matched control antibody stimulated the migration of HUVECs (data not shown). ARH-77 cells cultured in the presence of UV3 did not stimulate the migration of HUVECs. However, due to high standard deviations between experiments, there was no significant difference between the migration induced by ARH-77 cells alone vs. UV3 treated ARH-77 cells (P=0.44). The graph illustrates the average of 3 experiments performed.

Figure 13.

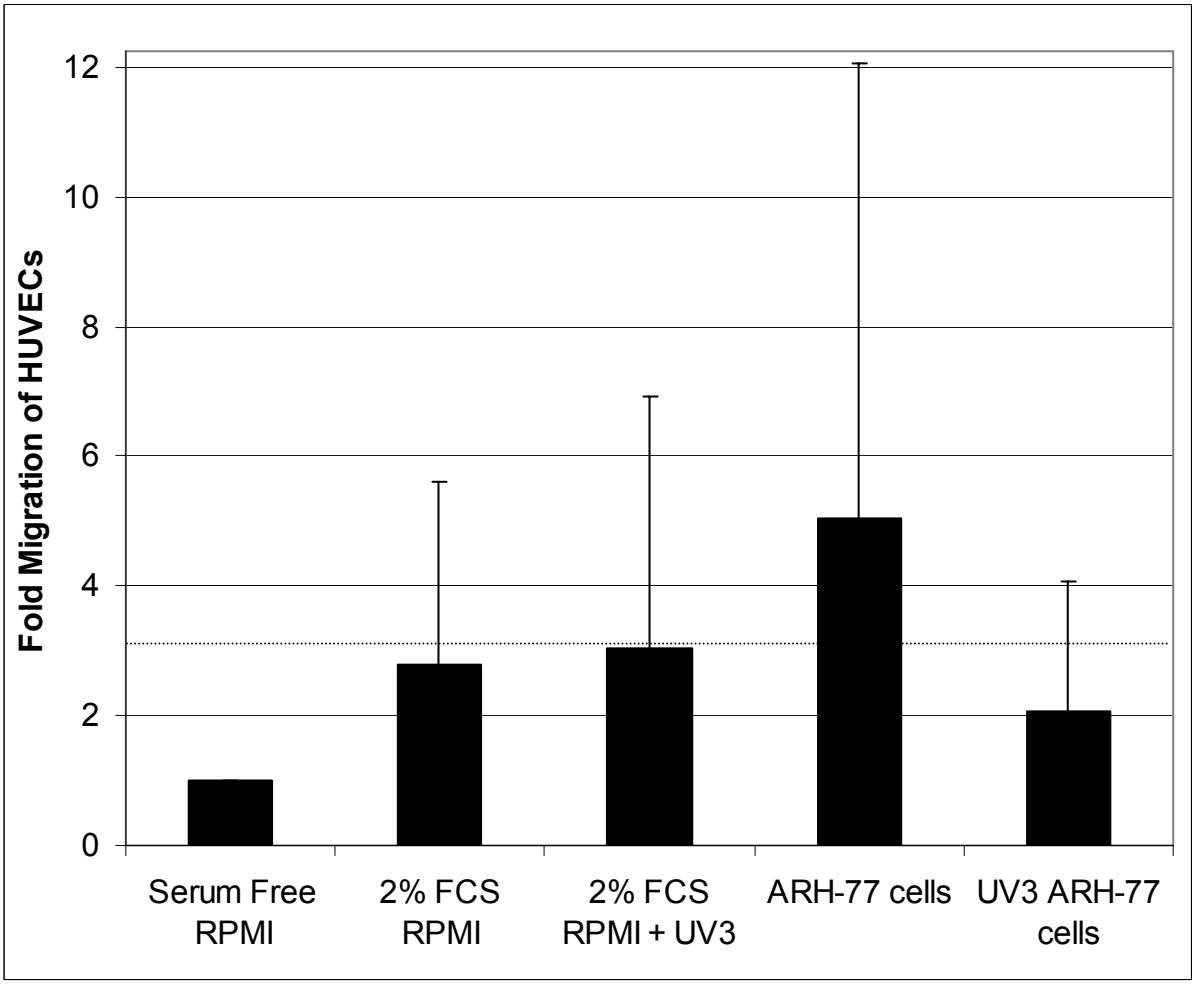
Fold Migration of HUVECs
12
10
8
6
4
2
0
Serum Free RPMI
2% FCS RPMI
2% FCS RPMI + UV3
ARH-77 cells
UV3 ARH-77 cells

C. Treatment of Cells with UV3 Did Not Alter Angiogenesis

UV3 Did Not Demonstrate a Decrease in the Expression of Angiogenic Genes Using Other Microarrays.

Microarrays have become a common technique used to analyze the expression levels of multiple genes at one time. This technique allows one to identify all of the genes expressed in a preparation of RNA. By comparing the expression profiles of two or more RNA preparations, one can obtain a profile of the genes transcribed under various conditions.

There are different types of microarrays. The SuperArray microarrays are nylon membrane arrays that are printed with cDNA fragments of specific genes, and the arrays used contain cDNA fragments for 20 genes involved in angiogenesis. The Microarray Core Oligo Arrays are glass slides printed with oligonucleotides that are unique for a given gene, and each microchip screens over 15,000 genes. The Affymetrix Arrays are also glass slide microchips, and each microchip screens over 20,000 genes. The membrane arrays have the advantage of being more sensitive, particularly when using ^{32}P. In addition, the smaller set of data allows one to focus in on the pathway in question. On the other hand, the advantages of the glass slides is that one can obtain more precise data for both a larger number and broader array of genes, which allows one to examine the effect of a given treatment on multiple pathways.

In order to study the effect of UV3 on the angiogenesis pathway and to determine whether UV3 altered gene expression in other pathways, RNA isolated from ARH-77 cells cultured in the presence of UV3 or an isotype control Ig was evaluated using oligo microarrays from the Microarray Core facility at UT Southwestern and the human U-133 2+ microarray from Affymetrix. **Table 2** compares the expression data obtained from the genes in the membrane microarray with expression data from the oligo microarray and Affymetrix microarray. The membrane microarrays demonstrated that several genes involved in angiogenesis are expressed by ARH-77 cells, and that UV3 significantly decreased the expression of the pro-angiogenic genes Angiopoietin-1, FGFR-3, and VEGF-D. However, in both microchip arrays, the same set of angiogenic genes was either not expressed or the expression level did not change by even 2 fold following UV3 treatment (**Table 2**).

In the oligo arrays, expression data from UV3-treated ARH-77 cells that changed two fold or more from isotype control-treated cells did not include any genes known to be involved in angiogenesis. In the Affymetrix array, expression data from UV3-treated ARH-77 cells demonstrated a 93% decrease in FGF-18 and an 81% decrease in FGF-5 compared to data from isotype control RNA. However, these affected genes represent only a small portion of all the angiogenic genes tested in each of the arrays. This suggests UV3 may not target the angiogenesis pathway. In addition, the microchip assays did not reveal UV3-induced expression changes that were targeted to any other pathway.

Angiopoietin-1 Expression Was Not Measurable by Quantitative PCR.

Using membrane microarrays, UV3-treated ARH-77 cells demonstrated a significant decrease in the expression of the pro-angiogenic gene Angiopoietin-1. In order to confirm and more precisely quantitate the expression of angiopoietin-1, RNA isolated from ARH-77 cells was reverse transcribed into cDNA and quantitated relative to a reference cDNA. When saturating amounts of ARH-77 cell cDNA were used, Angiopoietin-1 was amplified, but the expression of Angiopoietin-1 was not measurable (**Figure 14**). The range of concentrations used to obtain the standard curve was lowered and the number of amplification cycles was increased, but expression of Angiopoietin-1 was not measurable.

SuperArray Membrane Microarrays Did Not Reveal a UV3-Mediated Decrease in Angiogenic Gene Expression in Other Multiple Myeloma Cell Lines.

Other multiple myeloma cell lines cultured in the presence of UV3 or an isotype control antibody were examined using the membrane microarrays from SuperArray, Inc. to determine whether they would show a similar decrease in the expression of angiogenic genes. As illustrated in **Figure 15**, U-266 cells did not demonstrate a significant decrease in Angiopoietin-1 (P=0.87), FGFR-3 (P=0.63), or VEGF-D (P=0.81) following UV3 treatment. In two experiments with NCI-H929 cells, which were high expressers of Angiopoietin-1 and VEGF-D (**Figure 3**), there was no significant difference in the expression of Angiopoietin-1 (P=0.7) or

VEGF-D (*P*=0.4) in UV3-treated samples (data not shown). These data suggest that the anti-angiogenic effect of UV3 demonstrated in the membrane microarrays does not correlate with an anti-myeloma effect.

UV3 Did Not Affect the Secretion of VEGF by ARH-77 cells.

Using an ELISA assay, the levels of VEGF were examined in cell supernatants harvested from ARH-77 cells cultured for 24 or 48 hours in complete medium alone, complete medium with UV3, complete medium with an isotype control antibody, or in complete medium with UV3 added immediately prior to harvest. Out of four experiments performed on cell supernatants from 24 hour cultures, two experiments showed a minor decrease in VEGF secretion from UV3-treated ARH-77 cells, and the other two experiments showed no change in the VEGF secretion from UV3-treated ARH-77 cells. An additional two experiments performed on cell supernatants from 48 hour culture demonstrated that there was no change in the levels of VEGF among any of the cell supernatants tested (**Figure 16**). Collectively, these data demonstrate that UV3 treatment does not inhibit VEGF secretion by ARH-77 cells.

UV3 Did Not Significantly Affect the Secretion of VEGF in Other Human Multiple Myeloma Cell Lines.

VEGF levels were evaluated in cell supernatants from other multiple myeloma cell lines cultured for 48 hours in complete medium alone, complete medium with UV3, complete medium with an isotype control antibody, or in complete medium with UV3 added immediately prior to harvest. There was no significant difference in VEGF secretion between UV3-treated or control-treated HS-Sultan (P=0.7), IM-9 (P=0.4), or ILKM2 (P=0.2) human multiple myeloma cells (**Figure 17**). The fact that UV3 does not appear to interfere with VEGF secretion from any multiple myeloma cell line suggests that VEGF is not an important target in the UV3-mediated anti-tumor pathway.

Table 2. UV3 Did Not Induce a Decrease in the Expression of Angiogenic Genes as Determined by Other Microarrays

Gene Involved in Angiogenesis:	**SuperArray, Inc.** **% Decrease in Normal Gene Expression**	**Microarray Core Oligo Arrays**	**Affymetrix Human U-133 2+**
Angiopoietin-1	69*	Not Measurable	Not Measurable
Angiogenin	52	Not Measurable	Not Measurable
Collagen Type 18	45	Not Measurable	Not Measurable
Endothelin Receptor Type B	53	Not Measurable	< 2 fold Decrease
FGFR-3	42*	Not Measurable	< 2 fold Decrease (1/3 clones)
IFN-α 2	35	Not Measurable	Not Measurable
PAI	38	Not Measurable	Not Measurable
Prolactin	26	Not Measurable	Not Measurable
TGF-α	15	Not Measurable	< 2 fold Decrease (1/3 clones)
Tie-2	32	Not Measurable	Not Measurable
VEGF	42	No change in expression (2/3 replicates)	< 2 fold Decrease (3/4 clones)
VEGF-D	37*	Not Measurable	Not Measurable

* - represents a significant decrease

Table 2.

RNA was isolated from ARH-77 cells cultured in the presence of UV3 or the isotype control antibody, 13G10. In the SuperArray, Inc. microarray, the RNA was reverse transcribed in the presence of ^{32}P. In the Microarray Core Facility oligo arrays, aRNA was prepared from the cDNA and labeled with either Cy-3 or Cy-5, whereas in the Affymetrix human U-133 2+ array, biotin-labeled aRNA was used. The labeled cDNA or aRNA was hybridized to the respective membrane or microchip, as described in the methods. Microarray data from UV3-treated ARH-77 cells were analyzed for changes in the expression of angiogenic genes relative to the isotype-treated ARH-77 cells. As illustrated in Table 2 and Figure 9, the SuperArray membrane array demonstrated that UV3 decreased the expression of many genes involved in angiogenesis, and UV3 significantly decreased the expression of Angiopoietin-1, FGFR-3, and VEGF-D. However, in both microchip arrays, the signals from the same angiogenic genes were either non-existent, below background levels, not reproducible, or the expression of the genes in UV3 treated cells were not altered by 2-fold. The SuperArray data represent the average of greater than 7 experiments. The Microarray Core Oligo array experiments were performed 3 times, and the Affymetrix microarray data are based on one experiment performed.

Figure 14. Angiopoietin-1 Expression was Not Measurable Using Quantitative PCR.

ARH-77 RNA and Strategene's Human Reference RNA was reverse transcribed to cDNA in the presence or absence of reverse transcriptase. PCR reactions for angiopoietin-1 were set up in duplicate containing 1000 pg/µl, 200 pg/µl, 100 pg/µl, 50 pg/µl, or 10 pg/µl of the reference cDNA and 2000 pg/µl of ARH-77 cDNA, which was a saturating amount. The various concentrations of the reference cDNA were used to generate a standard curve of angiopoietin-1 expression. As illustrated in the graph below, the levels of expression for angiopoietin-1 in 3 different preparations of RNA from untreated ARH-77 cells were not measurable. This graph is representative of greater than 3 experiments performed.

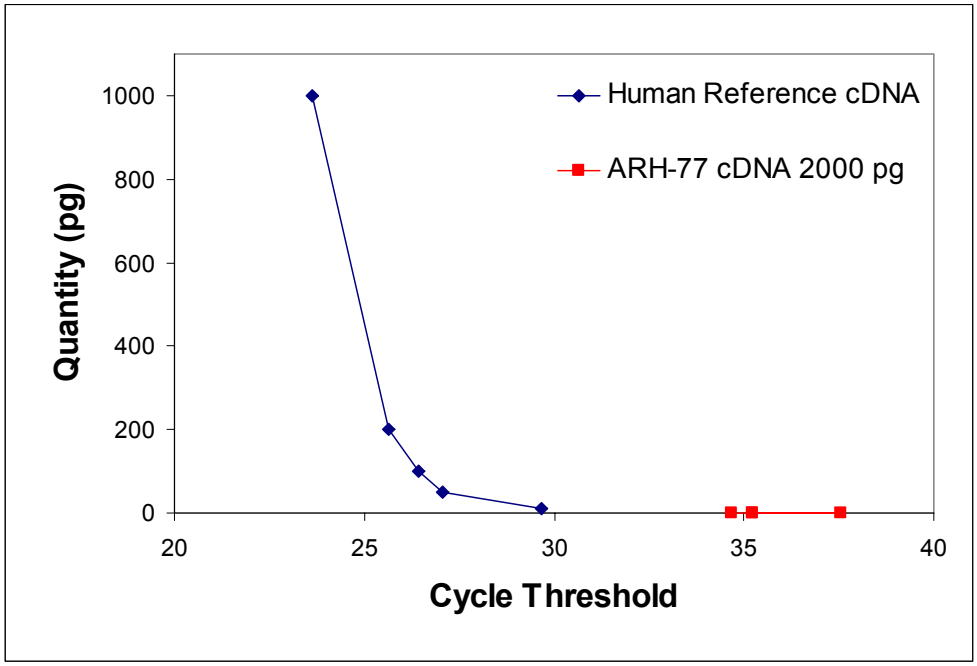

Figure 15. As Determined by SuperArray Analysis, UV3 Did Not Decrease Angiogenic Gene Expression in Other Human Multiple Myeloma Cell Lines.

RNA was isolated from U-266 cells cultured in the presence of UV3 or from U-266 cells that received UV3 immediately before harvest. U-266 RNA was reverse transcribed into cDNA in the presence of ^{32}P. The radiolabeled probes were hybridized to respective SuperArray membranes, and the data were analyzed by comparing the intensity of radioactivity of individual angiogenic genes to that of the positive controls. There was no significant change in the expression of Angiopoietin-1 (*P*=0.87), FGFR-3 (*P*=0.63), or VEGF-D (*P*=0.81) following UV3 treatment of U-266 cells. The graph represents an average of 3 experiments.

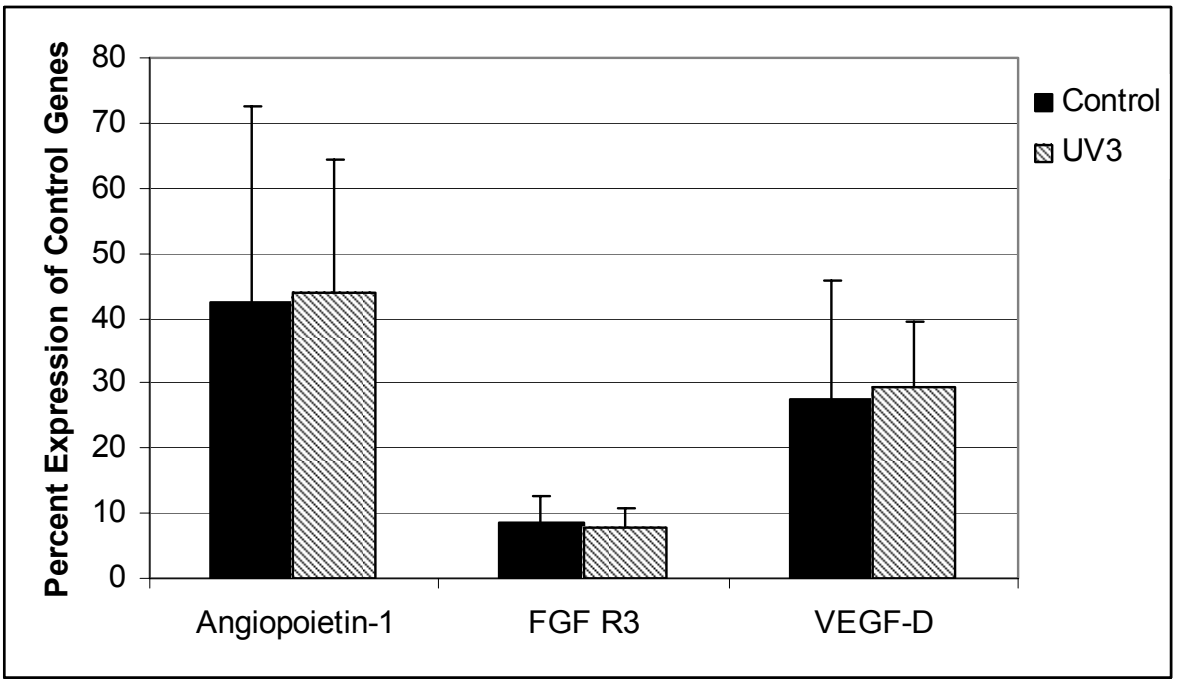

Figure 16. UV3 Did Not Affect the Secretion of VEGF by ARH-77 cells.

ARH-77 cells were cultured for 48 hours in complete medium (untreated), or in complete medium containing 100 µg/ml of UV3 or isotype control Ig, or they were cultured in complete medium and received UV3 immediately prior to harvesting (sham). Cells cultured as described were collected and centrifuged, and their respective supernatants were tested for the presence of VEGF using an ELISA assay. UV3 treated ARH-77 cells showed no change in levels of VEGF compared to controls (*P*=0.5). This graph is an average of 2 experiments.

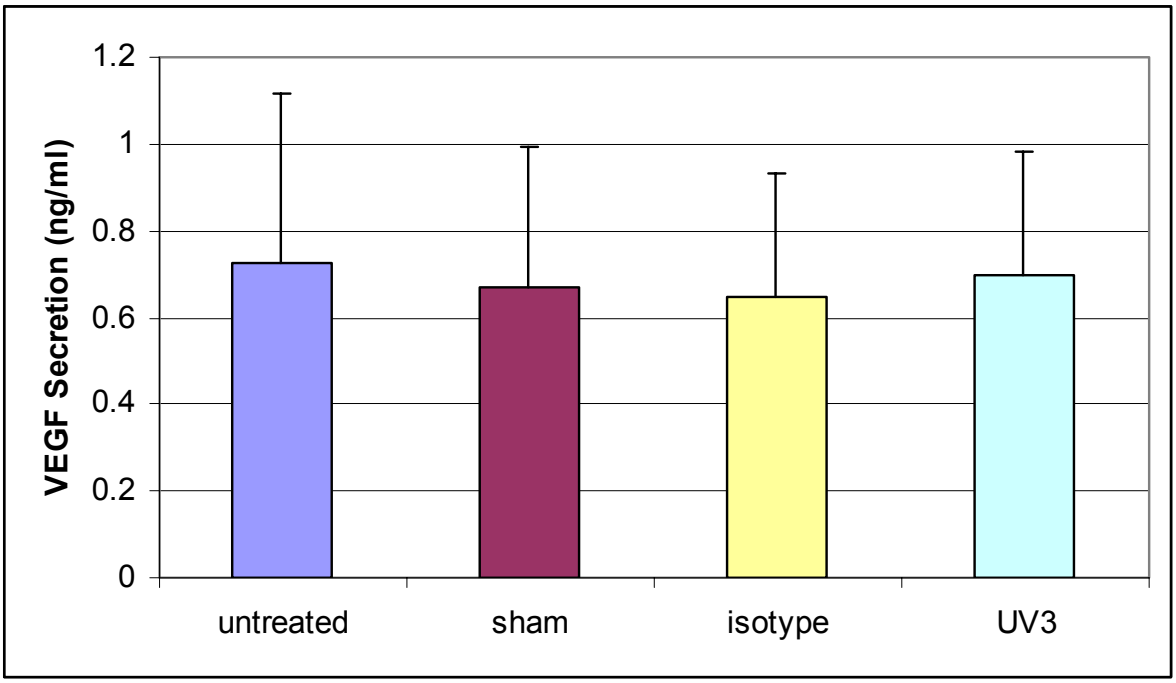

Figure 17. UV3 Did Not Significantly Alter the Secretion of VEGF in Other Human Multiple Myeloma Cell Lines.

HS-Sultan, IM-9, and ILKM2 cells were cultured in complete medium (untreated), or in complete medium containing 100 µg/ml of UV3 or isotype control Ig, or they were cultured in complete medium and received UV3 immediately prior to harvesting (sham). Cells were collected and centrifuged. Levels of VEGF in cell supernatants were measured using an ELISA. UV3 did not significantly inhibit the secretion of VEGF by HS-Sultan cells (*P*=0.7), IM-9 cells (*P*=0.4), or in ILKM2 cells (*P*=0.2) as compared to the controls. These results are based on the average of 2 experiments.

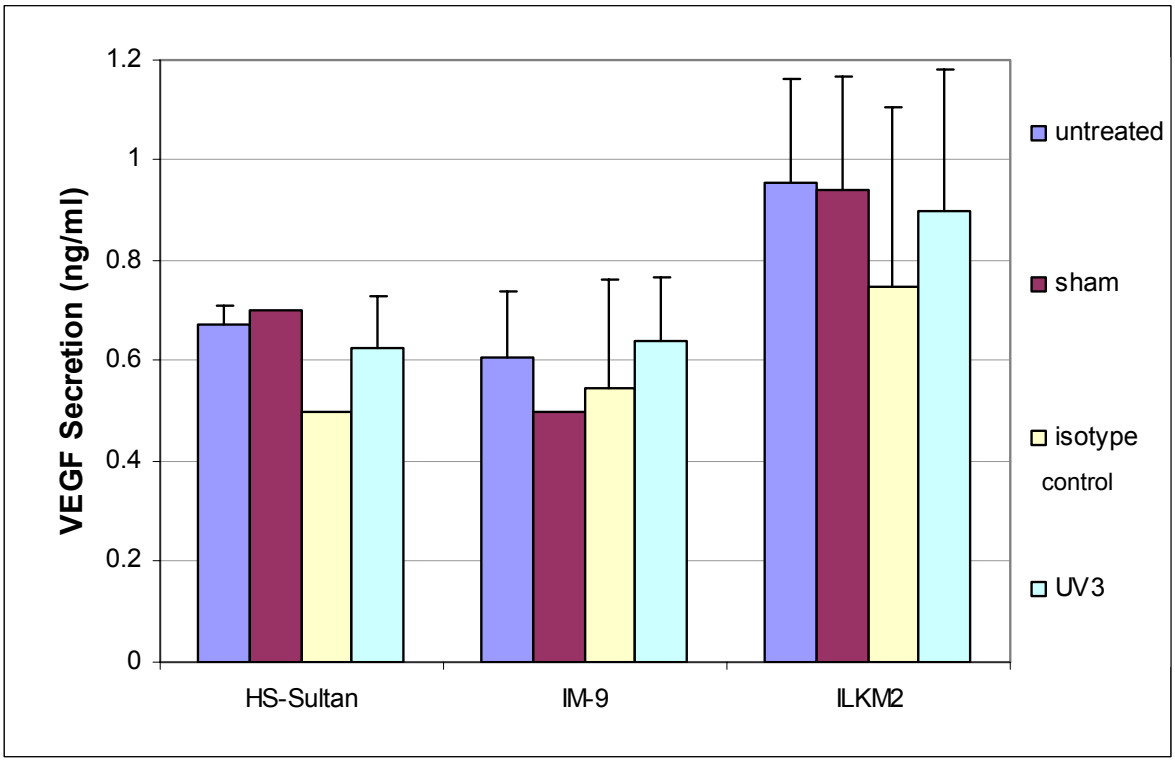

D. The Fc Portion of UV3 is Critical to its Anti-Tumor Activity

Effector Functions are the Predominant Mechanism of Anti-Tumor Activity of Monoclonal Antibodies

Previous data demonstrated that UV3 can induce both ADCC and CDC *in vitro* (150). However, the data suggested that UV3 did not act solely via effector mediated functions *in vivo* since $F(ab)'_2$ preparations of UV3 effectively prolonged the survival of SCID mice with ARH-77 multiple myeloma (92). This prompted an exploration of additional mechanisms underlying the anti-tumor activity of UV3.

In studies evaluating the mechanism of action of other monoclonal antibodies, it has been demonstrated that therapeutic antibodies can induce apoptosis or cell cycle arrest, mediate ADCC or CDC, or block signaling cascades such as angiogenesis (69). Most of these data are derived from *in vitro* studies. In some cases, antibodies are reported to utilize multiple mechanisms to mediate anti-tumor activity (67,71). Despite the many mechanisms by which antibodies mediate anti-tumor activity, a recent study in a mouse xenograft model demonstrated that the predominant mechanism of action of at least two therapeutic antibodies was related to their ability to mediate effector functions (71). Considering these new findings, the role of UV3 in mediating effector functions was re-evaluated.

In order to determine whether F(ab)'$_2$ preparations used previously (92) may have been contaminated with amounts of IgG sufficient to mediate effector function, F(ab)'$_2$ fragments of UV3 were concentrated to greater than 5 mg/ml and examined by gel electrophoresis. A faint IgG band appeared in the lane with the F(ab)'$_2$ fragments (data not shown). In order to determine whether the contaminating IgG may have influenced previous *in vivo* findings, new F(ab)'$_2$ fragments of UV3 were prepared for *in vivo* studies using additional purification steps to acquire highly purified preparations of F(ab)'$_2$. This "ultra-pure" F(ab)'$_2$ preparation was concentrated to greater than 5 mg/ml and evaluated by gel electrophoresis. As illustrated in lane 2 of **Figure 18**, no IgG bands appear with the ultra-pure F(ab)'$_2$ fragments. Lane 3 of **Figure 18**, however, illustrates a F(ab)'$_2$ preparation with 20% of the IgG dose added to the preparation. These preparations of UV3, ultra-pure F(ab)'$_2$, ultra-pure F(ab)'$_2$ with 20% IgG, the chimerized (c) UV3 monoclonal antibody and the isotype-matched control that are illustrated in **Figure 18** were used in further *in vivo* studies to address the role of UV3 in mediating effector functions.

Ultra-Pure UV3 F(ab)'$_2$ Bound to Multiple Myeloma Cells

The ultra-pure UV3 F(ab)'$_2$ was tested by flow cytometry to confirm that it bound to ARH-77 cells as well as UV3 IgG. As illustrated in **Figure 19**, ultra-pure UV3 F(ab)'$_2$ bound to 91% of ARH-77 cells, and UV3 IgG bound to 85% of ARH-77 cells. Twenty-two percent of the cells were positive when the isotype-

matched control was used. There was no significant difference between the number of cells stained with UV3 IgG vs. UV3 F(ab)'$_2$ (*P*=0.08).

Ultra-Pure UV3 F(ab)'$_2$ Did Not Prolong the Survival of SCID Mice with Multiple Myeloma.

In order to determine whether ultra-pure F(ab)'$_2$ fragments of UV3 would prolong the survival of NOD/SCID mice with advanced ARH-77 multiple myeloma, tumor-bearing mice were injected with 4 µg/g of cUV3, 8 µg/g of ultra-pure UV3 F(ab)'$_2$, or 4 µg/g of an isotype control antibody on days 14-17. As shown in **Figure 20**, all the mice receiving the ultra-pure F(ab)'$_2$ preparation of UV3 developed hind-leg paralysis or severe illness by day 65. Compared to control mice, there was no prolongation in the survival of mice receiving the ultra-pure F(ab)'$_2$. However, mice receiving cUV3, which was previously shown as effective as UV3 (150), demonstrated a significant increase in survival. This lack of therapeutic effect by ultra-pure F(ab)'$_2$ was also demonstrated in mice that received 20 µg/g of ultra-pure F(ab)'$_2$ (data not shown), and since the purity of a F(ab)'$_2$ preparation is still ultimately determined by what bands are visible, the absence of an anti-tumor effect at high doses of ultra-pure F(ab)'$_2$ confirms the absence of IgG in the F(ab)'$_2$ preparation. These data suggest that effector functions may be responsible for the predominant anti-tumor activity of UV3 *in vivo*. In addition, the change in survival results induced by the ultra-pure F(ab)'$_2$ suggests that previous *in vivo* studies using UV3 F(ab)'$_2$ may have had a small

amount of IgG in the preparation, which further suggests that lower doses of UV3 IgG may be highly effective in prolonging advanced multiple myeloma.

Figure 18. SDS-Page Analysis of the Purity of Ultra-pure UV3 F(ab)'$_2$

The UV3 hybridoma cell line was cultured, and UV3 was purified by affinity chromatography on a protein G sepharose column. Ultra-pure F(ab)'$_2$ fragments were purified from pepsin digests of UV3 by utilizing a Protein A column to remove any remaining IgG, followed by high performance liquid chromatography (HPLC) to separate F(ab)'$_2$ fragments from Fab' fragments. UV3 IgG, ultra-pure UV3 F(ab)'$_2$, and other preparations used in the *in vivo* experiments were electrophoresed on a 4-15% SDS page gel to test and compare the purity of the preparation. Lane 1 – UV3 IgG; Lane 2 – UV3 F(ab)'$_2$ ultra-pure; Lane 3 – UV3 IgG plus ultra-pure F(ab)'2 at a ratio of 1:50 (one *in vivo* dose of F(ab)'$_2$ plus 20% of one *in vivo* dose of IgG); Lane 4 – cUV3; Lane 5 – isotype control.

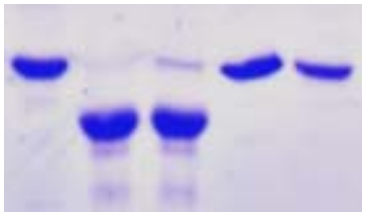

Lanes: 1 2 3 4 5

Figure 19. Ultra-Pure UV3 F(ab)'$_2$ Bound to ARH-77 Cells.

UV3 IgG, UV3 F(ab)'$_2$, and an isotype-matched control antibody were labeled with FITC and incubated with ARH-77 cells for 30 minutes on ice. Unbound antibody was removed by washing cells in PBS, and the amount of antibody bound to the cells was quantitated by FACS. Ultra-pure F(ab)'$_2$ fragments of UV3 bound to ARH-77 cells, and the percent of positive cells was comparable to that of the IgG. This graph represents the average of 3 experiments.

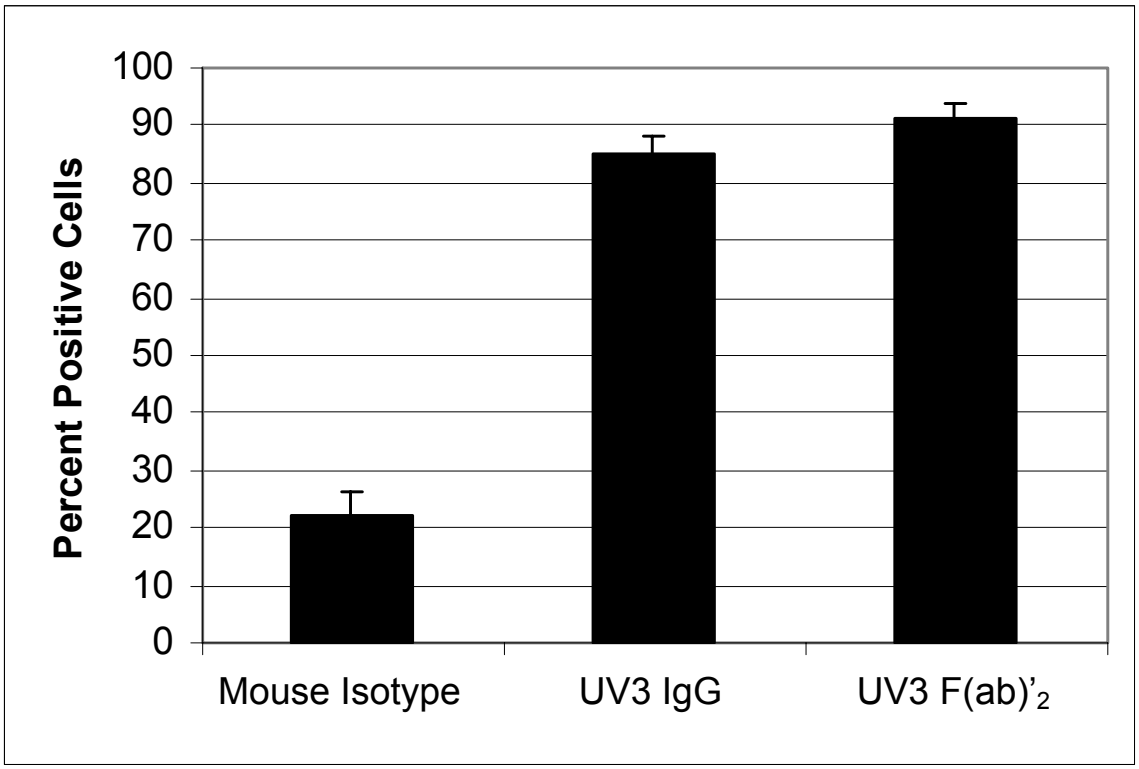

Figure 20. Ultra-Pure UV3 F(ab)'$_2$ Did Not Prolong Survival of SCID mice with Multiple Myeloma.

Female NOD/SCID mice at 6-7 weeks of age were irradiated with 150 rads, and 24 hours later, the mice were injected with 10^7 ARH-77 cells. On days 14-17 following tumor cell injection, mice received daily i.v. doses of one of the following: a PBS control, ultra-pure UV3 F(ab)'$_2$ (8 µg/g body weight), or cUV3 (4 µg/g body weight). Mice were sacrificed when they developed hind-leg paralysis or had lost 20% of their body weight. Mice receiving the dose of ultra-pure F(ab)'$_2$, showed no significant increase in survival as compared to control mice (*P*=0.76). Treatment with cUV3 significantly prolonged the survival of SCID/ARH-77 mice (*P*=0.02). This graph depicts one experiment of 3 performed.

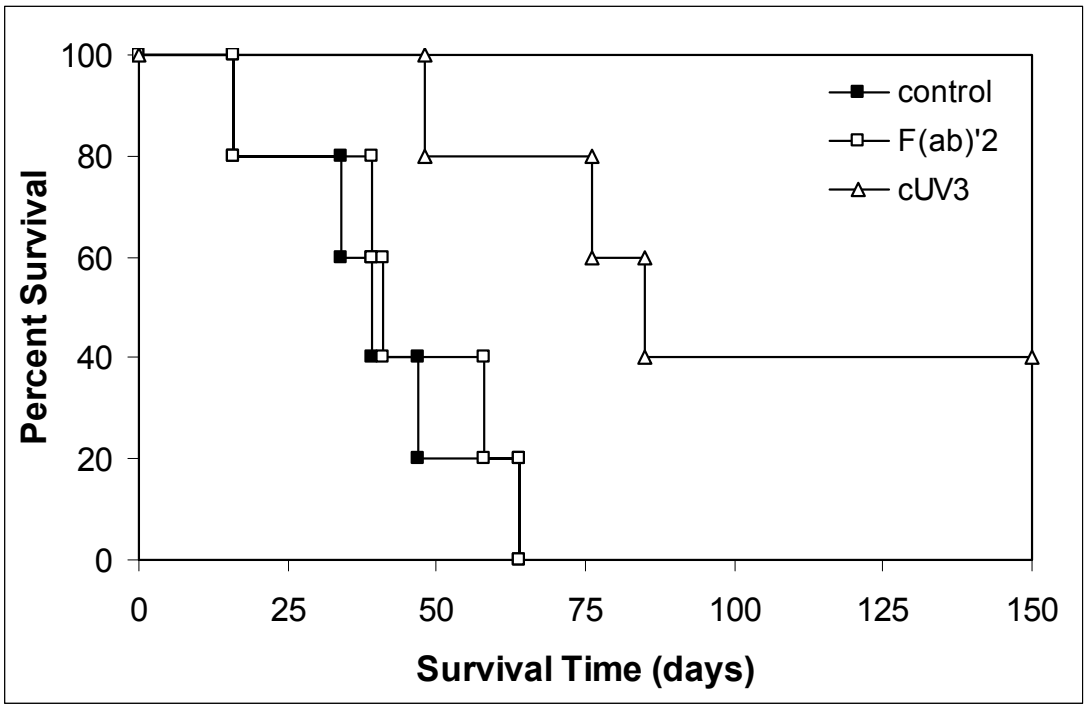

E. UV3 was Highly Effective in Treating SCID Mice with Daudi Human Burkitt's Lymphoma

UV3 was very effective in treating both early and advanced multiple myeloma in SCID mice (92). In order to determine whether UV3 might be a beneficial therapy for other hematopoietic tumors, the efficacy of UV3 and cUV3 in early stage human Burkitt's lymphoma (Daudi) was examined. In addition, the anti-tumor activity of UV3 was further explored with studies examining the role of UV3 in mediating effector functions in SCID mice xenografted with Daudi lymphoma cells.

UV3 IgG, UV3 F(ab)'$_2$, and cUV3 Bound to Daudi Lymphoma Cells

UV3 IgG, UV3 F(ab)'$_2$, cUV3 and control IgG's were evaluated by flow cytometry to determine whether each could bind to the human Burkitt's lymphoma cell line, Daudi. As shown in **Figure 21**, 58% of Daudi cells were positively stained by UV3 IgG, while 80% of the cells were positively stained by the ultra-pure UV3 F(ab)'$_2$. Twelve percent of Daudi cells were stained by the isotype-matched control in a direct immunofluorescent assay. In 3 experiments, there was no significant difference between the percent of Daudi cells stained with UV3 IgG vs. the ultra-pure F(ab)'$_2$ (P=0.11). In an indirect immunofluorescent assay, 94% of Daudi cells were stained by cUV3, and 21% were stained by the isotype control. Considering the standard deviations

between assays and the slightly higher number of cells stained positively by the human isotype control, there was no difference between the ability of UV3 and cUV3 to bind to Daudi lymphoma cells.

UV3 Significantly Prolonged the Survival of Mice with Daudi Lymphoma

In order to determine whether UV3 would prolong the survival of SCID mice with Daudi lymphoma, tumor-bearing mice received PBS or 0.8 μg/g of UV3 or an isotype control antibody on days 1-4 following tumor cell injection. As shown in **Figure 22**, all mice that received PBS or the isotype control antibody developed hind-leg paralysis by day 55, with an average survival of approximately 30 days. Mice that received UV3 survived up to 107 days, with an average survival of 60 days. These data demonstrate that UV3 extends the survival time of mice with Daudi lymphoma by two-fold (P=0.003).

Ultra-Pure UV3 F(ab)'$_2$ Significantly Prolonged the Survival of Mice with Daudi Lymphoma

The ability of ultra-pure UV3 F(ab)'$_2$ to prolong the survival of SCID mice with Daudi lymphoma was evaluated. Tumor-bearing mice received either PBS, 0.8 μg/g of UV3 IgG, 0.8 μg/g of an IgG isotype control antibody, or 8 μg/g of ultra-pure UV3 F(ab)'$_2$ on days 1-4 following tumor cell injection. As shown in **Figure 23**, mice that received ultra-pure UV3 F(ab)'$_2$ survived 1.36 times longer than mice that received PBS, and mice that received UV3 IgG survived 1.95

times as long as mice that received PBS. These data demonstrate that, as compared to the isotype control, ultra-pure UV3 F(ab)'$_2$ significantly prolonged the survival of mice with Daudi lymphoma (*P*=0.002). However, treatment with UV3 IgG was superior to treatment with F(ab)'$_2$ (*P*=0.001). This suggests that although the binding alone of UV3 to Daudi cells has some anti-tumor activity, the predominant mechanism of anti-tumor activity of UV3 is dependent upon the Fc portion of the antibody.

Small Amounts of UV3 IgG in the Ultra-Pure F(ab)'$_2$ Dose Reproduced the Effect Observed with UV3 IgG Alone.

In order to determine whether a small amount IgG in the F(ab)'$_2$ preparation could reproduce the therapeutic effect achieved with UV3 alone, 10, 20, or 30% of a UV3 IgG dose was added to a dose of ultra-pure F(ab)'$_2$ and tested in SCID mice with Daudi lymphoma. On days 1-4 following tumor cell injection, mice received PBS, 0.8 µg/g of UV3 IgG, 0.8 µg/g of an isotype control antibody, or 8 µg/g of ultra-pure F(ab)'$_2$ containing 0.08 µg/g, 0.16 µg/g, or 0.24 µg/g of IgG. As shown in **Figure 24**, mice that received UV3 survived up to 107 days, with an average survival of 60 days. Mice that received ultra-pure F(ab)'$_2$ plus 20% IgG survived up to 150 days, with an average survival of 77 days. These data demonstrate that, as compared to the isotype control, the addition of 20% IgG to ultra-pure F(ab)'$_2$ can significantly prolong survival of SCID mice with Daudi lymphoma (*P*=0.004). In addition, there was no significant difference in the

survival of mice that received a full dose (0.8 μg/g) of IgG or a 20% dose (0.16 μg/g) of IgG (*P*=0.33), suggesting that less UV3 IgG may achieve the same anti-tumor effect.

cUV3 Significantly Prolonged the Survival of Mice with Daudi Lymphoma.

The therapeutic effect of cUV3 was tested *in vivo* to determine whether cUV3 could prolong the survival of SCID mice with Daudi lymphoma in a manner comparable to that of UV3. Tumor-bearing mice received PBS, 0.8 μg/g of UV3 IgG, 0.8 μg/g of cUV3, or 0.8 μg/g of an isotype control antibody on days 1-4 following tumor cell injection. Mice that received cUV3 treatment survived up to 96 days, with an average survival of 59 days (**Figure 25**). cUV3 doubled the survival time of mice with Daudi lymphoma (*P*=0.002), performing as well as mouse UV3 IgG (*P*=0.89).

UV3 Did Not Affect the Proliferation of Daudi Lymphoma Cells *In Vitro*.

Daudi lymphoma cells were cultured for 24, 48, or 72 hours with UV3 IgG, an isotype control antibody, or Doxorubicin (positive control). Cells were then pulsed with ^{3}H-thymidine to determine whether UV3 would induce apoptosis or cell cycle arrest in Daudi lymphoma. In each of the time points tested, UV3 had no anti-proliferative effect on Daudi lymphoma cells (**Figure 26**). Doxorubicin, an anti-neoplastic agent, effectively inhibited the proliferation of Daudi cells. This

suggests that UV3 did not induce apoptosis or cell cycle arrest of Daudi lymphoma cells at doses of up to 1 mg/ml.

UV3 Did Mediate ADCC *In Vitro*

UV3 was evaluated for its ability to mediate ADCC of Daudi cells *in vitro*. BALB/c splenocytes were harvested and cultured with IL-2 for 5 days to activate Fc receptor positive NK cells. Daudi cells were labeled with $^{[51]-}$Chromium and incubated with an isotype-matched control antibody, UV3, or rabbit anti-human Ig serum (positive control). Excess antibody was removed by washing cells in serum-free medium, and the effector cells and target cells were mixed at a 10:1, 50:1, or 100:1 ratio and incubated for 4 hours at 37°C in a CO_2 incubator. Cells were centrifuged at 300 x g, and the amount of $^{[51]-}$Chromium remaining in the supernatant was used to calculate cell death. When effector cells were mixed with UV3-treated Daudi lymphoma cells at ratios of 50:1 or 100:1, there was a 13% increase in cell lysis compared to isotype-matched control-treated Daudi cells. The increase in lysis of UV3-treated cells was significant compared to the isotype-matched control treated cells (P=0.05, 50:1; P=0.004, 100:1), and the effect was comparable to the positive control. This suggests that UV3 mediates ADCC of Daudi lymphoma cells *in vitro*.

UV3 Did Not Mediate CDC *In Vitro*

Daudi cells were examined *in vitro* to determine whether UV3 induced CDC. Daudi cells were labeled with $^{[51]-}$Chromium and incubated with an isotype-matched control antibody, UV3, or rabbit anti-human Ig serum (positive control). After the removal of excess antibody, the cells were incubated for 4 hours at 37°C in a CO_2 incubator with various dilutions of rabbit serum (1/5, 1/25, or 1/50). Cells were centrifuged, and the amount of $^{[51]-}$Chromium remaining in the supernatant was used to calculate cell death. In 3 separate experiments, UV3-treated Daudi cells failed to demonstrate any increase in cell death compared to isotype-matched control-treated cells. However, the cells treated with the rabbit anti-human Ig serum had a significantly larger number of dead cells compared to the isotype-matched control-treated cells (P=0.005).

Figure 21. UV3 IgG, UV3 F(ab)'$_2$, and cUV3 Bound to Daudi Lymphoma Cells

Daudi lymphoma cells were collected and incubated with various concentrations of either UV3 IgG, ultra-pure UV3 F(ab)'$_2$, or mouse IgG isotype control antibodies. Unbound antibody was removed by washing cells in PBS, and the degree of antibody staining was measured by flow cytometry. Both UV3 IgG and ultra-pure UV3 F(ab)'$_2$ stained Daudi cells similarly (*P*=0.11). Daudi cells were also incubated with various concentrations of cUV3 or human isotype control antibodies. After washing cells in PBS to remove unbound antibody, the cells were incubated with a FITC-goat anti-human antibody. The secondary antibody was removed by washing cells in PBS, and the degree of antibody staining was measured by flow cytometry.

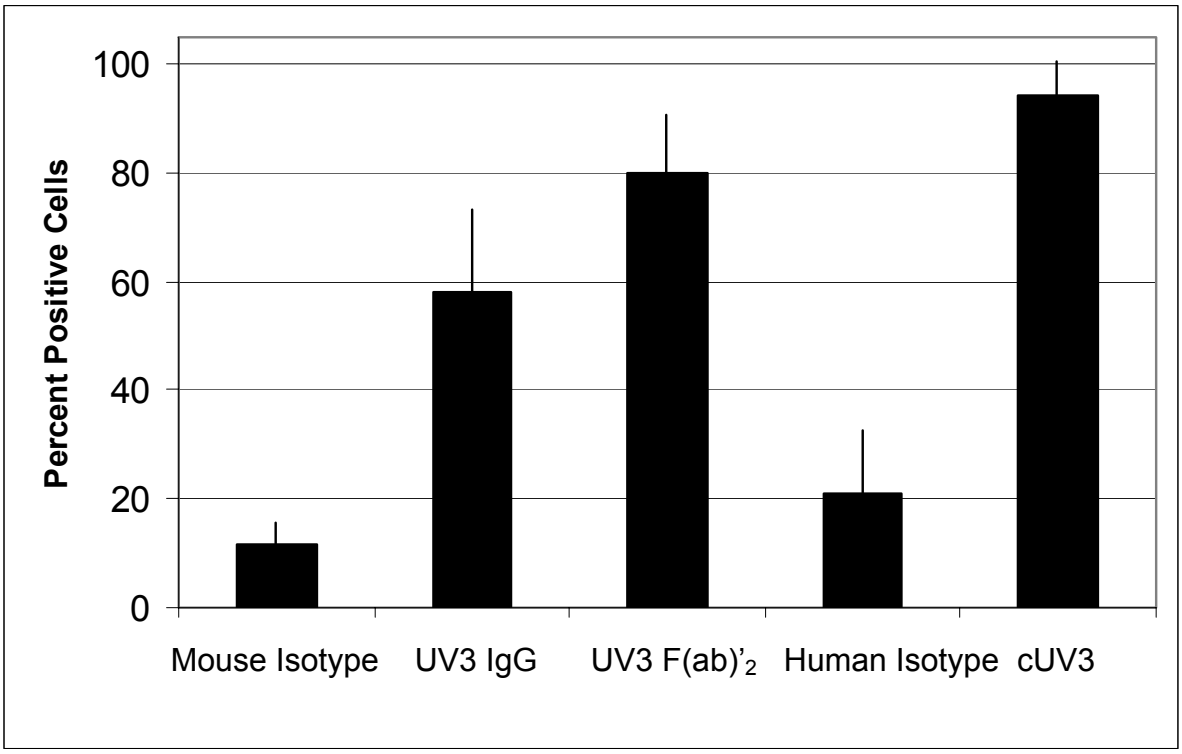

Figure 22. UV3 Significantly Prolonged the Survival of Mice with Daudi Lymphoma

Female SCID mice, 6-7 weeks of age, were injected i.v. with 10^7 Daudi lymphoma cells. Treatment was initiated one day following tumor cell injection, and mice received a single i.v. dose of PBS, isotype control (0.8 μg/g body weight), or UV3 IgG (0.8 μg/g body weight) each day for 4 consecutive days. Mice were sacrificed when they developed hind-leg paralysis. Compared to the isotype control, UV3 IgG significantly prolonged the survival of mice with Daudi lymphoma (*P*=0.003). This graph depicts the average of 3 experiments. In each experiment, there were 5 mice per group. Untreated (●), isotype control (○), and UV3 IgG (▲).

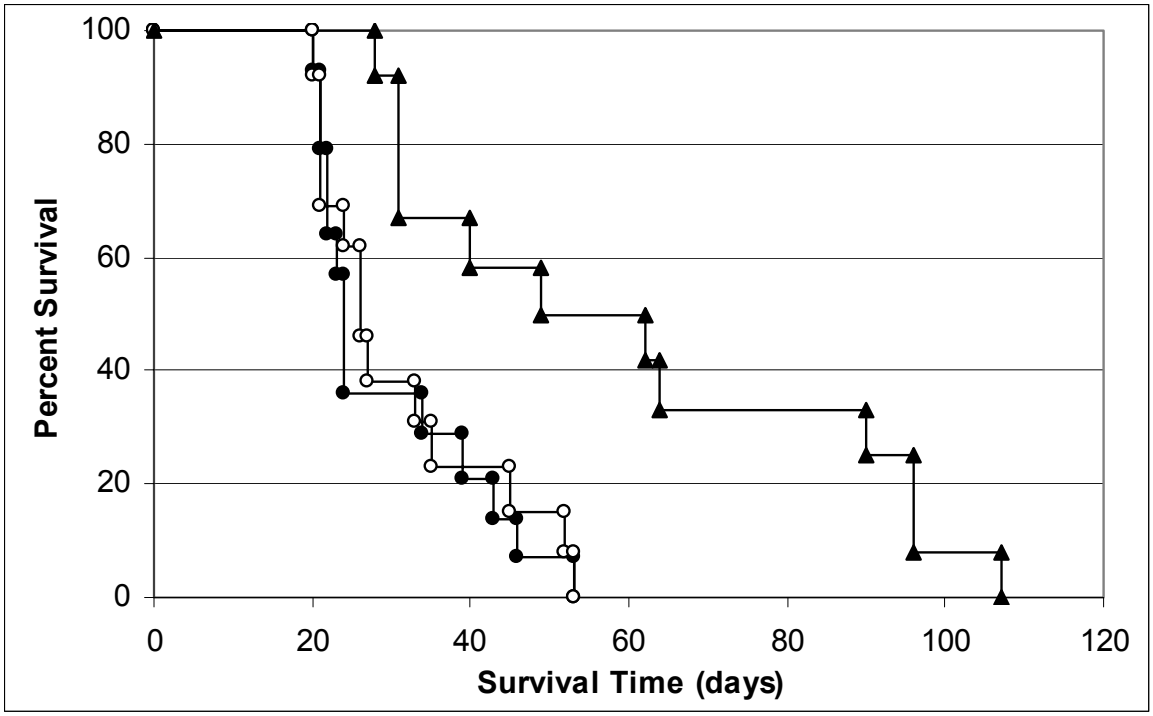

Figure 23. Ultra-Pure UV3 F(ab)'$_2$ Significantly Prolonged the Survival of Mice with Daudi Lymphoma

Female SCID mice, 6-7 weeks of age, were injected with 10^7 Daudi lymphoma cells. Treatment was initiated one day following tumor cell injection, and mice received a single i.v. dose of PBS, isotype control (0.8 µg/g body weight), ultra-pure UV3 F(ab)'$_2$ (20 µg/g body weight), or UV3 (0.8 µg/g body weight) each day for 4 consecutive days. Mice were sacrificed when they developed hind-leg paralysis. The graph depicts the fold increase in survival time of mice with Daudi lymphoma. The bars from left to right represent the survival of untreated mice, mice treated with the isotype control, UV3 F(ab)'$_2$, and with UV3 IgG. Ultra-pure UV3 F(ab)'$_2$ (*P*=0.002) and UV3 IgG (*P*=0.0000003) significantly prolonged the survival of mice with Daudi lymphoma as compared to the isotype control. However, treatment of Daudi lymphoma with UV3 IgG is clearly superior to F(ab)'$_2$ treatment (*P*=0.001). This graph illustrates the average of 3 experiments.

Figure 23.

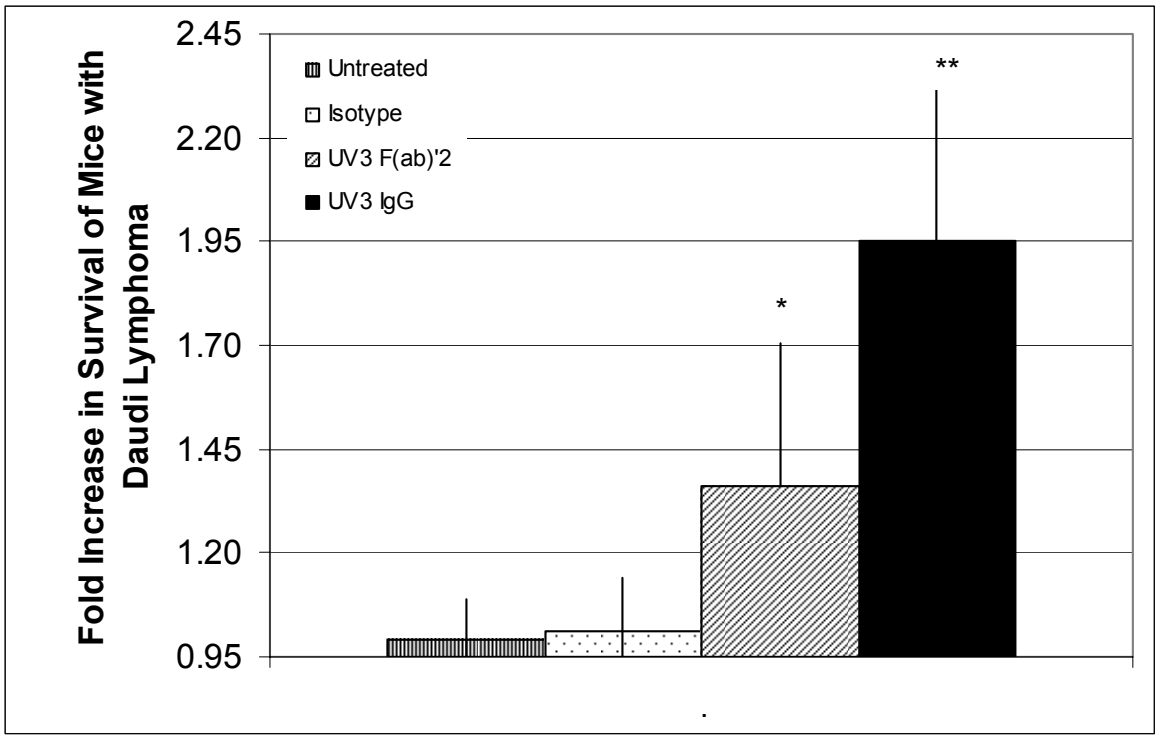
Fold Increase in Survival of Mice with Daudi Lymphoma
2.45
2.20
1.95
1.70
1.45
1.20
0.95
Untreated
Isotype
UV3 F(ab)'2
UV3 IgG
*
**

Figure 24. The Addition of 20% UV3 IgG to a F(ab)'$_2$ Preparation of UV3 was Enough to Reproduce the Anti-Tumor Activity Observed Using UV3 Alone.

Female SCID mice, 6-7 weeks of age, were injected i.v. with 10^7 Daudi lymphoma cells. Treatment was initiated one day following tumor cell injection, and mice received a single i.v. dose of PBS, isotype control (0.8 µg/g body weight), UV3 IgG (0.8 µg/g body weight), or ultra-pure UV3 F(ab)'$_2$ (20 µg/g body weight) plus 20% of the UV3 IgG dose (0.16 µg/g body weight) each day for 4 consecutive days. Mice were sacrificed when they developed hind-leg paralysis. Treatment with UV3 F(ab)'$_2$ that contained 20% IgG significantly prolonged the survival of mice with Daudi lymphoma compared to the isotype control (*P*=0.004). However, there was no significant difference in survival in mice treated with UV3 vs. treatment with F(ab)'$_2$ plus 20% IgG (*P*=0.33). This graph depicts the average of 3 experiments. In each experiment, there were 5 mice per group. Untreated (●), isotype control (○), UV3 IgG (▲), and 20% UV3 IgG (△).

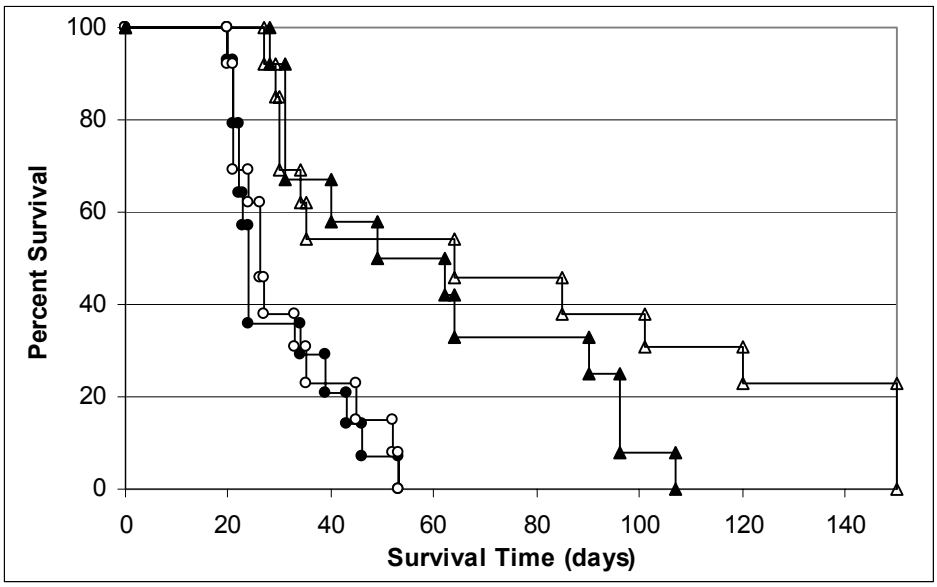

Figure 25. cUV3 Significantly Prolonged the Survival of Mice with Daudi Lymphoma.

Female SCID mice, 6-7 weeks of age, were injected i.v. with 10^7 Daudi lymphoma cells. Treatment was initiated one day following tumor cell injection, and mice received a single i.v. dose of PBS, isotype control (0.8 μg/g body weight), UV3 IgG (0.8 μg/g body weight), or cUV3 (0.8 μg/g body weight) each day for 4 consecutive days. Mice were sacrificed when they developed hind-leg paralysis. Treatment with cUV3 significantly prolonged the survival of mice with Daudi lymphoma compared to the isotype control (*P*=0.002), and cUV3 was equally as effective as UV3 (*P*=0.89) in treating mice with Daudi lymphoma. This graph represents the average of 2 experiments with cUV3 treatment and 3 experiments with UV3 treatment. There were 5 mice per group in the each experiment: untreated (●), isotype control (○), UV3 IgG (▲), and cUV3 (△).

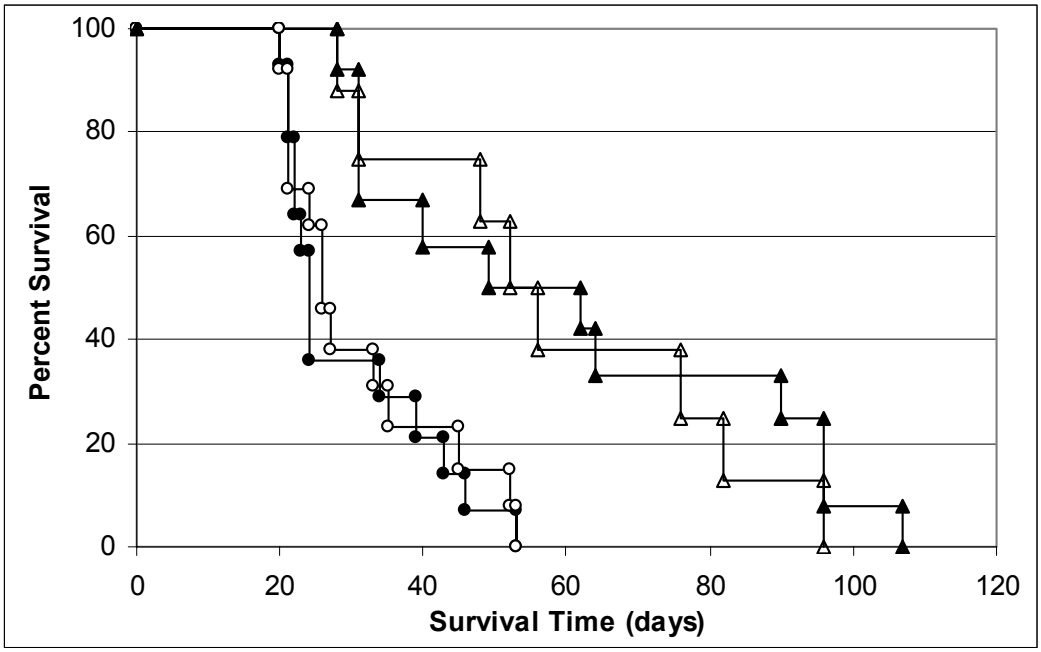

Figure 26. UV3 Did Not Affect the Proliferation of Daudi Lymphoma Cells *In Vitro*.

Daudi lymphoma cells were cultured in the presence of an isotype control, UV3 IgG, or Doxorubicin for 24 hours. The cells were pulsed with ^{3}H-thymidine during the final 8 hours of incubation, and the incorporated radioactivity was measured as a percent of that incorporated by untreated cells. Using up to 1 mg/ml of antibody, UV3 did not inhibit the proliferation of Daudi lymphoma cells (*P*=0.72). This graph is based on an average of 3 experiments.

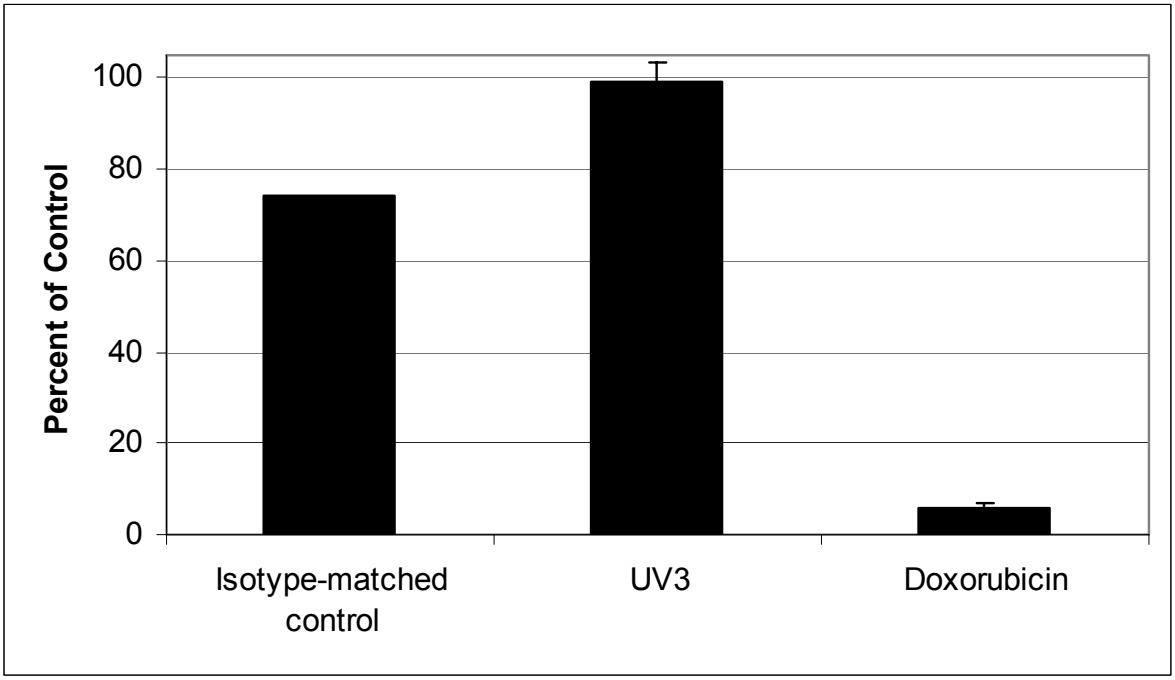

Figure 27. UV3 Mediated ADCC of Daudi Lymphoma Cells, *In Vitro*.

Daudi lymphoma cells were labeled with $^{[51]}$-Chromium and incubated with an excess of isotype-matched control antibody, UV3, or rabbit anti-human Ig serum (positive control). BALB/c splenocytes were isolated and cultured for 5 days in the presence of IL-2. These lymphokine-activated killer cells were then cultured for 4 hours at 37˚C in a CO_2 incubator with Daudi cells at effector to target ratios of 10:1, 50:1, and 100:1. The cells were centrifuged, and the amount of $^{[51]}$-Chromium present in the supernatant was used to calculate cell lysis. Compared to the isotype-matched control, Daudi cells treated with UV3 had a 13% higher specific lysis when cultured with effector cells at a 50:1 and 100:1 ratio. This difference was significant (*P*=0.05, E:T 50:1; *P*=0.004, E:T 100:1), and these results are based on the average of 3 experiments.

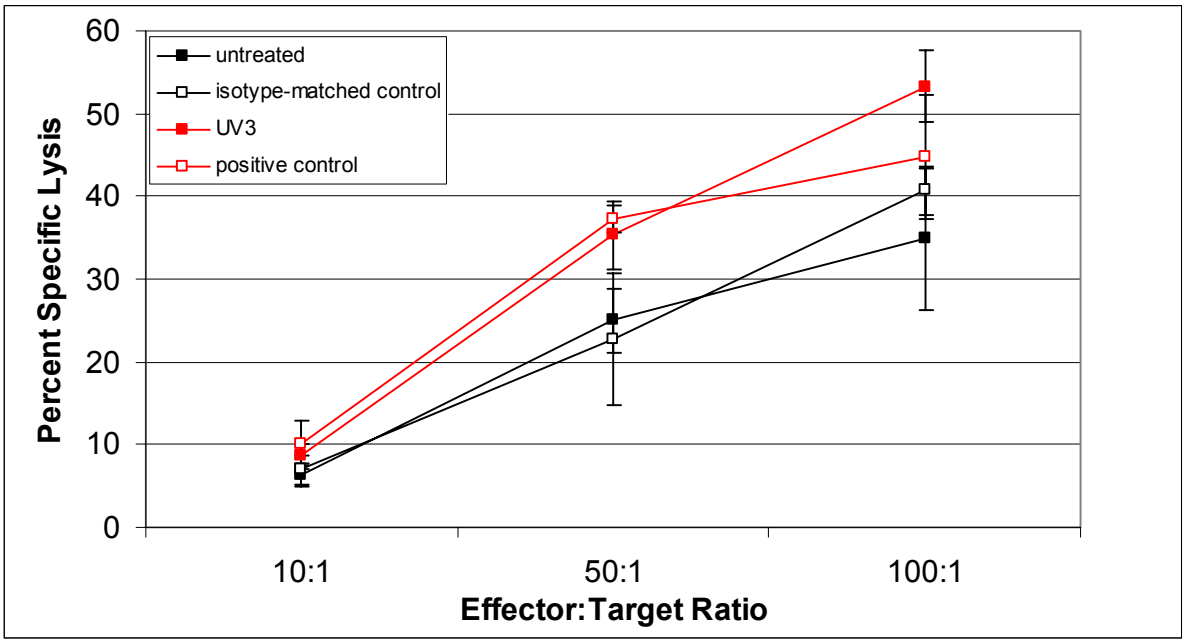

Discussion

A. Multiple Myeloma: an Incurable Disease

Multiple myeloma is responsible for 20% of all hematological malignancy-related mortality (10). If untreated, the average survival of multiple myeloma patients is 17 months. Regardless of the type or dose of the chemotherapeutic agent used, patients who receive chemotherapy have a median survival of 3 years, and patients who receive a combination of chemotherapy with autologous stem cell transplants have a median survival of 5 years (42,53). Multiple myeloma remains an incurable disease.

Despite the prolongation of life, the treatment regimens have significant morbidity, leading to immunosuppression and myelosuppression (42,49). Thalidomide holds promise for patients because, in its native form, it does not induce myelosuppression. However, thalidomide induces neuropathies (54).

B. Monoclonal Antibodies for Immunotherapy

Immunotherapy is an essential tool in the treatment of many diseases, particularly cancer. Passively administered monoclonal antibodies are a type of immunotherapy commonly used because of their specificity and low toxicity, resulting in prolonged survival and a better quality of life for patients. Monoclonal antibodies can destroy their target by inducing apoptosis or cell cycle arrest, inhibiting angiogenesis, blocking the binding of substrates by the tumor cell, and

recruiting effector cells and molecules (67). The unique aspect of monoclonal antibodies lies in their ability to exert a therapeutic effect by utilizing more than one of these mechanisms of action (71). In addition, antibodies can be engineered to further enhance their various functions by increasing antibody avidity, improving their binding to certain Fc receptors, improving tumor penetration, altering the half-life of the antibody, and/or conjugating the antibody to a toxic payload such as a toxin or a radionuclide (67,69,76).

The evidence for the success of monoclonal antibodies is clear. To date, five unconjugated monoclonal antibodies for the treatment of cancer have been approved by the FDA. Rituxan, a chimerized anti-CD20 antibody, has been approved for the treatment of non-Hodgkin's lymphoma (79). Campath, a humanized anti-CD52 antibody, has been approved for the treatment of chronic lymphocytic leukemia (85). Herceptin, a humanized anti-HER-2/neu antibody, has been approved for the treatment of metastatic breast cancer (69,76,82). Avastin, a humanized anti-VEGF antibody, and Erbitux, a chimeric anti-EGFR antibody, have been approved for the treatment of colorectal cancer (2,89). The clinical success of these agents suggests that immunotherapy with monoclonal antibodies may provide a novel avenue of therapy for other cancers as well.

In multiple myeloma, a variety of efforts are underway to explore this possibility. SGN-40, a humanized antibody recognizing CD40, demonstrated a modest cytotoxic effect on multiple myeloma cells from patients and a 2-4 fold reduction in IL-6 production *in vitro* (60). Rituxan, an anti-CD20 antibody,

induced one partial response and 5 stable disease in 19 evaluable multiple myeloma patients. However, few tumors in patients with multiple myeloma express CD20 (52,60). Other target antigens under investigation include anti-CD19, CD38, CD45, CD138, HM1.24, and MUC-1 (52).

C. UV3: a Monoclonal Antibody Against CD54 (ICAM-1)

UV3 was developed in an effort to create a specific monoclonal antibody to treat multiple myeloma. The ultimate goal in generating this monoclonal antibody was to provide not only a change in the therapeutic strategy for multiple myeloma, but also an improved therapeutic option for multiple myeloma patients.

In a SCID xenograft model, the therapeutic success of UV3 was evident in both early and advanced disease. SCID mice injected i.v. with ARH-77 multiple myeloma cells and treated with PBS or an isotype-matched control antibody developed hind-leg paralysis as a result of the growing tumor by day 35 following tumor cell injection. However, tumor-bearing mice treated with UV3 one day following tumor cell injection (early disease), survived for 150 days at which point the experiments were terminated. Mice receiving UV3 at an advanced stage of disease, which was 15 days following tumor cell injection, survived for over 124 days following tumor cell injection (92). Using very low doses of antibody, UV3 significantly prolonged the survival of SCID mice with ARH-77 multiple myeloma (67,69,92).

None of the monoclonal antibodies currently under development for multiple myeloma have demonstrated this degree of long-term therapeutic efficacy in advanced disease. Most of the current monoclonal antibodies tested were not specifically designed for multiple myeloma. In addition, with the exception of Rituxan, there are no available *in vivo* data that demonstrate the potential of these antibodies in treating multiple myeloma (52,60,62).

The therapeutic success of UV3 has led to its chimerization and development for phase I clinical trials(150). However, in addition to demonstrating the therapeutic success, it is important to understand how UV3 exerts its anti-tumor activity. The mechanism of action might suggest potential clinical side effects and provide information as to which of the current therapeutic options might work well in combination. It will also provide information that can predict its usefulness in other diseases.

Early studies aimed at evaluating the mechanism of action of the anti-CD54 antibody demonstrated that UV3 did not interfere with the adherence of one tumor cell to another, nor did it interfere with the adherence of tumor cells to the bone marrow stroma. UV3 did not induce cell cycle arrest or induce apoptosis. UV3 could mediate effector functions, but when $F(ab)'_2$ fragments demonstrated efficacy in the SCID-ARH-77 model, it was concluded that effector functions were not the only mechanism of action of UV3. The possibility that UV3 interfered with homing was unlikely given the success of UV3 in treating advanced disease (92). Therefore, considering all the possible mechanisms by

which antibodies produce their therapeutic effect, it was hypothesized that UV3 interfered with angiogenesis in multiple myeloma, either by signaling the down-regulation of angiogenic cytokines by the tumor cell or by blocking the reception of angiogenic molecules.

D. Objectives and Major Findings

The objectives of this study were as follows: 1) to determine whether ARH-77 cells expressed angiogenic genes and whether the trait is characteristic of ARH-77 cells only or is also present in a panel of multiple myeloma cell lines, 2) to determine whether ARH-77 cells secreted angiogenic proteins, 3) to determine whether the angiogenic proteins would affect the growth and proliferation of HUVECs, 4) to determine whether UV3 would block this cascade of angiogenic events by interfering with angiogenic gene expression, protein secretion, or by binding soluble angiogenic proteins, 5) to determine whether there is *in vivo* evidence for a reduced vascular supply in UV3-treated SCID/ARH-77 mice, and 6) to re-evaluate the role of the Fc portion of UV3 in mediating anti-tumor activity.

The major findings to emerge from this study are 1) ARH-77 cells, along with a panel of multiple myeloma cell lines, secrete some pro-angiogenic cytokines; 2) UV3 may induce a minor anti-angiogenic effect; 3) the Fc portion of UV3 is critical for its anti-tumor activity; and 4) UV3 prolongs the survival of SCID mice with Daudi lymphoma.

E. Multiple Myeloma Cells Secrete Pro-Angiogenic Cytokines

In this study, ARH-77 multiple myeloma cells demonstrate their pro-angiogenic capabilities in a variety of ways. Both microarray analysis and semi-quantitative PCR revealed that ARH-77 cells express a number of angiogenic genes. In addition, ARH-77 cells secrete pro-angiogenic cytokines/molecules such as VEGF and sCD54, which stimulate the migration of HUVECs across a fibronectin membrane. ARH-77 cells are not unique in their ability to do this. Several multiple myeloma cell lines are $CD54^{+}$, express a number of angiogenic genes, and secrete VEGF. This suggests that multiple myeloma cells, in general, might grow and develop by inducing angiogenesis.

The concept that multiple myeloma cells depend on angiogenesis for their growth and progression is well supported. As a patient's monoclonal gammopathy progresses to smoldering multiple myeloma, overt multiple myeloma, and finally relapsing multiple myeloma, the degree of angiogenesis in the bone marrow increases, directly correlating with the disease progression (157). Multiple myeloma cells secrete angiogenic proteins, such as VEGF, and there is a significant correlation between the density of microvessels in the bone marrow and the number of proliferating plasma cells (30,158). In SCID/ARH-77 mice, there is an increase in the vascularization of bone marrow compared to the bone marrow of healthy mice (data not shown). Conditioned media from plasma cells, which were isolated from multiple myeloma patients at various stages of disease progression and cultured without serum, induced angiogenesis *in vivo* in

the chick chorioallantoic membrane assay, and the amount of angiogenesis induced was directly proportional to the disease progression. In addition, the conditioned media stimulated HUVEC proliferation and migration *in vitro* (159).

Multiple myeloma cells secrete pro-angiogenic cytokines that induce angiogenesis to support their growth and differentiation, and in our studies, ARH-77 cells displayed similar characteristics. They expressed and secreted angiogenic cytokines and molecules, which promoted the migration of HUVECs *in vitro*.

F. UV3 May Induce a Minor Anti-Angiogenic Effect

Several experiments have been performed to determine whether UV3 either down-regulates or interferes with the angiogenic signals from multiple myeloma cells. Some microarray and PCR results support the hypothesis that UV3 is anti-angiogenic, while other microarray and PCR results do not support it. The fact that UV3 down-regulates sCD54, which is pro-angiogenic, supports the hypothesis, but no significant change could be demonstrated in migration of HUVECs. In addition, there was no measurable decrease in the levels of VEGF secreted by the cells. In order to come to a conclusion, the data must be examined both individually and collectively.

Reconciling Microarray Data

Microarrays are a relatively new technology. The assay uses a solid support, which is either a nylon membrane or a glass slide, that contains a library of cDNA fragments or oligonucleotides unique to various genes, which can fish out the genes expressed in target RNA. In this study, 3 different microarrays were used to determine the expression of angiogenic genes in UV3-treated vs. control-treated ARH-77 cell RNA. The SuperArray microarrays demonstrated a decrease in several anti-angiogenic genes, with a significant decrease in Angiopoietin-1, FGFR-3, and VEGF. These effects were not reproduced using the oligo arrays from the microarray core or the Affymetrix array.

cDNA Microarrays

SuperArray microarrays are nylon membranes printed with cDNA fragments of 20 different genes. There is one probe per gene, and the probes are printed on the array in duplicate. Data are acquired by evaluating the intensity of radioactivity at each probe and then determining the value of expression of a given gene relative to the positive control genes. To determine the effect of UV3 on gene expression, the expression of genes from UV3 treated ARH-77 cells are evaluated relative to the expression of genes from untreated ARH-77 cells, which are considered normal, and changes in gene expression are described as a percent increase or decrease of normal expression. Multiple experiments were performed to determine whether the effects of UV3 were

reproducible and significant. Although it appears that almost all the genes tested decreased in their expression as a result of UV3 treatment, the changes described are averages, and some averages fluctuated around zero. The expression of several cytokine genes, not involved in angiogenesis, did not change. However, three pro-angiogenic genes did decrease significantly, and the decrease in expression was reproducible.

Oligonucleotide Microarrays

As the field of microarray technology grew and improved, it was important to evaluate UV3-induced expression changes with microarrays that would examine a larger number of genes. Large scale microarrays could examine the expression of several genes at one time, thus providing information about other genes involved in angiogenesis as well as several other pathways known to contribute to cancer progression (160). However, analysis of the large scale array data revealed few, if any, UV3-induced changes in the expression of angiogenic genes.

Although the cDNA spotted arrays (SuperArray) are considered more sensitive, the oligo arrays (Affymetrix and Microarray Core) are considered more specific (161). For each gene examined in the oligo arrays, multiple probe pairs are designed to target different segments within a gene sequence, and with each probe pair, one probe is an exact sequence match while the other probe contains a single mismatch in sequence. In other words, each gene has its own internal

control. In addition, oligonucleotide sequences are generally designed to have similar hybridization temperatures and binding affinities. Further controls for specificity are utilized in data analysis. Genes with low levels of expression, for example, can lead to poor reproducibility and changes that are misleading. Due to these differences in cDNA spotted arrays vs. oligo arrays, it is expected that data obtained using these microarrays would differ (162).

Conclusions

The data acquired from the SuperArray microarrays could not be validated with quantitative PCR studies to examine the expression levels of Angiopoietin-1, and other multiple myeloma cell lines did not demonstrate the same expression changes. However, in UV3-treated cells, the Affymetrix microarray revealed large changes in the expression of some FGFs, and a number of genes with unknown function were affected, which may play a role in angiogenesis. In addition, although the decrease in the expression of VEGF observed in semi-quantitative PCR was not subsequently confirmed by a decrease in the levels of protein secretion, it is possible that the decrease in the expression of pro-angiogenic TGF-β and the increase in the expression of anti-angiogenic IFN-γ may alter secretion levels, leading to changes in downstream events. Most importantly, UV3 inhibited the secretion of sCD54, which has proven to be involved in pro-angiogenic activity (104). Considering the data, it is unlikely that the anti-angiogenic properties of UV3 play a prominent role in the anti-tumor

activity of UV3. However, because genetic and cellular changes do not equate to biological effects of similar proportions *in vivo*, it is possible UV3 may induce some anti-angiogenic effects.

CD54 and Angiogenesis

There are a variety of reasons that collectively implicate CD54 in the process of angiogenesis. Surface adhesion molecules modulate signal transduction pathways, and they can associate with other membrane receptors, such as growth factor receptors (163). CD54 plays a role in adhesion and inflammation, both of which are processes in angiogenesis, and ligands for CD54, such as fibrinogen, are endothelial cell matrix proteins involved in the angiogenic process (94,119,164). Several cytokines considered to be angiogenic promoters regulate CD54 expression and activation (94,165). In addition, sCD54 stimulates angiogenesis *in vitro* and *in vivo*. sCD54 stimulates the migration and tube formation of endothelial cells, the sprouting of aortic rings, and it stimulates angiogenesis in the chick chorioallantoic membrane assay (104,156).

Agents that modulate angiogenesis have become very important in the therapy of cancer (126,135). Thalidomide is an effective therapy for multiple myeloma as a single agent and in combination with chemotherapy or immunosuppressive therapy, and the effect is largely due to its role as an anti-angiogenic agent (55). Interestingly, thalidomide decreases the expression of

CD54 (41). UV3 may have a small, but real, downstream biological effect on angiogenesis.

G. The Fc Portion of UV3 is Critical for Anti-Tumor Activity

Mediating effector function is a predominant mechanism of anti-tumor activity of UV3, and it takes very small amounts of IgG to produce an effect. The ultra-pure UV3 F(ab)'$_2$ did not prolong the survival of mice with multiple myeloma. It slightly prolonged the survival of mice with daudi lymphoma, but UV3 IgG was clearly more effective. When small amounts of IgG were added to the F(ab)'$_2$, 20% of an original IgG dose was enough to reproduce the anti-tumor effect observed with a regular dose of UV3 IgG. The efficacy of the ultra-pure UV3 F(ab)'$_2$ suggests there may be some *in vivo* signaling, and considering data linking CD54 with angiogenesis (94,104,156,163,165) and data presented here, the signals may interfere with angiogenesis. However, the superior efficacy of UV3 IgG suggests that effector functions are the predominant mechanism of action.

As in the case of several antibodies, the role of effector functions in antibody-mediated effects appears to be more important than originally thought. In a study by Clynes et al (71), both Herceptin and Rituxan were unable to inhibit tumor growth in mice that lacked activating Fc receptors. It was demonstrated that both Herceptin and Rituxan relied on effector functions for their efficacy *in*

vivo, despite numerous studies demonstrating other mechanisms of action for these antibodies *in vitro* (71).

In contrast, a recent study by Wang et al (*Clinical Cancer Research*, submitted) demonstrated that the therapeutic efficacy of UV3 in a uveal melanoma model was independent of effector function. It is possible that, as a solid tumor, melanoma depends on angiogenesis for its growth more than tumors of myeloid or lymphoid origin. It has been demonstrated that the expression of CD54 increases with more adhesive tumors (111), and changes in CD54 expression can influence the regulation of angiogenesis (165). In addition, the levels of sCD54 in solid tumors are slightly elevated compared to lymphomas and myelomas (105).

Another factor that may contribute to the different therapeutic effect in uveal melanoma is the role of immune privilege in the eye. In the anterior chamber of the eye, there are regulatory proteins that inactivate the complement cascade, NK cell activity is impaired, and many more effector components of both the innate and the adaptive immune system are suppressed (166). UV3 $F(ab)'_2$ worked as well as IgG in treating tumors in the anterior chamber of the eye, but in the subcutaneous models of melanoma, UV3 IgG was slightly better. Indeed, UV3 IgG induced complement-mediated lysis of melanoma cells *in vitro* (167).

The tumor microenvironment is a highly complex network. Vascularity is different among various types of tumors, among tumor cells in various sites

within an organ, and among various sites within a tumor (168,169). UV3 may be capable of mediating the same activities in each environment, but because each environment is site-specific, certain functions of UV3 may have different degrees of importance *in vivo*.

H. UV3 May Induce Anti-Tumor Activity in Other Malignancies

The Therapeutic Efficacy of UV3

UV3 is highly effective in treating SCID mice with Daudi lymphoma. Compared to control mice, UV3 doubled the survival time of tumor-bearing mice. cUV3 also doubled the survival time of tumor-bearing mice, demonstrating equal therapeutic efficacy. The success of UV3 in the murine model of Daudi lymphoma suggests that UV3 may be a beneficial therapy for other malignant diseases. Indeed, in addition to the multiple myeloma and Daudi lymphoma models, UV3 demonstrated anti-tumor activity in a murine model of uveal melanoma (167), and preliminary studies reveal UV3 also reduces the growth and progression of prostate carcinoma and breast carcinoma in SCID xenograft models (Brooks and Spiridon, unpublished results).

CD54 and Cancer

There are a number of studies that implicate a role for CD54 in cancer growth and progression, yet reports are conflicting as to what that role is. In

melanoma, there is a correlation between increased CD54 expression and metastasis (115). However, in breast carcinoma, increased expression of CD54 correlates with a good prognosis (116). The expression of CD54 is influenced by inflammatory cytokines (97,170), angiogenic cytokines (119), adhesion (171) (111), and activated immune cells (111). Interestingly, the secretion of sCD54 does not necessarily correlate with the expression of membrane-bound CD54 (104,172).

It is possible that sCD54, rather than membrane-bound CD54, is the predominant source of the claimed impact of CD54 on cancer progression. sCD54 can be shed during inflammation(156), and it can be shed by cells surrounding the tumor (172). Compared to healthy individuals, sCD54 is significantly up-regulated in patients with multiple myeloma, non-Hodkin's lymphoma, Hodgkin's disease, ovarian carcinoma, breast carcinoma, renal cancer, gastrointestinal cancer, and bladder cancer (105) (173). Studies demonstrate, in addition to pro-angiogenic activity, sCD54 stimulates tumor growth *in vivo* (156). Furthermore, sCD54 can inhibit the binding of leukocytes to tumor targets, and it can suppress NK cell and T cell function (111,116,117). This interference may block the ability of membrane-bound CD54 to lyse tumor targets (112).

I. Future of UV3

This study emphasizes the importance of the Fc in UV3's ability to mediate anti-tumor activity. However, we could not define exactly why the Fc portion is so important. One possibility may be that it recruits effector cells, since stimulated-BALB/c splenocytes induced more specific lysis of UV3-labeled tumor targets. Another possibility is that anti-tumor signaling by UV3 may be concentration and time-dependant, and the Fc portion would assist in both by prolonging the half-life of UV3. Additionally, there may be a difference in the localization and distribution of the IgG in tumor tissue compared to the $F(ab)'_2$ since the binding of the Fc by the FcRn would affect the transcytosis of the IgG. The role of the Fc in mediating UV3's anti-tumor activity may encompass any or all of these possibilities.

In order to distinguish among these possibilities, there are a few experimental directions that could be taken. One option would be to test the therapeutic efficacy of a constant infusion of ultra-pure UV3 $F(ab)'_2$ administered through an osmotic pump. If a continuous infusion of the ultra-pure $F(ab)'_2$ prolonged the survival of tumor-bearing mice in a manner equal to the efficacy of UV3 IgG or significantly better than the efficacy of 4 day i.v. schedule, it would suggest the signaling role of UV3 is more important than originally thought. Additionally, the function of the Fc of UV3 could be examined by making UV3 IgG mutants that could only be bound by certain Fc receptors. By determining which receptor(s)

are involved in anti-tumor activity, we might obtain a clearer picture of why the Fc of UV3 is important.

Aside from further understanding the mechanism of UV3, a number of pre-clinical and clinical studies are underway. UV3 has been chimerized and will soon enter phase I clinical trials for patients with relapsed and refractory multiple myeloma (150). The fact that CD54 is present on a number cells in the body may raise safety concerns regarding the use of UV3, but previous phase I/II studies using another anti-CD54 antibody to treat rheumatoid arthritis demonstrated that another anti-CD54 was well-tolerated. Adverse effects were mild and included headache, fever, nausea/vomiting, light-headedness, and urticaria. The side effects occurred on the first or second day of treatment, and they lessened with time despite continued therapy (174,175). The anti-CD54 antibody was immunosuppressive, but there were no infectious complications related to the therapy (174).

In addition to the clinical use of UV3, there are number of pre-clinical studies to be completed. Further studies are needed to evaluate the efficacy of UV3 in the breast and prostate cancer models, and *in vivo* studies evaluating the efficacy of UV3 in murine models of lung and pancreas cancer are being carried out (Brooks, unpublished results). Studies are also needed to evaluate whether increased doses of UV3 or different dosing schedules would further improve the anti-tumor effect of UV3. Finally, the effect of UV3 must be evaluated in combination with other agents.

J. Conclusions

Monoclonal antibodies are beneficial for the treatment of cancer, and their success is largely due to their ability to target diseases by mechanisms that are different from other anti-tumor therapies. Multiple myeloma is an incurable disease, and, at this time, there are no monoclonal antibodies available for treatment. UV3 is a monoclonal antibody designed for the therapy of multiple myeloma, and it is highly effective in treating both early and advanced multiple myeloma in a murine model of human disease.

The objective of this study was to elucidate the mechanism(s) of action of UV3 or, more specifically, to determine whether UV3 interfered with angiogenesis by inhibiting the secretion of pro-angiogenic molecules. ARH-77 cells express and secrete angiogenic molecules, which can influence the migration of HUVECs. The expression and secretion of angiogenic molecules is a common feature of a number of multiple myeloma cell lines. When UV3 is added to the cell culture, the expression of some angiogenic genes is affected, but microarray analysis reveals that angiogenesis is not the only pathway targeted. UV3 affects genes from multiple pathways, and in combination with the biologically, multi-functional role of CD54, it suggests that UV3 mediates multiple of signals. Angiogenesis may be one pathway affected, and the evidence of a downstream effect of UV3 on sCD54 supports this. However, *in vivo* studies comparing ultra-pure $F(ab)'_2$ with IgG demonstrate that the predominant mechanism of action of

UV3 is dependant upon its Fc portion, either because it confers a longer half-life, or because it mediates CDC or ADCC.

In addition to a murine model of multiple myeloma, UV3 is highly effective in treating Daudi lymphoma. UV3 also demonstrated therapeutic efficacy in a murine model of uveal melanoma (167), and preliminary data indicate UV3 is effective in murine results models of breast and prostate cancer (Brooks and Spiridon, unpublished). Since previous Phase I and II clinical trials have demonstrated that an anti-CD54 monoclonal antibody is safe, UV3 is a candidate for clinical evaluation in the therapy of many cancers.

V. References

1. "What are the Key Statistics About Multiple Myeloma"? Detailed Guide: Multiple Myeloma. *American Cancer Society.* September 2004. http://www.cancer.org

2. "Monoclonal Antibody Therapy (Passive Immunotherapy)". *American Cancer Society*. September 2004. http://www.cancer.org

3. "Causes and Incidence". *Multiple Myeloma Research Foundation*. September 2004. http://www.multiplemyeloma.org/

4. Sirohi B. and Powles R. Multiple myeloma. Lancet 2004; 363:875-887.

5. Sonneveld P. and Segeren C.M. Changing concepts in multiple myeloma: from conventional chemotherapy to high-dose treatment. European Journal of Cancer 2003; 39:9-18.

6. Rosenthal D. S., Schnipper L. E., McCaffrey R. P., and Anderson K. C. "Multiple Myeloma and Other Plasma Cell Dyscrasias". Clinical Oncology. Atlanta, GA: American Cancer Society, 2001: 517-525.

7. Rajkumar S.V. and Greipp P.R. Prognostic factors in multiple myeloma. Hematology/Oncology Clinics of North America 1999; 13:1295-1314.

8. Riccardi A., Gobbi P.G., Ucci G., Bertoloni D., Luoni R., Rutigliano L. *et al*. Changing clinical presentation of multiple myeloma. European Journal of Cancer 1991; 27:1401-1405.

9. Berenson J.R. Etiology of multiple myeloma: What's new. Seminars in Oncology 1999; 26:2-9.

10. Kuehl W.M. and Bergsagel P.L. Multiple myeloma: Evolving genetic events and host interactions. Nature Reviews 2002; 2:175-187.

11. Nishida K., Tamura A., Nakazawa N., Ueda Y., Abe T., Matsuda F. *et al.* The Ig heavy chain gene is frequently involved in chromosomal translocations in multiple myeloma and plasma cell leukemia as detected by in situ hybridization. Blood 1997; 90:526-534.

12. Bergsagel P.L., Chesi M., Nardini E., Brents L.A., Kirby S.L., Kuehl W.M. Promiscuous translocations into immunoglobulin heavy chain switch regions in multiple myeloma. Proceeding of the National Academy of Sciences of the United States of America 1996; 92:13931-13936.

13. Boersma-Vreugdenhil G.R., Kuipers J., van Stralen E., Peeters T., Michaux L., Hagemeijer A. *et al.* The recurrent translocation t(14;20)(q32;q12) in multiple myeloma results in aberrant expression of MAFB: a molecular and genetic analysis of the chromosomal breakpoint. British Journal of Haematology 2004; 126:355-363.

14. Chesi M., Bergsagel P.L., Brents L.A., Smith C.M., Gerhard D.S., Kuehl W.M. Dysregulation of cyclin D1 by translocation into an IgH gamma switch region in two multiple myeloma cell lines. Blood 1996; 88:674-681.

15. Shaughnessy J. Jr., Gabrea A., Qi Y., Brents L., Zhan F., Tian E. *et al.* Cyclin D3 at 6p21 is dysregulated by recurrent chromosomal translocations to immunoglobulin loci in multiple myeloma. Blood 2001; 98:217-223.

16. Chesi M., Nardini E., Brents L.A., Schrock E., Ried T., Kuehl W.M. Frequent translocation t(4;14)(p16.3;q32.3) in multiple myeloma is associated with increased expression and activating mutations of fibroblast growth factor receptor 3. Nature Genetics 1997; 16:260-264.

17. Chesi M., Nardini E., Lim R.S., Smith K.D., Kuehl W.M., Bergsagel P.L. The t(4;14) translocation in myeloma dysregulates both FGFR3 and a novel gene, MMSET, resulting in IgH/MMSET hybrid transcripts. Blood 1998; 92:3025-3034.

18. Chesi M., Bergsagel P.L., Shonukan O.O., Martelli M.L., Brents L.A., Chen T. *et al*. Frequent dysregulation of the c-maf proto-oncogene at 16q23 by translocation to an Ig locus in multiple myeloma. Blood 1998; 91:4457-4463.

19. Bergsagel P.L. and Kuehl W.M. Chromosome translocations in multiple myeloma. Oncogene 2001; 20:5611-5622.

20. Neri A., Murphy J.P., Cro L., Ferrero D., Tarella C., Baldini L. *et al.* Ras oncogene mutation in multiple myeloma. Jounral of Experimental Medicine 1989; 170:1715-1725.

21. Mazars G.R., Portier M., Zhang X.G., Jourdan M., Bataille R., Theillet C. *et al.* Mutations of the p53 gene in human myeloma cell lines. Oncogene 1992; 7:1015-1018.

22. Drach J., Kaufman H., Urbauer E., Schrieber S., Ackermann J., Huber H. The biology of multiple myeloma. Journal of Cancer Research and Clinical Oncology 2000; 126:441-447.

23. Anderson K. Advances in the biology of multiple myeloma: Therapeutic applications. Seminars in Oncology 1999; 26:10-22.

24. Klein B. and Bataille R. Cytokine network in human multiple myeloma. Hematology/Oncology Clinics of North America 1992; 6:273-284.

25. Huang Y-W. and Vitetta E.S. A monoclonal anti-human IL-6 receptor antibody that inhibits the proliferation of human myeloma cells. Hybridoma 1993; 12:621-630.

26. Jelinek D.F. Mechanisms of myeloma cell growth control. Hematology/Oncology Clinics of North America 1999; 13:1145-1157.

27. Lauta V.M. A review of the cytokine network in multiple myeloma. Cancer 2003; 97:2440-2452.

28. Merico F., Bergui L., Gregoretti M.G., Ghia P., Aimo G., Lindley I.J.D. *et al.* Cytokines involved in the progression of multiple myeloma. Clinical and Experimental Immunology 1993; 92:27-31.

29. Anderson K.C. and Lust J.A. Role of cytokines in multiple myeloma. Seminars in Hematology 1999; 36:14-20.

30. Podar K., Tai Y-T., Davies F.E., Lentzsch S., Sattler M., Hideshima T. et al. Vascular endothelial growth factor triggers signaling cascades mediating multiple myeloma cell growth and migration. Blood 2001; 98:428-435.

31. Dalton W.S. The tumor microenvironment: Focus on myeloma. Cancer Treatment Reviews 2003; 29:11-19.

32. Huang Y-W., Hamilton A., Arnuk O.J., Chaftari P., Chemaly R. Current drug therapy for multiple myeloma. Drugs 1999; 57:485-506.

33. Bosanquet A.G. and Gilby E.D. Pharmacokinetics of oral and intravenous melphalan during routine treatment of multiple myeloma. European Journal of Cancer and Clinical Oncology 1982; 18:355-362.

34. Cooper M.R. and Cooper M.R. "Basis for current major therapies of cancer: Systemic Therapy". Clinical Oncology. Atlanta, GA: American Cancer Society, 2001:175-229.

35. Kornel L. On the effects and the mechanism of action of corticosteroids in normal and neoplastic target tissues: findings and hypotheses, with a review of information on intracellular steroid receptors in genereal. Acta Endocrinologica.Supplementum. 1973; 178:1-45.

36. Munshi N.C., Barlogie B., Desikan K.R., Wilson C. Novel approaches in myeloma therapy. Seminars in Oncology 1999; 26:28-34.

37. Duflos A., Kruczyski A., Barret J.M. Novel aspects of natural and modified vinca alkaloids. Current Medicinal Chemistry - Anti-Cancer Agents 2002; 2:55-70.

38. Moore M.J. Clinical pharmacokinetics of cyclophosphamide. Clinical Pharmacokinetics 1991; 20:194-208.

39. Bono V.H., Jr. Review of mechanism of action studies of the nitrosoureas. Cancer Treatment Reports 1976; 60:699-702.

40. Rajkumar S.V., Kyle R.A., Gertz M.A. Myeloma and the newly diagnosed patient: A focus on treatment and management. Seminars in Oncology 2002; 29:5-10.

41. Zweegman S. and Huijgens P.C. Treatment of myeloma: Recent developments. Anti-Cancer Drugs 2002; 13:339-351.

42. Barlogie B., Shaughnessy J., Tricot G., Jacobson J., Zangari M., Anaissie E. *et al.* Treatment of multiple myeloma. Blood 2004; 103:20-32.

43. Pinguet E., Martel P., Fabbro M., Petit I., Canal P., Culine S. Pharmacokinetics of high-dose intravenous melphalan in patients undergoing peripheral blood hematopoietic progenitor-cell transplantation. Anticancer Research 1997; 17:605-612.

44. Fermand J.P., Chevret S., Ravaud P., Divine M., Leblond V., Dreyfus F. *et al.* High-dose chemoradiotherapy and autologous blood stem cell transplantation in multiple myeloma: results of a phase II trial involving 63 patients. Blood 2004; 82:2005-2009.

45. Lenhoff S., Hjorth M., Holmberg E., Turesson I., Westin J., Nielsen J.L. *et al.* Impact on survival of high-dose therapy with autologous stem cell support in patients younger than 60 years with newly diagnosed multiple myeloma: a population-based study. Blood 2000; 95:7-11.

46. Barlogie B., Jagannath S., Vesole D.H., Naucke S., Cheson B., Mattox S. Superiority of tandem autologous transplantation over standard therapy for previously untreated multiple myeloma. Blood 1997; 89:789-793.

47. Bertz H., Burger J.A., Junzmann R., Mertelsmann R., Finke J. Adoptive immunotherapy for relapsed multiple myeloma after allogeneic bone marrow transplantation (BMT): evidence for a graft-versus-myeloma effect. Leukemia 1997; 11:281-283.

48. Gertz M.A., Witzig T.E., Pineda A.A., Greipp P.R., Kyle R.A., Litzow M.R. Monoclonal plasma cells in the blood stem cell harvest from patients with multiple myeloma are associated with shortened relapse-free survival after transplantation. Bone Marrow Transplantation 1997; 19:337-342.

49. Bensinger W.I. Allogeneic hematopoietic cell transplantation for multiple myeloma. Biomedicine and Pharmacotherapy 2002; 56:133-138.

50. Strasser K. and Ludwig H. Thalidomide treatment in multiple myeloma. Blood Reviews 2002; 16:207-215.

51. D'Amato R.J., Loughnan M.S., Flynn E., Folkman J. Thalidomide is an inhibitor of angiogenesis. Proceedings of the National Academy of Sciences of the United States of America 1994; 91:4082-4085.

52. Gorschluter M., Ziske C., Glasmacher A., Schmidt-Wolf I.G.H. Current clinical and laboratory strategies to augment the efficacy of immunotherapy in multiple myeloma. Clinical Cancer Research 2001; 7:2195-2204.

53. Hideshima T. and Anderson K.C. Molecular mechanisms of novel therapeutic approaches for multiple myeloma. Nature Reviews 2002; 2:927-937.

54. Cool R.M. and Herrington J.D. Thalidomide for the treatment of relapsed and refractory multiple myeloma. Pharmacotherapy 2002; 22:1019-1028.

55. Matthews S.J. and McCoy C. Thalidomide: A review of approved and investigational uses. Clinical Therapeutics. 2003; 25:342-395.

56. Ng S., MacPherson G.R., Gutschow M., Eger K., Figg W.D. Antitumor effects of thalidomide analogs in human prostate cancer xenografts implanted in immunodeficient mice. Clinical Cancer Research 2004; 10:4192-4197.

57. Richardson P.G., Schlossman R.L., Weller E., Hideshima T., Mitsiades C., Davies F. *et al.* Immunomodulatory drug CC-5013 overcomes drug resistance and is well tolerated in patients with relapsed multiple myeloma. Blood 2002; 100:3063-3067.

58. Bross P.F., Kane R., Farrell A.T., Abraham S., Benson K., Brower M.E. *et al.* Approval summary for Bortezomib for injection in the treatment of multiple myeloma. Clinical Cancer Research 2004; 10:3954-3964.

59. Hussein M.A., Saleh M., Ravandi F., Mason J., Rifkin R.M., Ellison R. Phase 2 study of arsenic trioxide in patients with relapsed or refractory multiple myeloma. British Journal of Haematology 2004; 125:470-476.

60. Tai Y-T., Catley L.P., Mitsiades C.S., Burger R., Podar K., Shringpaure R. *et al.* Mechanisms by which SGN-40, a humanized anti-CD40 antibody, induces cytotoxicity in human multiple myeloma cells: Clinical implications. Cancer Research 2004; 64:2846-2852.

61. Bataille R., Barlogie B., Lu Z.Y., Rossi J.F., Lavabre-Bertrand T., Beck T. *et al.* Biologic effects of anti-interleukin-6 murine monoclonal antibody in advanced multiple myeloma. Blood 1995; 86:685-691.

62. Ozaki S., Kosaka M., Wakahara Y., Ozaki Y., Tsuchiya M., Koishihara Y. *et al.* Humanized anti-HM1.24 antibody mediates myeloma cell cytotoxicity that is enhanced by cytokine stimulation of effector cells. Blood 1999; 93:3922-3930.

63. Lin B., Podar K., Gupta D., Tai Y.T., Li S., Weller E. *et al.* The vascular endothelial growth factor receptor tyrosine kinase inhibitor PTK787/ZK222584 inhibits growth and migration of multiple myeloma cells in the bone marrow microenvironment. Cancer Research 2002; 62:5019-5026.

64. Ruffini P.A., Biragyn A., Kwak L.W. Recent advances in multiple myeloma immunotherapy. Biomedicine and Pharmacotherapy 2002; 56:129-132.

65. Kohler G. and Milstein C. Continuous cultures of fused cells secreting antibody of predefined specificity. Nature 1975; 256:495-497.

66. Ehrlich P. Croonian Lecture: On immunity with special reference to cell life. Proceedings of the Royal Society of London 1900; 66:424-448.

67. von Mehren M., Adams G.P., Weiner L.M. Monoclonal antibody therapy for cancer. Annual Reviews in Medicine 2003; 54:343-369.

68. Waldman T.A. Immunotherapy: past, present and future. Nature Medicine 2003; 9:269-277.

69. von Mehren M. and Weiner L.M. Monoclonal antibody-based therapy. Current Opinion in Oncology 1996; 8:493-498.

70. Stockwin L.H. and Holmes S. The role of therapeutic antibodies in drug discovery. Biochemical Society Transactions 2003; 31:433-436.

71. Clynes R.A., Towers T.L., Presta L.G., Ravetch J.V. Inhibitory Fc receptors modulate *in vivo* cytoxicity against tumor targets. Nature Medicine 2000; 6:443-446.

72. Shawler D.L., Bartholomew R.M., Smith L.M., Dillman R.O. Human immune responses to multiple injections of murine monoclonal IgG. Journal of Immunology 1985; 135:1530-1535.

73. Wright A., Shin S.U., Morrison S.L. Genetically engineered antibodies: progress and prospects. Critical Reviews in Immunology 1992; 12:125-168.

74. Mendez M.J., Green L.L., Corvalan J.R.F., Jia X.C., Maynard-Currie C.E., Yang X.D. *et al.* Functional transplant of megabase human immunoglobulin loci recapitulates humn antibody response in mice. Nature Genetics 1997; 15:146-156.

75. Winter G., Griffiths A.D., Hawkins R.E., Hoogenboom H.R. Making antibodies by phage-display technology. Annual Review of Immunology 1994; 12:433-435.

76. Carter P. Improving the efficacy of antibody-based cancer therapies. Nature Reviews Cancer 2001; 1:118-129.

77. Hudson P.J. Recombinant antibody constructs in cancer therapy. Current Opinion in Immunology 1999; 11:548-557.

78. Shields R.L., Namenuk A.K., Hong K., Meng Y.G., Rae J., Briggs J.C. *et al.* High resolution mapping of the binding site on human IgG1 for FcγRI, FcγRII, FcγRIII and FcRn and design of IgG1 variants with improved binding to FcγR. Journal of Biological Chemistry 2001; 276:6591-6604.

79. Forero A. and LoBuglio A.F. History of antibody therapy for non-Hodgkin's lymphoma. Seminars in Oncology 2003; 30:1-5.

80. Speth P.A.J., van Hoesel Q.G.C.M., Haanen, C. Clinical Pharmacokinetics of Doxorubicin. Clinical Pharmacokinetics 1988; 15:15-31.

81. Boye J., Elter T., Engert A. An overview of the current clinical use of the anti-CD20 monoclonal antibody rituximab. Annals of Oncology 2003; 14:520-535.

82. Kaklamani V. and O'Regan R.M. New targeted therapies in breast cancer. Seminars in Oncology 2004; 31:20-25.

83. Young R.C., Ozols R.F., Myers C.E. The anthracycline antineplastic drugs. New England Journal of Medicine 1981; 305:139-153.

84. Pettitt A.R. Mechanism of action of purine analogues in chronic lymphocytic leukaemia. British Journal of Haematology 2003; 121:692-702.

85. Robak T. Monoclonal antibodies in the treatment of chronic lymphoid leukemias. Leukemia & Lymphoma 2004; 45:205-219.

86. Ulukan H. and Swaan P.W. Camptothecins: a review of their chemotherapeutic potential. Drugs 2002; 62:2039-2057.

87. Tanaka F., Fukuse T., Wada H., Fukushima M. The history, mechanism and clinical use of oral 5-fluorouracil derivative chemotherapeutic agents. Current Pharmaceurical Biotechnology 2000; 1:137-164.

88. Grem J.L. Systemic treatment options in advanced colorectal cancer: perspectives on combination 5-flluorouracil plus leucovorin. Seminars in Oncology 1997; 24:S18-8-S18-18.

89. Veronese M.L. and O'Dwyer P.J. Monoclonal antibodies in the treatment of colorectal cancer. European Journal of Cancer 2004; 40:1292-1301.

90. Huang Y.W., Burrows F.J., Vitetta E.S. Cytotoxicity of a novel anti-ICAM-1 immunotoxin on human myeloma cell lines. Hybridoma 1993; 12:661-675.

91. Schulz T.F., Vogetseder W., Mitterer M., Johnson J.P., Dierich M.P. Individual epitopes of an 85,000 MW membrane adherence molecule are variably expressed on cells of different lineage. Immunology 1988; 64:581-586.

92. Huang Y.W., Richardson J.A., Vitetta E.S. Anti-CD54 (ICAM-1) has anti-tumor activity in SCID mice with human myeloma cells. Cancer Research 1995; 55:610-616.

93. Huang Y-W., Richardson J.A., Tong A.W., Zhang B.Q., Stone M.J., Vitetta E.S. Disseminated growth of a human multiple myeloma cell line in mice with severe combined immunodeficiency disease. Cancer Resear 1993; 53:1392-1396.

94. van de Stolpe A. and van der Saag P.T. Intercellular adhesion molecule-1. Journal of Molecular Medicine 1996; 74:13-33.

95. Staunton D.E., Marlin S.D., Stratowa C., Dustin M.L., Springer T.A. Primary structure of ICAM-1 demonstrates interaction between members of the immunoglobulin and integrin supergene families. Cell 2004; 52:925-933.

96. Wang J.H. and Springer T.A. Structural specializations of immunoglobulin superfamily members for adhesion to integrins and viruses. Immunological Reviews 1998; 163:197-215.

97. Roebuck K.A. and Finnegan A. Regulation of intercellular adhesion molecule-1 (CD54) gene expression. Journal of Leukocyte Biology 1999; 66:876-888.

98. Rothlein R., Dustin M.L., Marlin S., Springer T.A. A human intercellular adhesion molecule (ICAM-1) distinct from LFA-1. Journal of Immunology 1986; 137:1270-1274.

99. van Seventer G.A., Shimizu Y., Horgan K.J., Shaw S. The LFA-1 ligand ICAM-1 provides an important costimulatory signal for T cell receptor-mediated activation of resting T cells. Journal of Immunology 1990; 144:4579-4586.

100. Hibbs M.L., Xu H., Springer T.A. Regulation of adhesion ICAM-1 by the cytoplasmic domain of LFA-1 integrin beta subunit. Science 1991; 251 :1611-1613.

101. Sellak H., Franzini E., Hakim J., Pasquier C. Reactive Oxygen Species Rapreaase Endothelial ICAM-1 Abiliy to Bind Neutrophils Without Detectable Upregulation. Blood 1994; 83:2669-2677.

102. Hanasaki K., Varki A., Stamenkovic I., Bevilacqua M.P. Cytokine-induced β-galactoside α-2,6-sialytransferase in human endothelial cells mediates α2,6-sialylation of adhesion molecules and CD22 ligands. The Journal of Biological Chemistry 1994; 269:10637-10643.

103. Rothlein R., Mainolfi E.A., Czajkowski M., Marlin S.D. A form of circulating ICAM-1 in human serum. Journal of Immunology 1991; 147:3788-3793.

104. Gho Y.S., Kleinman H.K., Sosne G. Angiogenic activity of human soluble intercellular adhesion molecule-1. Cancer Research 1999; 59:5128-5132.

105. Banks R.E., Gearing A.J.H., Hemingway I.K., Norfolk D.R., Perren T.J., Selby P.J. Circulating intercellular adhesion molecule-1 (ICAM-1), E-selectin and vascular cell adhesion molecule-1 (VCAM-1) in human malignancies. British Journal of Cancer 1993; 68:122-124.

106. Becker J.C., Termeer C., Schmidt R.E., Brocker E-B. Soluble intercellular adhesion molecule-1 inhibits MHC-restricted specific T cell/tumor interaction. Journal of Immunology 1993; 151:7224-7232.

107. Gearing A.J.H. and Newman W. Circulating adhesion molecules in disease. Immunology Today 1993; 14:506-512.

108. Leeuwenberg J.F.M., Smeets E.F., Neefjes J.J., Shaffer M.A., Cinek T., Jeunhomme T.M.A.A. *et al.* E-selection and intercellular adhesion molecule-1

are released by activated human endothelial cells in vitro. Immunology 1992; 77:543-549.

109. Seth R., Raymond F.D., Makgoba M.W. Circulating ICAM-1 isoforms: diagnostic prospects for inflammatory and immune disorders. Lancet 1991; 338:83-84.

110. Poritz L.S., Page M.J., Tilberg A.F., Koltun W.A. Amelioration of graft versus host disease with anti-ICAM-1 therapy. Journal of Surgical Research 1998; 80:280-286.

111. Boyd A.W., Dunn S.M., Fecondo J.V., Culvenor J.G., Duhrsen U., Burns G.F. *et al.* Regulation of expression of a human intercellular adhesion molecule (ICAM-1) during lymphohematopoietic differentiation. Blood 1989; 73:1896-1903.

112. Vanky F., Wang P., Patarroyo M., Klein E. Expression of the adhesion molecule ICAM-1 and major histocompatibility complex class I antigens on human tumor cells is required for their interaction with autologous lymphocytes in vitro. Cancer Immunology, Immunotherapy 1990; 31:19-27.

113. Raspadori D., Lauria F., Ventura M.A., Rondelli D., Tura S. Expression of adhesion molecules on acute leukemic blast cells and sensitivity to normal LAK activity. Annals of Hematology 1993; 67:213-216.

114. Van Riet I., De Waele M., Remels L., Lacor P., Schots R., Van Camp B. Expression cytoadhesion molecules (CD56, CD54, CD18 and CD29) by myeloma plasma cells. British Journal of Haematology 1991; 79:421-427.

115. Johnson J.P., Stade B.G., Holzmann B., Schwable W., Riethmuller G. *De novo* expression of intercellular adhesion molecule-1 in melanoma correlates with increased risk of metastasis. Proceeding of the National Academy of Sciences of the United States of America 1989; 86:641-644.

116. Mills P.J., Parker B., Jones V., Adler K.A., Perez C.J., Johnson S. *et al*. The effects of standard anthracycline-based chemotherapy on soluble ICAM-1 and vascular endothelial growth factor levels in breast cancer. Clinical Cancer Research 2004; 10:4998-5003.

117. Altomonte M., Gloghini A., Bertola G., Gasparolo A., Carbone A., Ferrone S. *et al.* Differential expression of cell adhesion molecules CD54/CD11a and CD58/CD2 by human melanoma cells and functional role in their interaction with cytotoxic cells. Cancer Research 1993; 53:3343-3348.

118. Johnson J.P. The role of ICAM-1 in tumor development. Chemical Immunology 1991; 50:143-163.

119. Griffioen A.W., Damen C.A., Martinotti S., Blijham G.H., Groenewegen G. Endothelial intercellular adhesion molecule-1 expression is suppressed in human malignancies: The role of angiogenic factors. Cancer Research 1996; 56:1111-1117.

120. Yoshida A., Yoshida S., Ishibashi T., Inomata H. Intraocular neovascularization. Histology and Histopathology 1999; 14:1287-1294.

121. Folkman J. Clinical applications of research on angiogenesis. New England Journal of Medicine 1995; 333:1757-1763.

122. Folkman J. Therapeutic Angiogenesis in Ischemic Limbs. Circulation 1998; 97:1108-1110.

123. Hanahan D. and Folkman J. Patterns and emerging mechanisms of the angiogenic switch during tumor angiogenesis. Cell 1996; 86:353-364.

124. Klagsbrun M. and Moses M.A. Molecular angiogenesis. Chemistry and Biology 1999; 6:R217-R224.

125. Eliceiri B.P. and Cheresh D.A. Adhesion events in angiogenesis. Current Opinion in Cell Biology 2001; 13:563-568.

126. Folkman, J. “Tumor angiogenesis”. The Molecular Basis of Cancer. Philadelphia: W. B. Saunders, 1995: 206-232.

127. Folkman J. What is the evidence that tumors are angiogenesis dependent? Journal of the National Cancer Institute 1990; 82:4-6.

128. Beckner M.E. Factors promoting tumor angiogenesis. Cancer Investigation 1999; 17:594-623.

129. Desai S.B. and Libutti S.K. Tumor angiogenesis and endothelial cell modulatory factors. Journal of Immunotherapy 1999; 22:186-211.

130. Veikkola T., Karkkainen M., Claesson-Welsh L., Alitalo K. Regulation of angiogenesis via vascular endothelial growth factor receptors. Cancer Research 2000; 60:203-212.

131. Huang Z. and Bao S-D. Roles of main pro- and anti-angiogenic factors in tumor angiogenesis. World Journal of Gastroenterology 2004; 10:463-470.

132. Holmgren L., O'Reilly M.S., Folkman J. Dormancy of micrometastases: balanced proliferation and apoptosis in the presence of angiogenesis suppression. Nature Medicine 1995; 1:149-153.

133. Verheul H., Voest E.E., Schlingemann R.O. Are tumors angiogenesis-dependent? Journal of Pathology 2004; 202:5-13.

134. Lyden D., Hattori K., Dias S., Costa C., Blaikie P., Butros L. *et al.* Impaired recruitment of bone-marrow-derived endothelial and hematopoietic precursor cells blocks tumor angiogenesis and growth. Nature Medicine 2001; 7:1194-1201.

135. Eskens F. Angiogenesis inhibitors in clinical development; where are we now and where are we going? British Journal of Cancer 2004; 90:1-7.

136. Kumar C.C., Malkowski M., Yin Z., Tanghetti E. Yaremko B., Nechuta T. *et al*. Inhibition of Angiogenesis and Tumor Growth by SCH221153, a Dual $\alpha_v\beta_3$ and $\alpha_v\beta_5$ Integrin Receptor Antagonist. Cancer Research 2001; 61:2231-2238.

137. Shaheen R.M., Davis D.W., Liu W., Zebrowski B.K., Wilson M.R., Bucana C.D. *et al.* Antiangiogenis therapy targeting the tyrosine kinase receptor for vascular endothelial growth factor receptor inhibits the growth of colon cancer liver metastasis and induces tumor and endothelial cell apoptosis. Cancer Research 1999; 59:5412-5416.

138. Cuadros C., Dominguez A.L., Frost G.I., Borgstrom P., Lustgarten J. Cooperative effect between immunotherapy and antiangiogenic therapy leads to effective tumor rejection in tolerant Her-2/neu mice.Cancer Research 2003; 63:5895-5901.

139. Burk K.H., Drewinko B., Turjillo J.M., Ahearn M.J. Establishment of a human plasma cell line *in vitro*. Cancer Research 1978; 38:2508-2513.

140. Nilsson K., Bennich H., Johansson S.G., Ponten J. Established immunoglobulin producing myeloma (IgE) and lymphoblastoid (IgG) cell lines from an IgE myeloma patient. Clinical & Experimental Immunology 1970; 7:477-489.

141. Matsuoka Y., Moore G.E., Yagi Y., Pressman D. Production of free light chains of immunoglobulin by a hematopoietic cell line derived from a patient with multiple myeloma. Proceeding of the Society for Experimental Biology and Medicine 1967; 125:1246-1250.

142. Fahey J.L., Buell D.N., Sox H.C. Proliferation and differentiation of lymphoid cells: studies with human lymphoid cell lines and immunoglobulin synthesis. Annals of the New York Academy of Sciences 1971; 190:221-234.

143. Harris N.S. Plasma cell surface antigen on human blood lymphocytes. Nature 1974; 250:507-509.

144. Olsson L. and Kaplan H.S. Human-human hybridomas producing monoclonal antibodies of predefined antigenic specificity. Proceedings of the National Academy of Sciences of the United States of America 1980; 77:5429-5431.

145. Shimizu S., Yoshioka R., Hirose Y., Sugai S., Tachibana J., Konda S. Establishment of two interleukin 6 (B cell stimulatory factor 2/interferon beta 2)-dependent human bone marrow-derived myeloma cell lines. Journal of Experimental Medicine 1989; 169:339-344.

146. Ritts R.E. Jr., Ruiz-Arguelles A., Weyl K.G., Bradley A.L., Weihmeir B., Jacobsen D.J. *et al.* Establishment and characterization of a human non-secretory plasmacytoid cell line and its hybridization with human B cells. International Journal of Cancer 1983; 31:133-141.

147. Gazdar A.F., Oie H.K., Kirsch I.R., Hollis G.F. Establishment and characterization of a human plasma cell myeloma culture having a rearranged cellular myc proto-oncogene. Blood 1986; 67:1542-1549.

148. Klein E., Klein G,, Nadkarni J.S., Nadkarni J.J., Wigzell H., Clifford P. Surface IgM-kappa specificity on a Burkitt lymphoma cell *in vivo* and in derived culture lines. Cancer Research 1968; 28:1300-1310.

149. Robertson S.M., Kettman J.R., Miller J.N., Norgard M.V. Murine monoclonal antibodies specific for virulent treponema pallidum (Nichols). Infection and Immunity 1982; 36:1076-1085.

150. Smallshaw J.E., Coleman E., Spiridon C., Vitetta E.S. The generation and anti-myeloma activity of a chimeric anti-CD54 antibody, cUV3. Journal of Immunotherapy 2004; in press.

151. Coloma M.J., Hastings A., Wims L.A., Morrison S.L. Novel vectors for the expression of antibody molecules using variable regions generated by polymerase chain reaction. Journal of Immunological Methods 1992; 152:89-104.

152. Schageman, J. and Garner, H.R. “MarC-V: Microarray Calculation and Visualization”. *University of Texas Southwestern Medical Center*. 2002. http://pga.swmed.edu/Information/marcV_Info.htm

153. Schageman J.J., Basit M., Gallardo T.D., Garner H.R., Shohet R.V. MarC-V: A spreadsheet-based tool for analysis, normalization, and visualization of single cDNA microarray experiments. Biotechniques 2002; 32:338-344.

154. “Source”. *Stanford University Genetics Department*. 2004. www.source.stanford.edu/cgi-bin/source/sourceSearch

155. “Net Primer”. *Premier Biosoft International*. 2002. www.premierbiosoft.com

156. Gho Y.S., Kim P.N., Li H-C., Elkin M., Kleinman H.K. Stimulation of tumor growth by human soluble intercellular adhesion molecule-1. Cancer Research 2001; 61:4253-4257.

157. Rajkumar S.V., Mesa R.A., Fonseca R., Schroeder G., Plevak M.F., Dispenzieri A. et al. Bone marrow angiogenesis in 400 patients with monoclonal gammopathy of undetermined significance, multiple myeloma, and primary amyloidosis. Clinical Cancer Research 2002; 8:2210-2216.

158. Vacca A., Ribatti D., Roncali L., Ranieri G., Serio G., Silvestris F. *et al.* Bone marrow angiogenesis and progression in multiple myeloma. British Journal of Haematology 1994; 87:503-508.

159. Vacca A., Ribatti D., Presta M., Minischetti M., Lurlaro M., Ria R. *et al.* Bone marrow neovascularization, plasma cell angiogenic potential, and matrix metalloproteinase-2 secretion parallel progression of human multiple myeloma. Blood 1999; 93:3064-3073.

160. "Whole genome microarrary *vs* focused microarray". *SuperArray Bioscience Corporation* 2004. www.superarray.com

161. Kuo W.P., Jenssen T-K., Butte A.J., Ohno-Machado L., Kohane I.S. Analysis of matched mRNA measurements from two different microarray technologies. Bioinformatics 2002; 18:405-412.

162. Butte A. The use and analysis of microarray data. Nature Reviews. Drug Discovery 2002; 1:951-960.

163. Cavallaro U. and Christofori G. Cell adhesion and signalling by cadherins and Ig-CAMs in cancer. Nature Reviews 2004; 4:118-132.

164. Szekanecz Z. and Koch A.E. Vascular endothelium and immune responses: implications for inflammation and angiogenesis. Rheumatic Diseases Clinics of North America 2004; 30:97-114.

165. Griffioen A.W., Damen C.A., Mayo K.H., Barendsz-Janson A.F., Martinotti S., Blijham G.H. *et al.* Angiogenesis inhibitors overcome tumor induced endothelial cell anergy. International Journal of Cancer 1999; 80:315-319.

166. Streilein J.W. Ocular immune privilege: the eye takes a dim but practical view of immunity and inflammation. Journal of Leukocyte Biology 2003; 74:179-185.

167. Wang S., Coleman E.J., Pop L.M., Brooks K., Vitetta E.S., Niederkorn J.Y. Effect of an anti-CD54 (ICAM-l) monoclonal antibody (UV3) on the growth of human uveal melanoma cells transplanted heterotopically and orthotopically in SCID mice. Clinical Cancer Research 2004;*submitted.*

168. Fidler I.J. Angiogenic heterogeneity: regulation of neoplastic angiogenesis by the organ microenvironment. Journal of the National Cancer Institute 2001; 93:1040.

169. Fidler I.J., Singh R.K., Yoneda J., Kumar R., Xu L., Dong Z. *et al.* Critical determinants of neoplastic angiogenesis. Cancer Journal 2000; 6:S225-236.

170. Giavazzi R., Chirivi R.G.S., Garofalo A., Rambaldi A., Hemingway I., Pigott R. *et al.* Soluble intercellular adhesion molecule-1 is released by human melanoma cells and is associated with tumor growth in nude mice. Cancer Research 1992; 52:2628-2630.

171. Yasuda M., Tanaka Y., Tamura M., Fujii K., Sugaya M., So T. *et al*. Stimulation of β_1 integrin down-regulates ICAM-1 expression and ICAM-1-dependent adhesion of lung cancer cells through focal adhesion kinase-1. Cancer Research 2001; 61:2022-2030.

172. Pastore L., Tessitore A., Martinotti S., Toniato E., Alesse E., Bravi M.C. *et al*. Angiotensin II stimulates intercellular adhesion molecule-1 (ICAM-1) expression by human vascular endothelial cells and increases soluble ICAM-1 release in vivo. Circulation 1999; 100:1646-1652.

173. Kostler W.J., Tomek S., Brodowicz T., Budinsky A.C., Flamm M., Hejna M. et al. Soluble ICAM-1 in breast cancer: Clinical significance and biological implications. Cancer Immunology and Immunotherapy 2001; 50:483-490.

174. Kavanaugh A.F., Davis L.S., Nichols L.A., Norris L.A., Rothlein R., Scharschmidt L.A. *et al.* Treatment of refractory rheumatoid arthritis with a monoclonal antibody to intercellular adhesion molecule-1. Arthritis and Rheumatism 1994; 37:992-999.

175. Kavanaugh A.F., Davis L.S., Jain R.I., Nichols L.A., Norris S.H., Lipsky P.E. A phase I/II open label study of the safety and efficacy of an anti-ICAM-1 (intercellular adhesion moledule-1; CD54) monoclonal antibody in early rheumatoid arthritis. The Journal of Rheumatology 1996; 23:1338-1344.

VITAE

Elaine Coleman was born in Dearborn, Michigan on July 23, 1975 to Ted and Sylvia Craig. After completing her work at Jackson High School in Jackson, Michigan in 1993, she entered Oklahoma Christian University of Science and Arts in Edmond, Oklahoma. During the summer of 1996, she did a summer research internship with Dr. Paula Grammas at the Oklahoma University Health Science Center in the pathology department. Her work, entitled "Endothelial Derived Toxic Factor Attacks Neurons in Alzheimer's Disease", took first place in a student colloquium contest at Oklahoma Christian in April 1997. She received the degree of Bachelor of Science from Oklahoma Christian University with a major in biology in April 1997.

In August 1997, Elaine entered the Anatomy Graduate Program at the University of North Texas Health Science Center, which she attended for 1 year. In August 1998, she transferred to the Division of Cell and Molecular Biology Graduate School at the University of Texas (UT) Southwestern Medical Center, and she entered the Immunology Graduate Program in 1999. During her time at UT Southwestern, she has served as conference leader for the immunology module of the medical microbiology course; she has served as a volunteer for the STARS program, presenting her research to junior high and high school students; and she has served as a career representative to local 5th and 6th grade gifted and talented

programs, performing science experiments with the students and teaching them about experimental design. In honor of her service to both the school and the community, Elaine received a Dean's award in July 2004.

Elaine has given oral presentations of her work at both local and international meetings. A large portion of her work has been funded through a training grant from the National Institutes of Health. In addition, her collaborative involvement with other scientists has led to four journal articles, co-authorship of a book chapter in William Paul's *Fundamental Immunology*, and an instructional guide describing how to write a thesis. A manuscript based on the results in the thesis is in preparation.

Permanent Address:

2710 Amberton Pl.
Euless, TX 76040

Publications:

1. Patterson, C. E., Schaub, T., **Coleman, E.**, Davis, E. C. Developmental Regulation of FKBP65: An ER-localized Extracellular Matrix Binding-Protein. *Molecular Cell Biology*. 11, 3925-3935. 2000

2. Baluna, R., **Coleman, E.**, Jones, C., Ghetie, V., Vitetta, E.S. The Effect of a Monoclonal Antibody Coupled to Ricin A Chain-Derived Peptides on Endothelial Cells *in Vitro*: Insights into Toxin-Mediated Vascular Damage. *Experimental Cell Research*. 258, 417-424. 2000

3. Vitetta, E.S., **Coleman, E.**, Ghetie, M.A., Ghetie, V., Michalek, J., Pop, L.M., Smallshaw, J.E., Spiridon, C. Immunotherapy. In: Fundamental Immunology, 5th Edition, ed: W. Paul, Lippincott, Williams and Wilkens, New York, Chapter 50, pp-1621-1659, 2003.

4. Smallshaw, J., **Coleman, E.**, Spiridon, C., Vitetta, E.S. The Generation and Anti-Myeloma Activity of a Chimeric Anti-CD54 Antibody, cUV3. *Journal of Immunotherapy*, in press. 2004

5. Wang, S., **Coleman, E. J.**, Pop, L. M., Brooks, K. J., Vitetta, E. S., Niederkorn, J. Y. Effect of an Anti-CD54 (ICAM-1) Monoclonal Antibody (UV3) on the Growth of Human Uveal Melanoma Cells Transplanted Heterotopically and Orthotopically in SCID Mice. *Clinical Cancer Research*, submitted. 2004

6. **Coleman, E.J.**, Brooks, K., Vitetta, E.S. The Fc portion of UV3, an anti-CD54 monoclonal antibody, is critical for its anti-tumor activity *in vivo*. *In preparation*.